Universitetet i Stavanger

FACULTY OF SCIENCE AND TECHNOLOGY

MASTER'S THESIS

Study programme/specialisation: MSc in Offshore Technology Marine and Subsea Technology	Spring semester, 2017 Open/~~Confidential~~
Author: Thamilinian Kannamanaickanur Muruganandam	…… (signature of author)
Faculty Supervisor: Prof. Muk Chen Ong External Supervisors: Dr. Xiaopeng Wu (IKM Ocean Design) Per Nystrøm (IKM Ocean Design)	
Title of master's thesis: Numerical analysis of interference between an otter trawl board and a pipe-in-pipe system	
Credits: 30	
Keywords: pipe-in-pipe, otter trawl, impact analysis, pull over analysis, new contact element	Number of pages: 100 +supplemental material/other: 17 Stavanger, 29 June 2017

Numerical analysis of interference between an otter trawl board and a pipe-in-pipe system

Thamilinian Kannamanaickanur Muruganandam

Spring 2017

MASTER THESIS

Department of Mechanical and Structural Engineering and Materials Science

University of Stavanger

Main supervisor: Prof. Muk Chen Ong

Co-supervisors: Dr. Xiaopeng Wu (IKM Ocean Design)

Per Nystrøm (IKM Ocean Design)

(This page intentionally left blank)

Abstract

Subsea pipelines are likely to be exposed to fishing activity, which may results in trawl gear interacting with a pipeline. The interaction is classified into impact, pull-over and a special case called hooking. The trawl load is considered to be an important design load in pipeline design. In the recent developments of the subsea pipelines, the pipe-in-pipe (PIP) system is a solution for high-pressure/high-temperature requirements. Previous research and findings mainly focus on trawl gear interaction with a single pipe wall pipeline. There is limited research on trawl gear-PIP interaction. The main objective of this thesis work is to simulate and investigate the impact and pull-over responses of a pipe-in-pipe system during the interference with an otter trawl board.

The numerical study were carried out based on nonlinear finite element (FE) method by means of the computer software SIMLA. Based on the previous models for the single pipe wall pipe, modifications on the models were made to account for PIP. An advanced impact model was enabled to study the impact response of PIP. Later, a detailed clump weight pull-over model was modified and studied by using the new contact element (cont153) in SIMLA. Finally, a detailed trawl board pull-over model (with simplified geometry) was modified with the cont153 element to study the PIP response under pull-over loads. More details are described as follows.

Firstly, a study was carried out to investigate the impact response of a single pipe wall pipe and a PIP system. The impact model was established according to the Recommended Practice DNV-RP-F111 (RP) by using an advanced impact calculation method. Various pipeline parameters like pipe wall thickness, content density, concrete coating, specified minimum yield strength (SMYS), different trawl gears, and position of centralisers for PIP were considered. The purpose is to check how these parameters influence the impact response.

For pull-over analysis, to gain more understanding of the cont153 element, the clump weight model from Maalø's work was tested. As a result of this study, a contact stiffness with good contact behaviour was obtained and then used in further study. It is also found that the

friction coefficient has important influence on the results. The new contact element was then used in a trawl board model with the stiffness defined in the clump weight case. The warp line tension results are compared with previous model test results. The comparisons show that for lower span heights (0.5 m and 1.0 m), good agreements were achieved, but noticeable deviations were found for higher span heights (5.0 m).

Finally, the detailed trawl board model was used to investigate the pull-over responses (displacement, bending moment, strain, etc.) of a PIP at low span height (up to 1.0 m). The pull-over responses from the detailed model were compared with those from RP load. The main finding is that the responses increases as the span height increases, and the responses from the detailed model are in general lower than the RP case. This finding indicates the possibility to further optimise PIP design in the view point of trawl board pull-over loads at low span heights.

Acknowledgement

This thesis has been submitted in partial fulfillment of the requirement for completing the degree of Master of Science in Offshore Technology at the University of Stavanger.

I take this opportunity to express my gratitude to all those who have provided me with valuable guidance and support.

I would like to thank my faculty supervisor Prof. Muk Chen Ong for his excellent encouragement, guidance and motivation throughout the process of writing this project report. I would also thank him for being supportive to choose the topic and available all time during the semester.

I would like to extend my heartfelt gratitude external supervisor, Dr. Xiaopeng Wu (IKM Ocean Design) for his wonderful guidance, comments and support from scratch to final level of writing this report. I would thank him for his excellent motivation, especially his great knowledge and contribution towards modelling and analysis in SIMLA software.

I would also like to thank Per Nystrøm, Engineering Manager for his support and IKM Ocean Design, Stavanger for providing office space with all accessories.

Finally, I must express my very profound gratitude to my parents and to my brother and frirnds for providing me with unfailing support throughout the studies in Stavanger.

Contents

List of Figures

List of Tables

List of Abbreviations

DEH	Direct Electric Heating Cable
DNV	Det Norske Veritas
FE	Finite Element
HP	High Pressure
HT	High Temperature
ID	Inner Diameter
IP	Inner Pipe
NPD	Norwegian Petroleum Directorate
OD	Outer Diameter
OP	Outer Pipe
PIP	Pipe-In-Pipe
RP	Recommended Practice
SYMS	Specified Minimum Yield Strength
TB	Trawl Board
VIV	Vortex Induced Vibrations

List of Symbols

H_t	dent depth
k_i	in-plane stiffness of trawl board
L_w	warp line length
OD	overall outside diameter of the pipeline, including coating
t	pipe wall thickness ($t_{nom} - t_{corr}$)
α	factor to be included in the dent calculation
β	factor to be included in the dent calculation
σ	standard deviation for impact test results
A_E	cross-sectional area of the steel pipe exposed to external pressure
A_i	cross-sectional area exposed to internal pressure
A_w	warp line cross-sectional area
B	half height of trawl board
C_F	coefficient of pull-over force
C_h	coefficient of effect of span height on impact velocity
C_T	coefficient for pull-over duration
D	steel pipe nominal outside diameter
d	water depth
E	young's modulus
E_a	impact energy due to hydrodynamic added mass

E_{LOC}	impact energy absorbed locally by the pipe shell and coating
E_s	impact energy due to steel mass of the trawl board, beam with shoe or clump weight
F_b	impact force due to trawl board bending action
F_{sh}	maximum impact force experienced by the pipe shell
F_T	maximum pull-over force on pipe, horizontal direction
$f_{y,temp}$	derating value due to the temperature of the yield stress dimensionless height
F_Z	maximum pull-over force on pipe, vertical direction
h	trawl board height(=2B)
$H_{p,c}$	permanent plastic dent depth
H_{sp}	span height
I	trawl vessel density (annual mean number of trawlers per unit seabed)
imp	trawl gear impact frequency
k_{c1}	stiffness of the protective cover for heating cables attached to the pipeline (when applicable)
k_{c2}	stiffness of coating
k_{c3}	coating stiffness due to interaction effect between coating and steel pipe
k_{pb}	effective bending stiffness of the pipe in impact calculation
k_{pS}	effective soil stiffness acting on the pipe in impact calculation
k_s	local shell stiffness of the steel pipeline

k_w	stiffness of trawl warp
L	trawl board length, beam length or clump weight width
m_a	hydrodynamic added mass
m_p	plastic moment capacity for a plate
m_t	steel mass of the trawl gear
n_g	number of trawl boards, beam shoe or clump weight per trawl vessel
P_e	external pressure
p_i	internal pressure
R_{fa}	reduction factor associated with added mass
R_{fs}	reduction factor associated with steel mass
t_{corr}	corrosion allowance
t_{nom}	nominal thickness of the pipe
T_p	pull over duration
V	trawl velocity
y	yield stress to be used in design $[y = (SMYS) - f_{y,temp}\alpha_u]$

Chapter 1

Introduction

1.1 Background and motivation

Subsea pipelines are used for many purposes in the offshore oil and gas industry, from small diameter pipelines for infield transportation of products to larger diameter export pipelines. Pipelines are installed in the seabed using various pipe laying methods. All subsea pipelines are exposed to environmental loads, operational loads, and external interference loads such as dropped objects and fishing activities. The free span of pipeline occurs due to seabed irregularities, soil condition etc and it lead to fatigue damage, vortex induced vibration (VIV) and hooking of fishing gear. Various span correction measures like rock dumping, mechanical supports etc are used to reduce free spans. However there exists short free spans with evident heights and parts where the pipeline is laid freely on the seabed.

On the Norwegian continental shelf, a large network of subsea pipelines has been installed. The recent developments of the subsea pipelines are usage of PIP system. PIP is a solution for high-pressure/high-temperature requirements and it consists of a carrier pipe and an inner pipe. The two pipes are kept apart by centralisers which are fixed at regular intervals. The main idea is to use thermal insulation layer between the carrier pipe and the inner pipe to enhance the insulation performance of the inner pipe. To a certain extent, the carrier pipe also provides extra protection to the inner pipe against external damage. The PIP also

exposed to environmental loads, operational loads, and external interference loads such as dropped objects and fishing activities.

The offshore oil and gas industry and fishing industry often operates in the same area. In general, subsea structures attract fishes and this lead to increase in fishing activities in this area. According to Norwegian petroleum directorate (2010) the fishing activities are carried out based on three different trawling methods namely, midwater trawl, demersal or semi-demersal trawl and bottom otter trawl. The midwater trawl is characterised by the fishing gear which is not in contact with the seabed as illustrated in 1.2. This method will not go deeper than 500-600 m and used in a small extent. Semi-demersal trawling is a combination of the bottom and midwater trawling methods when a midwater trawl is lowered down towards the seabed. A bottom otter trawl is a trawl which is towed along or close to the seafloor. As the name indicates, a bottom otter trawl will always be in contact with the seabed and are most commonly used trawl as illustrated in figure 1.3.

In Norwegian sea, the trawling activities are carried out in the area, where the subsea structures and pipelines are exposed freely on the seabed. The bottom otter trawl or bottom trawling is the most common method used for trawling and this trawling activity leads to the interference of the trawl gear and the pipelines. Figure1.1 illustrated the crossing of trawl board over pipeline. The interference during the crossing causes three different scenarios, impact, pullover, and hooking phases to occur on the pipeline and are discussed detail in chapter 3.

The Norwegian authorities require that subsea installations shall not unnecessarily or to an unreasonable extent impede or obstruct fishing activities (DNV-RP-F111, 2014). The hazard of over trawling cannot be completely avoided even if the pipeline is laid outside of fishing zone because the subsea equipment attracts the fishes. This requirement leads to the over-trawlability of the pipelines. Initially the model testing is the preferred method for determining trawl loads. Such methods suffer from high costs, need for truncated models etc (Longva, 2010). So this requirement leads to usage and development of software to predict such trawl loads.

The previous research methods and existing guidelines focus mainly on trawl gear interaction

with a single wall pipeline. There is limited discussion on the response of pipe-in-pipe system under trawl loads. So, the study should be carried out to measure the response and risk of the PIP exposed to trawl loads. The trawl gear design loads are generally considered according to DNV-RP-F111 (2014). This recommended practice was published by Det Norske Veritas (DNV) and describes specifically on design methods regarding trawl gear interference with subsea pipeline. The calculation methods provided within DNV-RP-F111 are mainly based on experimental test. According to DNV-RP-F111 (2014) the largest trawl board used in Norwegian sea can have a mass of 6000kg and the clump weight can have a mass of up to 9000kg.

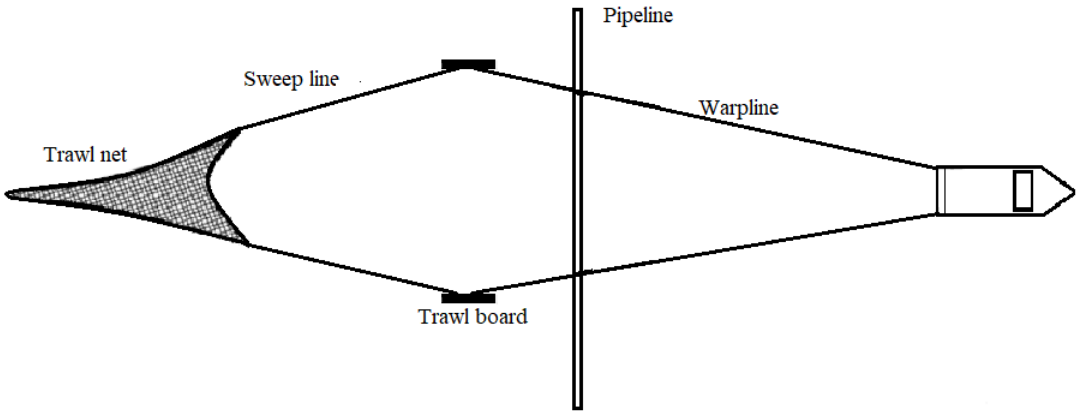

Figure 1.1 Trawl board crossing pipeline (DNV-RP-F111, 2014)

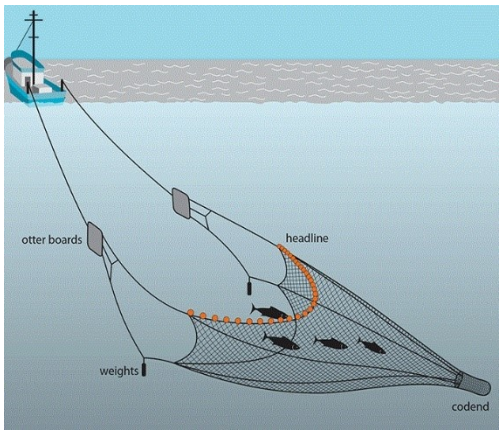

Figure 1.2 Midwater trawl (FRDC, 2014)

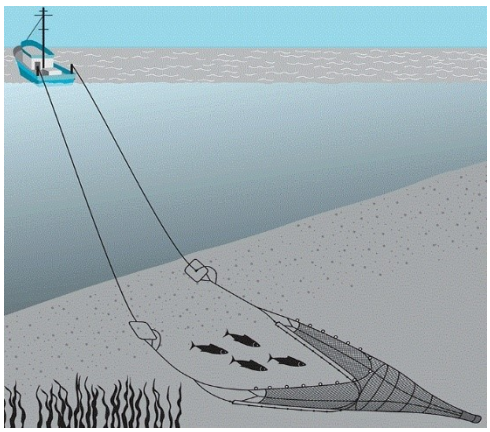

Figure 1.3 Bottom otter trawl (FRDC, 2014)

1.2 Previous work on trawl gear pipeline interaction

Subsea pipelines are exposed to fishing activity loads, such interaction of trawl gear. The interaction problem was studied earlier by Moshagen and Kjeldsen (1980). The laboratory and field study was performed in River and Harbour Laboratory in Trondheim now Division VHL of the Norwegian Hydrodynamic Laboratories in 1974. The study consists of the conflict between rigid and fixed pipeline with different bottom trawl gears. Later on, Horenberg and Sriskandarajah (1987) investigated specifically on the response of beam-trawl gear interaction with the rigid and fixed pipeline.

Moreover, Verley et al. (1991) studied the response of trawl forces on free-spanning pipeline by conducting model test. The test was carried out for three different trawl doors namely v-door, oval and polyvalent door. Also, three degrees of span flexibility are considered in the tests, ranging from a rigid, fixed pipe to a very flexible condition. Furthermore, Verley (1994) focused on the straight pipeline laid on a flat seabed exposed to trawling and he discussed particularly about the response of point of impact load and pull-over load caused by the trawl board on pipeline, which is the first phase of the trawl gear and pipeline interaction.

One specific accident related to trawl gear pipeline interaction has been well analysed and the report was published by (Ellinas et al., 1995). The main discussion is about the damage of the pipeline caused by the trawl gear. The pipeline is in the Hewett field in the southern North Sea. The interaction leads to lifting of the pipeline accompanied by the plastic deformation, so that it formed a vertical span about 15m above the seabed. The assessment study focusses mainly on the integrity of the pipeline and the strain level induced during the installation of the pipeline and strains developed during the damage process.

In addition, Hval et al. (2009) assessed the structural integrity of pipelines subjected to large strains caused by trawl pull-over load. The study is carried out for the pipeline laid in phase 2 development of the Ormen Lange gas field. This assessment is made before the real-time incident, to determine whether the pipeline would survive the incident of trawl impact during operation without resulting in failure or leakage.

Igland and Søreide (2008) developed a finite-element model in ANSYS to analyse a heavy

clump weight pulled over the pipeline. Pull-over analysis is mainly focused. The pull-over loads and duration are compared with loads, amplitude and duration given in DNV-RP-F111. Realistic trawl pull-over loads are established using actual stiffness of the pipeline and the pipe-soil interaction and the result shows that the method in DNV-RP-F111 are conservative.

Maalø (2011) worked on the simulation of clump weight-pipeline interaction of a fixed pipe section at low span heights and compared with model test results by using FE analysis software SIMLA. He developed input files based on the model test. The simulation results are also compared with the design loads calculated from the RP. He concluded that the increasing in pipeline flexibility resulted in a decrease in pull-over force. Following him, Johnsen (2012) mentioned that the pull-over load of clump weight calculation methods in DNV-RP-F111 was based on an experimental model test executed at MARINTEK in 2004. The author carried out many sensitivity studies. The full-scale pipeline model was also analysed to investigate the effect of flexibility in pipeline comparing with design loads. He concluded that the DNV design loads have higher pullover force and longer pullover time than those observed in full-scale test particularly for smaller diameter pipeline.

Longva (2010) examined the crossing of trawl board over the pipeline by using analysis software SIMLA. He developed a new hydrodynamic model by considering the seabed proximity and forward-speed effects of the trawl board. Also, he examined the oblique trawl board crossing in his analysis, stating that perpendicular crossing did not predict the largest pullover loads. Further, Longva and Sævik (2012) developed a new contact element that helps interaction between 3-dimension rigid body and pipeline model by beam element. The study is carried out by comparing with model test results to verify the performance of new contact element.

Pipe-in-pipe systems is emerging for Norwegian offshore projects in the North Sea. PIP system is used for the High Pressure and High Temperature (HP/HT) subsea field and it has superior thermal conductivity performance and can provide necessary thermal insulation with very low overall heat transfer coefficient. For the PIP, the outer pipe gives extra protection for the inner pipe and it does not have to resist the internal pressure and it accepts greater level of dent depth when compared to sing wall pipe. The PIP is also exposed to trawling

loads. Sriskandarajah et al. (1999), is first to describe the fishing gear interaction of HP/HT PIP systems. The study is based on impact analysis and pull-over analysis of heavy dutch beam trawl. The effects of impact in terms of dent depth are examined by both empirical formulae and by the Finite Element (FE) method. Pullover analyses were performed using an implicit non-linear dynamics solution within the FE method in ABAQUS.

Zheng et al. (2012) studied the impact damage on PIP by conducting indentation test and comparing the results with FE model analysis results. The model analysis is carried out using the software ABAQUS. The test is carried out for both the single wall pipe and PIP. Furthermore, Zheng et al. (2014a) demonstrated the overtrawlability of the PIP and single pipe by using quasi-static indentation tests and impact tests, as well as the corresponding finite element (FE) models. Based on the experiments and FE models, the authors demonstrate that the quasi-static analysis can replace the dynamic analysis to some extent, as the quasi-static process is not much different compared to impact response.

Offshore pipelines are exposed to external pressure and internal pressure. The trawl gear impact creates a dent that pushes the pipe wall inward along with the external pressure, in this case the dent might be severe when compared to impact on pipe with no external pressure. A finite-element model of denting under external pressure for single wall pipe and pipe-in-pipe using hydrostatic fluid element has been established and verified Zheng et al. (2014b) . Also, the study is carried out for the combination of external pressure, internal pressure and the indentation. The study concludes that the collapse induced by reducing the internal pressure has a high possibility to happen for single wall pipe, but for PIP the inner pipe is not sensitive to outer pipe due to the space between the outer pipe and inner pipe, therefore a buckle is less likely to propagate.

Small scale pullover test is carried out by Zheng et al. (2014b) to study the pullover force for different pipes and different conditions. The model test was conducted in the wave basin in the Hydraulic Engineering Laboratory in National University of Singapore. The trawl gear used for the model test is beam trawl gear and the pipeline is fixed at both ends. The test is carried out for both PIP and single wall pipe and the results are compared.

It can be noticed that there was only limited study carried out for the interaction of trawl

equipment with PIP. Therefore, more study should be carried out for the influence of trawl loads on PIP to understand the behaviour. The interference between trawl gear and pipelines are explained in recommended practice DNV-RP-F111 (2014). The recommended practice RP has the design data for the trawl board, clump weight. Also, design basis for pipeline. The detailed procedure of advance impact calculation, pull-over and hooking are described in this RP. This is considered as the reference for the work related to interference of trawl gear and PIP.

1.3 Scope of the thesis

All the simulation in this thesis are related to impact and pull-over analysis performed using the finite element program SIMLA. The impact model for single pipe established in IKM Ocean Design according to advance impact calculation method described in DNV-RP-F111, was extended to accont for the PIP system. For single wall pipeline, analysis is carried out to check, how different pipeline properties will influence the impact result. The various pipeline properties considered are wall thickness, coating thickness, content density, specified minimum yield stress and different trawl mass. The basic pipeline data is referred from recommended practice. For PIP, the centralizers are used to connect the inner pipe and the carrier pipe. These centralisers are arranged in consecutive distance in the pipeline. In this thesis, the centrlisers are modelled as stiff springs that connect the inner pipe and the outer pipe. The simulations are carried out for two different cases and they are 1) when the trawl board hits at the place where exactly the centralizers are placed and 2) hits in between the gap of two centralizers. This analysis is carried out to check, how these parameters influence the result.

Trawl gear pull-over interference has previously been investigated by Johnsen (2012) by using SIMLA. In this thesis, the work is continued by establishing a new contact model for the clump weight. The simulation of clump weight pull-over interference is caried out for short pipeline. The aim of the work is to investigate the behaviour of new contact element (cont153).Various simulation are carried out for different contact stiffness and friction

coefficient. The horizontal pull-over results were measured from simulation and compared with previous model test and the results of Johnsen (2012). The previous model test configuration was illustrated in detail by Maalø (2011) This study served as the basis for the developing the trawl board model with the new contact element.

A validation study was carried out for a trawl board pipeline interaction. The trawl board model was developed based on previous model by using the new contact element with the simplified geometry. The model used in the previous model is illustrated by Wu et al. (2015) in detail. The friction coefficient and stiffness were added based on the previous work on clump weight interaction. This model consists of 1360m fixed and rigid pipeline length and 350 mm diameter. From this model, the warp line tension is measured and compared with previous model test results. The study was carried out for three different span heights 0.5 m, 1.0 m, and 5.0 m, and also the influence of different warp line angle also investigated.

Finally, the PIP model was established with the trawl board model developed in the previous case. The pull-over analysis is carried out for the interference of trawl board - PIP model and the pull-over results are compared with the analysis carried out for RP load calculated using DNV-RP-F111.The various results like horizontal force, vertical force, strains, bending moment are compared are compared for three different span heights 0.0 m, 0.5 m, and 1.0 m.

Finally, in total three different SIMLA pull-over models have been established for pull-over analysis, a new contact model for the clump weight pipeline interaction, a new contact model for measuring the warp line tension during the interaction of trawl board with single wall pipeline and finally the pull-over analysis is carried out for the trawl board-PIP interaction and are compared with the current engineering practice DNV-RP-F111 (2014) in order to identify and explain eventual differences such as, unnecessary conservatism that can be avoided in future pipeline designs.

1.4 Structure of the thesis

Chapter 2: Describes briefly about different trawling methods and types of trawl board used in Norwegian water. A short description of clump weight is also addressed.

Chapter 3: Contains the detail of PIP and its mass calculation. The effect of different loads acting in pipeline like temperature effect, pressure effect etc., are also discussed

Chapter 4: Presents the different phases of trawl gear and pipeline interaction. The simplified calculation method and advanced impact calculation method are discussed to calculate the trawl gear impact loads. The DNV-RP-F111 calculation method for estimation of trawl board pull-over loads is reviewed.

Chapter 5: Describes all aspects of modelling in SIMLA, including the trawl gear configuration, clump weight and trawl board model with new contact element. The description of different pipeline models, seabed interaction with pipeline and trawl board, pipe warp line contact and trawl board pipeline contact are also discussed.

Chapter 6: Contains all the results part and its discussion. First it has the discussion on horizontal pull-over force on pipeline by clump weight developed based on new contact element, followed by the results of warp line tension exerted by the trawl board developed with new contact element for different span heights. Finally, the results of trawl board interaction with PIP and comparison with RP load are discussed.

Chapter 7: The conclusion regarding the simulation results and the recommendations for the further work are discussed.

Chapter 2

Trawl Methods

Trawling is an important method of fishing practice carried out worldwide. The trawling process is carried out by a vessel and the vessel tows a trawl net or fishing net with an opening along the direction of travel. The warp-line connects the trawl bag with vessel. The trawling process can be carried even at 5000 m water depths and it depends on the kind of the target species. According to DNV-RP-F111 (2014), there are three different types of bottom trawling methods are used, namely

- Otter trawl
- Beam trawl
- Twin trawl

The main focus of this chapter is to introduce different types of bottom trawling methods used in Norwegian sea.

2.1 Otter trawl

The configuration of a typical otter trawl is shown in figure 2.1. The otter trawl gear consists of a trawl net which is connected to trawl boards through sweep line. There are two trawl boards connected at each side of the trawl net. These trawl boards help to open the trawl

net by hydrodynamic force. The trawl boards are further connected to the surface vessel by

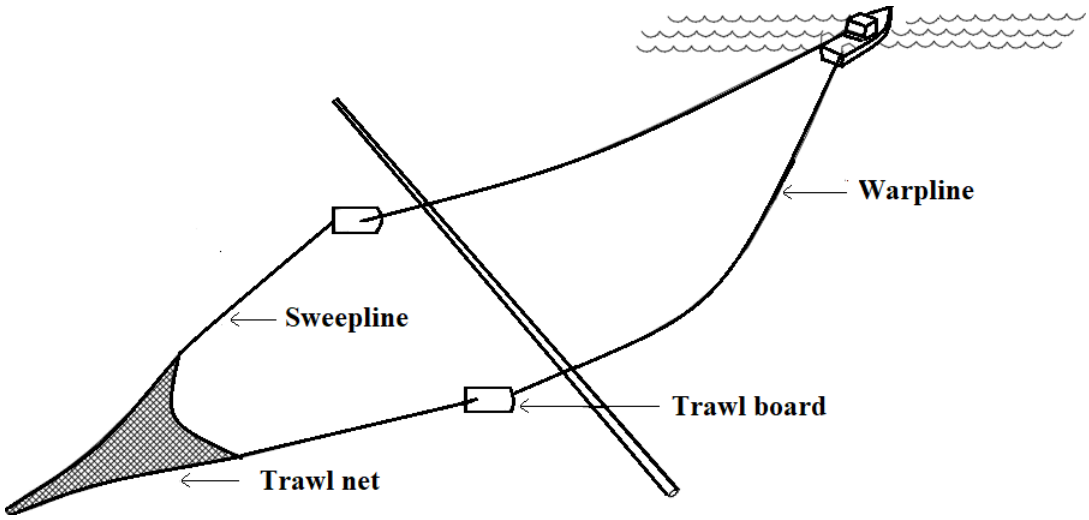

Figure 2.1 Otter trawl (DNV-RP-F111, 2014)

means of warp line. The sweep lines and warp lines are connected at suitable positions on the trawl board to ensure the maximum spreading of the trawl net. The required angle of attack relative to the direction of travel is achieved by adjusting these connections. Around the circumference of the trawl net mouth, the upper part consists of float and lower part consists of mounted weights. These weights and floats also help to open the trawl net.

During trawling, fish will lose speed and get trapped in the trawl net, because the boards are dragged along the seabed which make noise and set up a cloud of mud. The otter trawl is the most common and frequently used bottom trawl in Norwegian waters. The trawl boards are classified into different types and the most commonly used trawl boards are as follows,

- Polyvalent board or rectangular board
- V-shaped board

Figure 2.2 Polyvalent board (Skibssmedie/Thyborøn)

The polyvalent board is used in this thesis work. The polyvalent boards have a curved surface with an oval shape which improves the ability to slide over obstacles. The polyvalent boards have generally been found to give the highest loads on pipelines. The polyvalent board is used for both hard and soft seabed. For hard seabed, the board is desirable to have small contact area and for soft seabed the contact area should be larger. Figure 2.2 shows the polyvalent type rawl board.

2.2 Beam trawl

The beam trawl consists of a transverse steel beam mounted on the trawl net to keep the net open as shown in figure 2.3. Beam shoes are connected at each end of the beam which have sharp edges. The outline of a beam shoe is seen in figure 2.4. The beam trawl is normally used in pair and is towed by outriggers on each side of the vessel. The beam keeps the trawl net open regardless of the vessel speed. These beam trawls are used to catch various species of fish. The beam keeps the trawl net open regardless of the vessel speed. These beam trawls are used to catch various species of fish. The beam trawl mainly used on flat, sandy seabed

in shallow waters in the southern parts of North Sea.

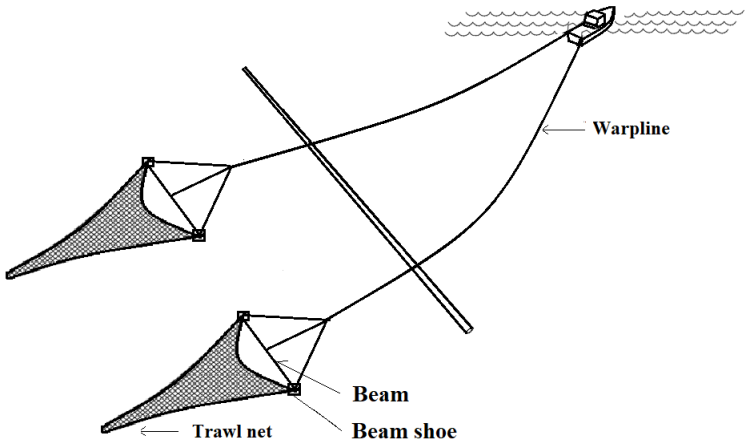

Figure 2.3 Beam trawl (DNV-RP-F111, 2014)

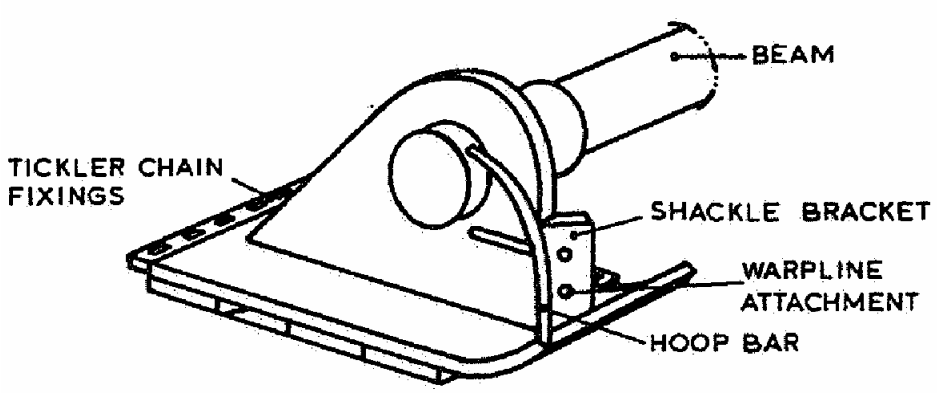

Figure 2.4 Beam shoe (DNV-RP-F111, 2014)

2.3 Twin trawl

The twin trawl shown in figure 2.5, is a new concept developed during last decades. The twin trawl is an extension of otter trawl in which a single vessel tows two trawl nets side by side. The twin trawl consists of a heavy clump weight located at the centre of two trawl net connected by a centre warp line. The clump weight with two trawl boards, keep the trawl net separated and mouths open and this is due to hydrodynamic forces. The fishing quantity is raised compared to a normal otter trawl. At the time of trawling process most

of the towing force are absorbed by the centre wrapline. This results in the reduction of the necessary spreading force due to a reduction of tension in warp lines connected to the trawl boards. This leads to a larger trawl bag opening than for a single otter trawl and is the main advantage of using a twin trawl.

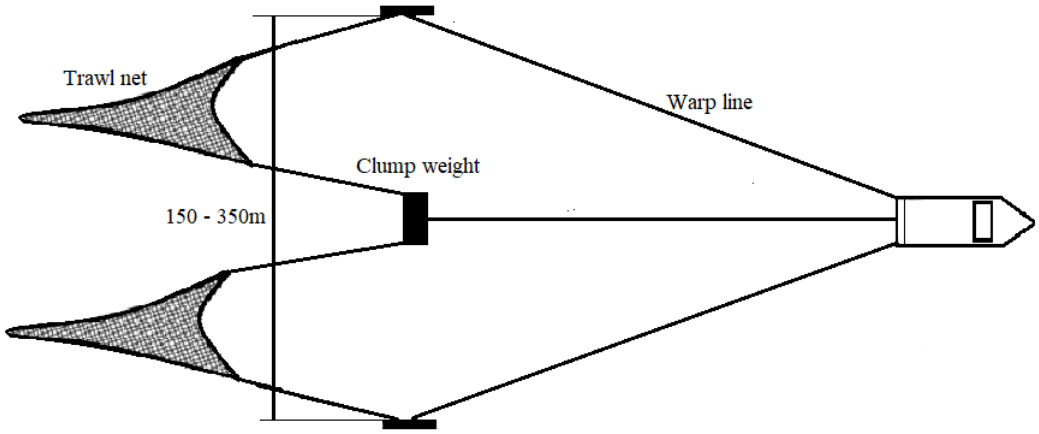

Figure 2.5 Twin trawl (DNV-RP-F111, 2014)

Clump weight

The clump weight has a mass ranging between 2 to 9 tonnes because, the clump weight should be heavy to resist the increase of upward pull. Comparing with trawl board, the clump weight can result in higher impact energy and pull-over loads. There are various types of clump weight design exist, in that two common clump weight designs are the roller type and the bobbin type as shown in figure 2.6 and figure 2.7.

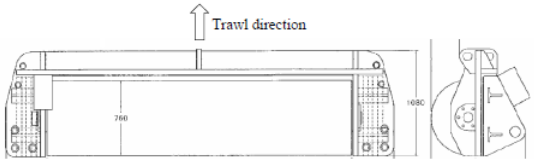

Figure 2.6 Roller type clump weight (DNV-RP-F111, 2014)

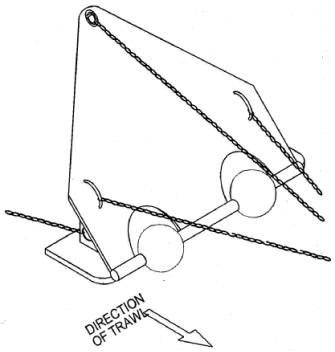

Figure 2.7 Bobbin type clump weight (DNV-RP-F111, 2014)

Chapter 3

Theoretical Background of Pipeline

The following chapter covers the theoretical backgrounds for the areas that need to be considered when carrying out the analysis. Most important subjects related to the analysis are the temperature and pressure loading on the pipeline. This section gives brief explanation of PIP configuration, calculation of pipeline mass, causes of pipeline span, different loads on pipeline, effect of temperature and pressure loadings.

3.1 General description of pipe-in-pipe

The pipe-in-pipe system consists of an inner "flowline" pipe and a protective outer pipe called carrier pipe. The function of inner pipe is to convey fluids and is designed for internal pressure containment. Inner pipe is insulated with thermal insulation material to achieve the required operational temperature. The outer pipe protects the insulation material from external hydrostatic pressure and other mechanical damage. Two pipes are kept apart by centralisers which are fixed at regular intervals. Figure 3.1 shows the illustration of PIP.

There are several conditions in which the pipe-in-pipe systems may be considered for particular flowline application over a conventional or flexible pipeline. The first condition is insulation-high pressure (HP) and high temperature (HT) reservoir condition. The HP/HT flowlines require high insulation to prevent formation of wax and hydrate deposit (Bai and

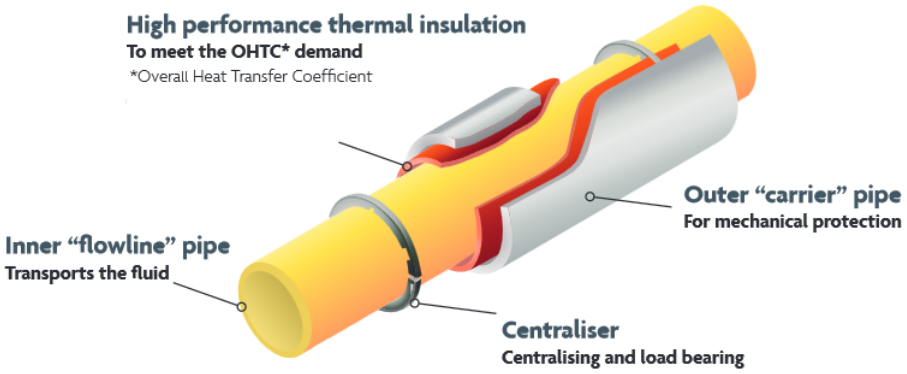

Figure 3.1 A sketch illustration of PIP (Technip)

Bai, 2005). There are different thermal coatings available that can be applied to steel pipe but they tend not to be particular robust mechanically and also not been proven at the temperature in present HP/HT field. An alternative is to place the flowline inside another larger pipe called carrier pipe. There are guidelines to estimate trawl board interaction with single wall pipe, but there is no specified method to access the trawl board interaction with pipe-in-pipe. The carrier of pipe-in-pipe is not required to resist the internal pressure and can occupy a greater level of indentation than a single wall pressure containing pipe (Bai and Bai, 2005). The result will be conservative if one applies the approach for single wall pipe to pipe-in-pipe. Therefore, the interference of trawl board and PIP assessment should be conducted. The various configuration of PIP should be considered are gap thickness between the internal and external pipes, thermal stability, and overall feasibility.

3.2 Mass of the pipe

The mass of the pipe is the product of density and volume and the formula for calculating the mass is described below

$$m = (d_0^2 - d_i^2) \times l \times \rho \tag{3.1}$$

where,

d_o= outer diameter of the pipe

d_i = inner diameter of the pipe

ρ = density (pipe, concrete, content)

l = length of the pipe (per unit length)

The mass of the outer pipe and the mass of the inner pipe is calculated using the equation below. The total mass is the dry mass of the pipe.

Mass of the outer pipe

$$m_{outer\ pipe} = (OD^2_{outer\ pipe} – ID^2_{outer\ pipe}) \times \rho_{outer\ pipe} \tag{3.2}$$

Mass of inner pipe

$$m_{inner\ pipe} = (OD^2_{inner\ pipe} – ID^2_{inner\ pipe}) \times \rho_{inner\ pipe} \tag{3.3}$$

Total mass $m_T = m_{outer\ pipe} + m_{inner\ pipe}$

The submerged mass of the pipe is the difference between dry mass and the buoyancy mass

Submerged mass = Dry mass – Buoyancy mass

Buoyancy mass is calculated using Buoyancy mass = total volume $\times \rho_{sw}$

where,

ρ_{sw} = density of sea water

The total mass of the single pipe wall is calculated by considering the coating thickness

Mass of the outer pipe

$$m_{pipe} = (ID^2_{concrete} – ID^2_{pipe}) \times \rho_{pipe} \tag{3.4}$$

Mass of concrete coating

$$m_{concrete} = (OD^2_{concrete} – ID^2_{concrete}) \times \rho_{concrete} \tag{3.5}$$

Total mass

$m_T = m_{concrete} + m_pipe$

3.3 Pipeline span

In offshore the spanning can occur when pipeline and seabed contact lost over an appreciable distance. In other words, free spanning is an unsupported length of pipeline. Excessive yielding and fatigue can occur when the pipeline has the free spans and may result in failure of pipelines. The free span occurs due to various reason and some of the main reasons are described below

- Seabed irregularities (rough seabed)
- Subsequent scouring movement (mobile seabed)
- Sand Waves
- Rock Berm
- Rocks and Boulders
- Dynamic loads (waves and currents)

3.4 Loads in pipeline

The pipelines are subjected to various types of loads including functional loads, environmental loads, installation loads (Palmer and King, 2004). The loads occur due to various parameters. These loads are categeroized
Functional loads – The functional loads acting on the pipeline includes

- internal pressure loads,
- thermal expansion,
- weight of the pipe,
- external pressure.

Environmental loads – The environmental loads are caused by

- waves,

- current and
- other external forces.

Installation loads – The installation loads are occurred at the time of pipeline installation by using different methods.

3.5 Pipeline expansion

The operating temperature and pressure of the pipeline laid on the seabed will be normally higher than the installation temperature and pressure, so when the pipeline is exposed to operating temperature and pressure it tends to expand. The three-main reason for the end force and expansion of the pipeline are temperature, pressure and poison contraction associated with pressure effects. This leads to lateral/upheaval buckling and walking of pipeline.

3.5.1 Effect of thermal strain

The pipeline operates at higher temperate, while the pipeline will be installed at ambient temperatures. So, the Pipelines experience thermal strain or stress when subjected to temperature difference during operation phases and it develops to pipeline expansion. When the pipeline is unrestrained, the temperature rise causes the expansion whereas when it is totally constrained, the pipeline cannot expand and therefore the effects can be seen as a compressive stress in the pipe (Palmer and Ling, 1981).
The thermal strain is given by equation 3.6

$$\varepsilon_{thermal} = \alpha.\Delta T \tag{3.6}$$

Where,
$\varepsilon_{thermal}$ = thermal strain
α = linear thermal expansion coefficient
ΔT = temperature difference

The thermal stress is given by equation 3.7

$$\sigma_{thermal} = -\alpha.E_{steel}.\Delta T \tag{3.7}$$

Where,

$\sigma_{thermal}$ = thermal strain

E_{steel} = elastic modulus

A pipeline which is fully constrained experiences buckling when it is exposed to increase in temperature during operation. Any imperfection or out of straightness in the pipeline initiate thermal buckling of the pipeline. The imperfection will create a perpendicular component of the axial compressive force induced by operational/design temperature of the pipeline. Then the pipeline will start to move side-ways if the perpendicular force exceeds the soil frictional restraining force.

3.5.2 Effect of pressure

Pressure induces axial loading due to end cap force which contribute to the expansion of pipeline. The first pressure effect is the end cap loading and this occurs at any curvature in the pipeline. The end-cap force which is caused due to pressure difference is given in equation 3.8, (Berhe, 2014)

$$F_{end} = p_i A_i + p_e A_e \tag{3.8}$$

Where,

p_i = internal pressure

p_e= external pressure

A_i = internal cross-sectional area of pipeline

A_e = outer cross-sectional area of pipeline

The corresponding stress for unrestrained pipeline is given by equation 3.9

$$\sigma_{end\ cap} = \frac{F_{end\ cap}}{A_{steel}} \tag{3.9}$$

The corresponding strain for unrestrained pipeline is given by equation 3.10

$$\varepsilon_{end\ cap} = \frac{\sigma_{end\ cap}}{E_{steel}} \tag{3.10}$$

Where,

$\sigma_{end\ cap}$ = stress at curvature end of pipeline

A_{steel}= area of steel

$\varepsilon_{end\ cap}$= strain at curvature end of pipeline

The next effect is the poisson's effect. The internal pressure induces a hoop stress and the hoop stress induces circumferential expansion of a pipeline and simultaneous axial contraction i.e. the pipe expands in hoop direction, the poisson's effect results in an axial contraction. For unrestrained pipeline, the corresponding strain and stress due to Poisson's effect are given by equation 3.11 and 3.12.

$$\varepsilon_p = \frac{-\nu\sigma_h}{E_{steel}} \tag{3.11}$$

$$\sigma_p = 0 \tag{3.12}$$

For restrained pipeline, the corresponding strain and stress due to poisson's effect are given equation 3.13 and 3.14

.

$$\varepsilon_p = 0 \tag{3.13}$$

$$\sigma_p = -\nu\sigma_h \tag{3.14}$$

where,

ν= Poisson ratio

σ_h = hoop stress

3.5.3 Combined effect of thermal strain and pressure

Normally pipeline is subjected to a combined effect of thermal strain, pressure and poisson effects. And hence the pipeline has to be designed considering these cases. The longitudinal stress due to this effect has two components, a tensile stress from pressure and a compressive stress from thermal loads. These stresses and strains are in the axial direction. Induced strain and stress by the combined effect of temperature and pressure for restrained and unrestrained pipeline conditions is given by the following equations (Berhe, 2014)

. For unrestrained case, the longitudinal strain and longitudinal stress which is directly related to pipeline expansion are given by equation 3.15 and 3.16

respectively.

$$\varepsilon_L = \alpha.\Delta T + \frac{\sigma_h}{2}.\frac{1-2\nu}{E_{steel}} \tag{3.15}$$

$$\sigma_L = \frac{PD}{4t} \tag{3.16}$$

For restrained case, the longitudinal strain and Longitudinal stress which is directly related to pipeline expansion is given by equation 3.17 and 3.19

respectively.

$$\varepsilon_L = 0 \tag{3.17}$$

$$\sigma_L = \alpha.E_{steel}.\Delta T + \nu\sigma_h \tag{3.18}$$

Hoop stress

The circumferential stress or hoop stress is developed in thin wall pipe by action of a radial force distributed around the circumference when the pipeline is subjected to internal pressure.

$$\sigma_L = \frac{PD}{2t} \tag{3.19}$$

where,

σ_h = hoop stress

D = internal diameter

t = wall thickness

P = net internal pressure

ε_L = Longitudinal strain

σ_L = Longitudinal stress

3.5.4 Effective axial force

The effective axial force is often considered as a virtual force in contrast to the so-called "true" axial force given by the integral of stress over the steel cross-section (Fyrileiv and Collberg, 2005). The influence of external and internal pressure in the pipeline is described by using the concept of effective axial force. Therefore, for the pipeline designer it is very important to understand this concept.

According to law of Archimedes effect of external pressure is defined as, "The effect of the water pressure on a submerged body is an upward directed force equal in size to the weight of the water displaced by the body". The law is based on the assumption that pressure acts over a closed surface.

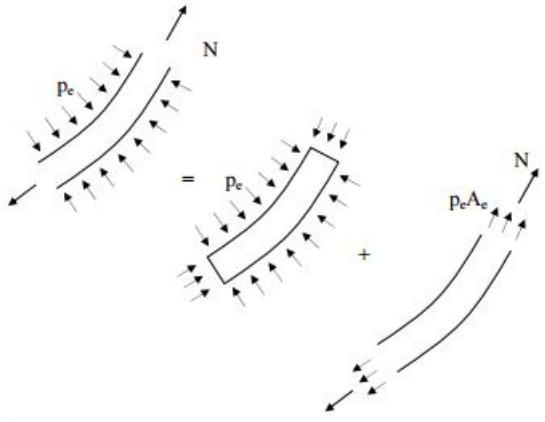

Figure 3.2 Pipe section with external pressure (Fyrileiv and Collberg, 2005)

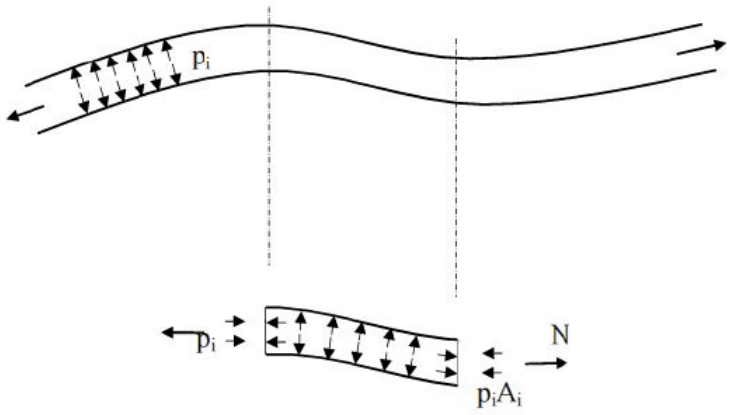

Figure 3.3 Pipe section with internal pressure (Fyrileiv and Collberg, 2005)

Consider a pipe exposed to external pressure as shown in figure 3.2, only the axial force N is included in the section. This axial force with external pressure $p_e$can be replace replaced by a section where the external pressure acts over a closed surface and the gives the resulting force equal to the weight of the displaced water, the buoyancy of the pipe section and an axial force equal to $N + p_e A_e$. The external pressure effect does not change physics or add any forces to the pipe section. However, it significantly simplifies the calculation.

For the internal pressure, similar consideration is accounted. Figure 3.3 shows a section of a pipeline with internal pressure, the external forces acting on this section is the axial force N and the end cap force, $N + p_i A_i$. The internal pressure acts always on a closed surface when the pressure acts in all direction in every point in the liquid.

From these considerations of the external and internal pressures acting on a pipeline section it becomes clear that the effect of these may be accounted for effective axial force. The effective axial force is given in the equation 3.20

$$S = N - p_i A_i + p_e A_e \tag{3.20}$$

The effective axial force for the shorter pipeline and long pipe is illustrated in the figure 3.4 and 3.5

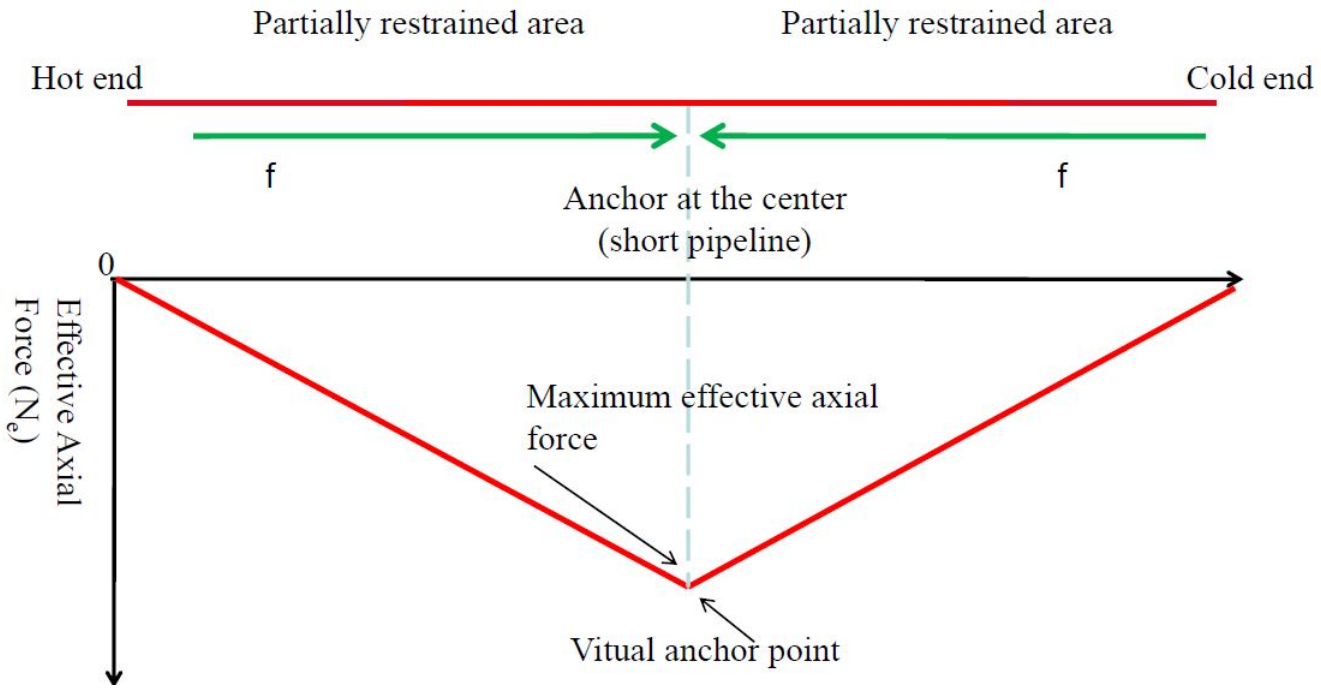

Figure 3.4 Typical effective axial force for short pipeline (Palmer and King, 2004)

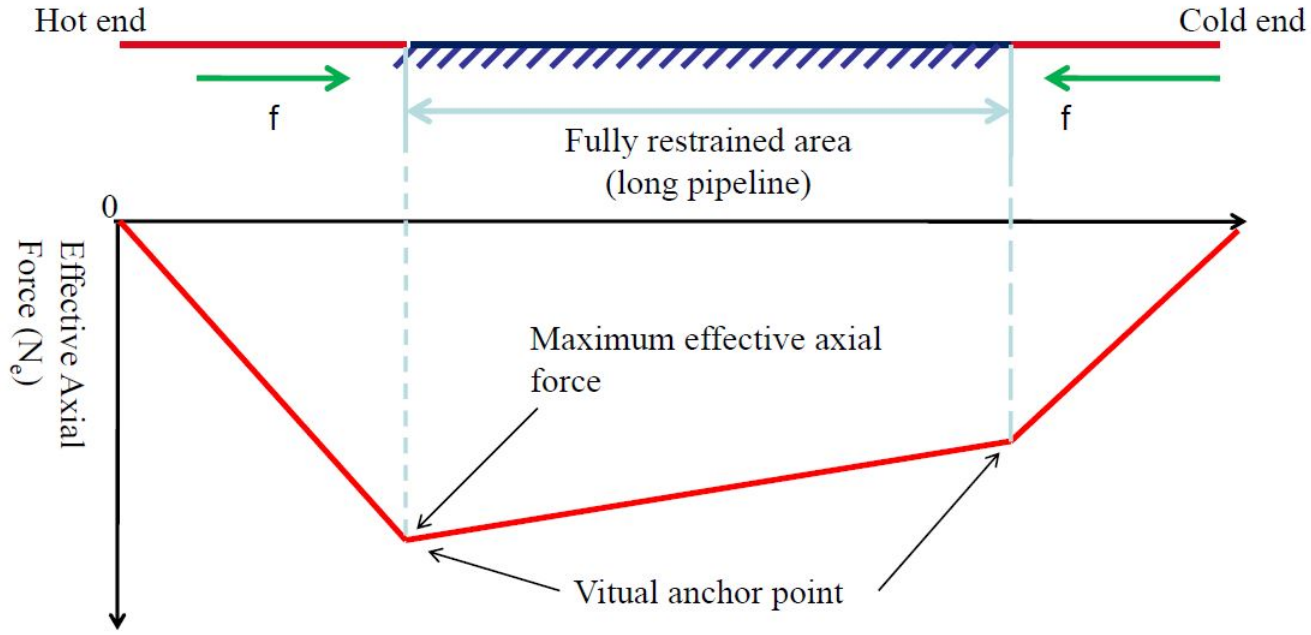

Figure 3.5 Typical effective axial force for long pipeline (Palmer and King, 2004)

Chapter 4

DNV-RP-F111

4.1 Trawl gear – pipeline interaction

When a bottom trawling operation is carried out, the trawl gear may interact with pipeline. According to the DNV-RP-F111 (2014), the interaction is divided into three different phases as follows

- Impact
- Pull-over
- hooking

4.1.1 Impact phase

This is the first phase also called as initial impact phase, where the trawl equipment first hits the pipeline. The trawl equipment may be either a trawl board, a beam shoe, or a clump weight. This impact lasts for some hundredths of a second. The local resistance of the pipe shell mainly resists the impact force, including any coating or attached electric cable protection structure. A method to determine the impact energy of a trawl board and the impact energy absorbed by the pipe shell was proposed initially by Mellem et al. (1996).

4.1.2 Pull-over phase

Pull-over is the second phase occurring after the impact. In this stage the trawl board, beam trawl or clump weight is dragged over the pipeline by the warp line. The pull-over phase last from 1 second to some 10 seconds and the duration depends on water depth, span height, and other factors. A more global response of the pipeline is observed in this phase.

4.1.3 Hooking phase

In the hooking phase the trawl equipment gets stuck under the pipeline. This is a rarely occurring event. During this phase the forces at the pipeline could be as large as the breaking strength of the warp line. In this project the focus will be on the response of the pipeline during the impact phase and pull/over phase.

4.2 Brief description of impact analysis

When the trawl equipment hits the pipeline, an impact force is induced on the pipeline. The transfer of kinetic energy from the impacting trawl equipment to the pipeline, its coating etc., is called as impact loads. During this impact the duration of energy transfer is very short and this amount of transferred energy is absorbed as a local dent or local deformation of the pipe. The impact energy transferred to the pipe depends on the front-end shape of the trawl equipment. The impact energy comprises of towing velocity and mass of the trawl equipment, impact velocity, pipeline property, span height, soil etc.,
The block diagram in the figure 4.1 shows the design overview of impact analysis, pull-over analysis and hooking of trawl board interference with the pipeline. The initial step of the process is to select the type of trawl gear and its mass, velocity, size , frequency etc.

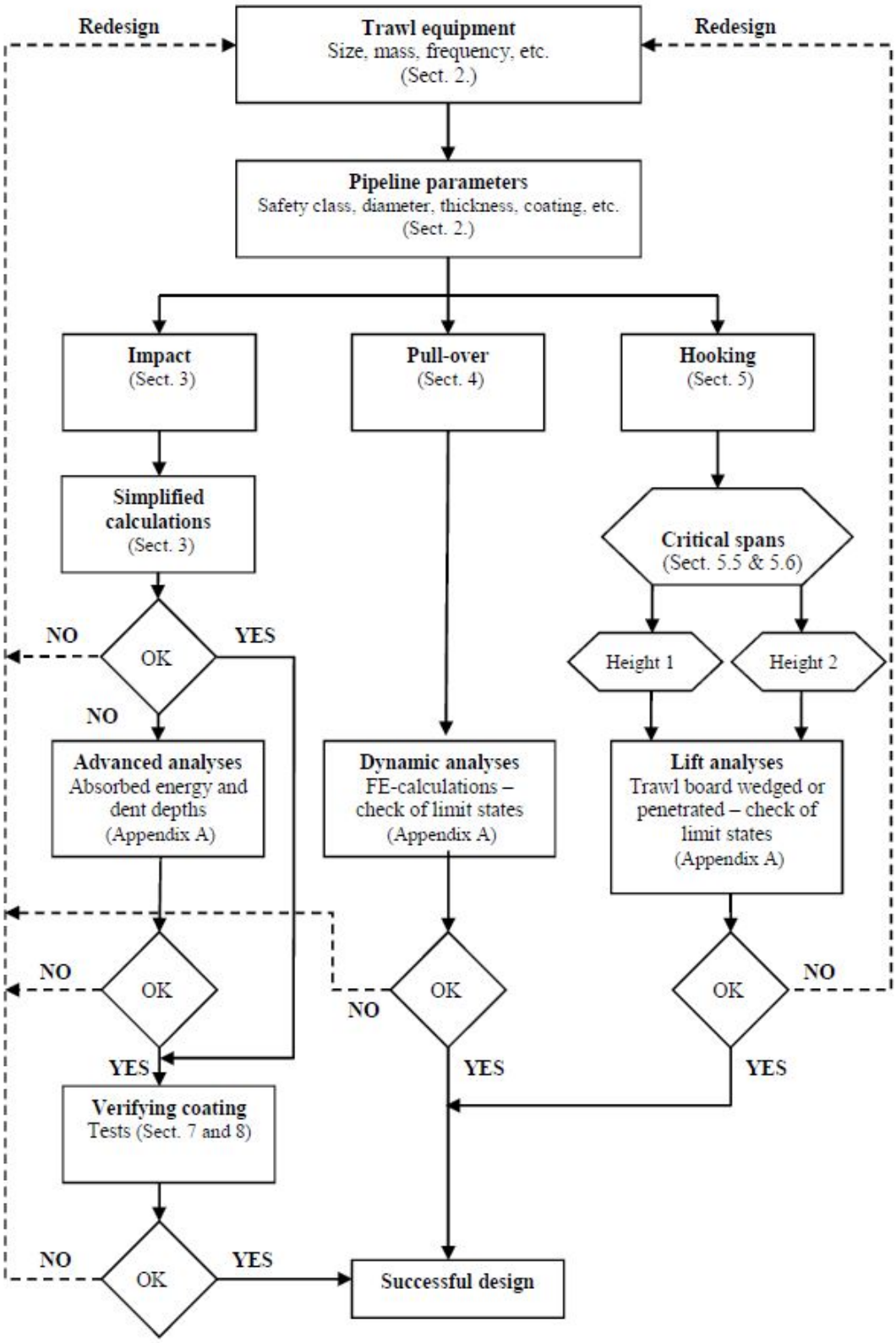

Figure 4.1 Overview of the design of pipeline with respect to interference with trawl gear (DNV-RP-F111, 2014)

The second step is to choose the pipeline parameters like diameter, thickness, coating, material etc. Once the parameter is defined the simplified calculations is carried out and then the advanced analysis is done with help of software to obtain the accurate results for impact analysis. And finally, coating is verified and the results are ok then it is a successful design if not the design should be carried out from first. For the pull-over analysis the FE calculation the dynamic analysis is carried out.

4.2.1 Simplified calculation method

The simplified method applies only for steel pipelines like bare pipes, painted pipes and pipes with thin corrosion coating or concrete coating. For other cases, advance impact calculation method is applied. The simplified method of calculation is conservative and used to calculate the impact energy absorbed by the pipe and to estimate the permanent dent depth. This simplified calculation method is based on the recommended practice (DNV-RP-F111, 2014).

4.2.1.1 Trawl board

The impact energy is calculated separately for steel mass and the associated added mass of the trawl board.
For steel mass

$$E_s = R_{fs}.\frac{1}{2}.m_t.(C_h.V^2) \tag{4.1}$$

where,
E_s= impact energy due to steel mass of the trawl board
R_{fs} = reduction factor associated with steel mass
m_t = steel mass of trawl board
C_h = coefficient of effect of span height on impact velocity
V^2 = trawl velocity
The impact energy equation is the simple Kinetic Energy equation as shown in equation 4.2

Palmer and Ling (1981)

$$KE = \frac{1}{2}mv^2 \tag{4.2}$$

The kinetic energy is defined as the work needed to accelerate a body of a given mass from rest to its stated velocity. Having gained this energy during its acceleration, the body maintains this kinetic energy unless its speed changes. The same amount of work is done by the body in decelerating from its current speed to a state of rest. The kinetic energy is directly proportional to the mass that means when the mass increases the kinetic energy increases and when the mass decreases the kinetic energy decreases and also, the kinetic energy is directly proportional to the square of the velocity.
For added mass

$$E_a = R_{fa}.\frac{\alpha.m_p.D}{\beta+1}.\left[\frac{F_b}{\alpha.m_p}\right]^{(\beta+1/\beta)} \tag{4.3}$$

where,
m_p = plastic moment capacity is illustrated in equation 4.4
F_b = impact force is illustration in equation 4.5
R_{fa} = reduction factor associated with added mass
D = steel pipe nominal outside diameter
α, β = calculated using equation 4.6 and 4.7

$$m_p = \frac{1}{4}.f_y.t^2 \tag{4.4}$$

$$F_b = c_b.V.(m_a.k_b)^{0.5} \tag{4.5}$$

$$\alpha = 37\left[ln\frac{D}{t} - \frac{1}{2}\right] \tag{4.6}$$

$$\beta = 0.125\left[ln\frac{D}{t} + \frac{1}{2}\right] \tag{4.7}$$

where,

f_y = specified minimum yield stress

t = pipe wall thickness (tnominal thickness -tcorrosion allowance)

The maximum of Es and Ea is the conservative of kinetic energy absorbed by the local deformation of the coating and the pipe wall.

$$E_{loc} = max(E_s, E_a) \tag{4.8}$$

4.2.1.2 Clump weight

For clump weights, the total absorbed energy is calculated by using equation 4.9

$$E_{loc} = R_{fs}.\frac{1}{2}.(m_t + m_a)V^2 \tag{4.9}$$

where

m_t = Ddry steel mass of the clump weight.

m_a = hydrodynamic added mass including mass of water entrained in the hollow section.

R_{fs} = reduction factor associated with steel mass

V^2 = trawl velocity

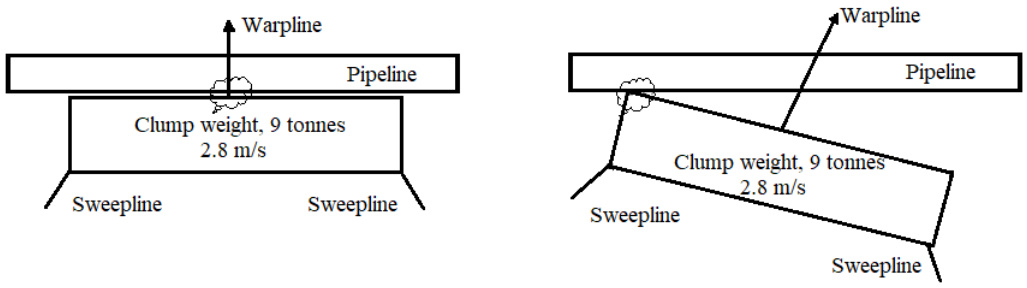

Figure 4.2 Scenerio-1 and senerio-2 (DNV-RP-F111, 2014)

Two impact scenarios are considered for clump weight. The first scenario is the trawl direction is normal to the pipeline as shown in figure 4.2. In this case the clump weight hits the pipeline with its total mass at the center of the clump weight. In second scenario, the corner of the clump weight hits the pipeline with inclined trawl direction as shown in 4.2. In this aspect, the impact energy is reduced compared to scenario 1.

4.2.1.3 Permanent plastic dent depth

The permanent plastic dent depth is calculated by using th eequation 4.10

$$H_{pc} = D\left[\frac{F_{sh}}{m_p.\alpha}\right]^{1/\beta} - \left[\frac{F_{sh}}{m_p.6\times 10^3}.\sqrt{\frac{D^3}{t}}\right] \tag{4.10}$$

H_{pc}= permanent plastic dent depth

$$F_{sh} = m_p.\alpha.\left[\frac{z_{loc}}{m_p.D}.\frac{B+1}{\alpha}\right]^{\beta/(\beta+1)} \tag{4.11}$$

F_{sh} = impact force experienced by the pipe shell

4.2.2 Advanced impact calculation method

The simplified calculation method is conservative. To achieve a more accurate result, the advanced impact calculation method can be applied. The advanced impact calculation method is done by considering the whole system as a spring-mass system (DNV-RP-F111, 2014).

Trawl Equipment

- m_a and m_t the added mass and steel mass of the trawl board
- k_b and k_i are the trawl board out-of-plane and in-plane-stiffness

For trawl board, the hydrodynamic added mass is applied through the out-of-plane stiffness and the steel mass is applied through the in-plane-stiffness. For clump weight, the

hydrodynamic added mass is added directly to the mass of the clump weight that is through the in-plane-stiffness. The total mass for the clump weight is the combination of addeded mass and dry steel mass (m_a and m_t) and k_i is the associated stiffness.

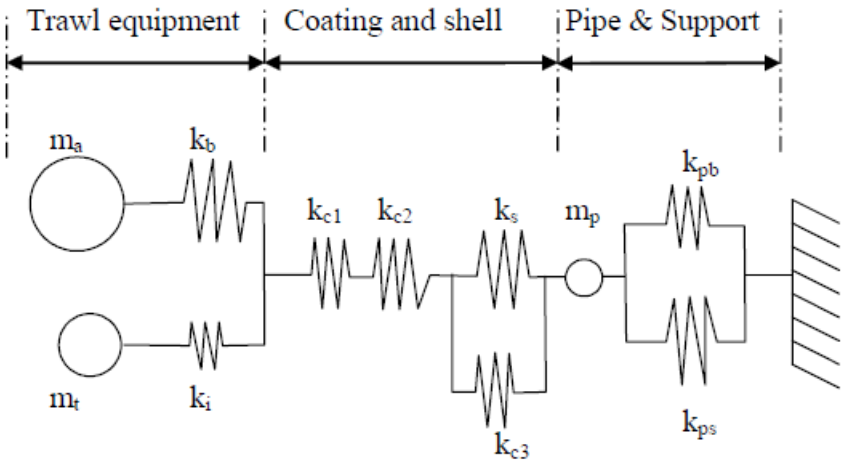

Figure 4.3 Mass-spring system for impact process (DNV-RP-F111, 2014)

Coating and shell

- k_{c1} represents the stiffness of the protective cover for heating cable attached to the pipeline, when applicable
- $k_{c2}$is the stiffness of coating
- k_{c3} represents any possible effect it has on the steel shell stiffness by distributing the impact force over a larger area by shear deformation in the coating
- k_s is the local shell stiffness of the steel pipeline

Pipe and support

- $m_p$is the effective mass of the pipe, including hydrodynamic added mass effects
- k_{pb} is the effective bending stiffness of the pipe
- k_{ps} is the effective soil stiffness acting on the pipe

The local stiffness of a concrete coated pipe may conservatively be approximated by the following relationship between the impact force and the indentation depth of a bare steel

pipe.

$$F_{sh} = m_p.\alpha.\left[\frac{H_t}{D}\right]^{\beta} \tag{4.12}$$

The energy absorbed locally by the steel pipe can be calculated directly from the maximum force obtained from the impact analysis as

$$E_{ab} = \int F_{sh}(H_t)dH_t = \frac{\alpha.m_p.D}{(\beta+1)}.\left[\frac{F_{sh}}{\alpha.m_p}\right]^{(\beta+1)/\beta} \tag{4.13}$$

There are different steps involved in advanced impact calculation method. First step is to perform static analysis and then the force-dent relation of local pipe shell is established. But in this report the force-dent relationship is established using the formula as mentioned in equation4.12. The third step is to perform dynamic analysis, in this analysis the pipe shell performance is included as non-linear spring. Trawl equipment stiffness is included as spring and the soil stiffness is modelled with discrete ground springs both vertical and lateral. Figure 5.1 shows such a model. Finally, the values are plotted between impact force and time to find the maximum impact force. With help of this impact force, the energy absorbed locally by the pipe shell is calculated using the equation 4.13, and also the permanent dent depth is calculated.

4.3 Brief description of pull-over analysis

4.3.1 Trawl board

According to DNV-RP-F111 (2014) it is recommended that a dynamic analysis is carried out to calculate the pull-over response from trawl gear. Pull-over analysis deals with the global response of the pipeline as the trawl gear is pulled or forced to cross over the pipeline. The pull-over load is to be applied as a single point load represented by a force time history.
The pull-over load is divided into horizontal force and vertical force. The maximum horizontal pull-over force is calculated according to the following equation 4.14 and it is denoted by Fp

Trawl boards:

$$F_P = c_F.V(m_t.k_w)_{1/2} \tag{4.14}$$

Where,

k_w = warp line stiffness

V = trawling velocity

m_t= steel mass of board

c_F = empirical coefficient

The empirical coefficient for polyvalent and rectangular boards is calculated by using equation 4.15

$$C_F = 8.0(1 - e^{-0.8\bar{H}}) \tag{4.15}$$

$$\bar{H} = \frac{H_{sp} + (OD/2) + 0.2}{B} \tag{4.16}$$

Where $\bar{H}$ = is a dimensionless height

H_{sp} = span height

OD = pipe outer diameter

B = half the trawl board height

The maximum vertical force for Polyvalent and rectangular boards acting in the downward direction can be estimated by using equation 4.17.

$$F_z = F_p(0.2 + 0.8.e^{-2.5\bar{H}}) \tag{4.17}$$

This downward acting force may be assumed to have the same force-time history as the corresponding horizontal force.

The pull-over duration is an important parameter in trawl boardpipeline impact, as it is usually closely related to the pull-over force. DNV-RP-F111 lists four parameters assumed to govern pull-over duration Trawl velocity, Pipeline induced movement at interaction,

Warp line stiffness and trawl board mass.

The total pull-over time, T_P is calculated by using equation 4.18.

$$T_P = C_T.C_F.\left(\frac{m_t}{k_w}\right)^{1/2} + \frac{\delta p}{V} \tag{4.18}$$

Where,

k_w = warp line stiffness

V = trawling velocity

δp = displacement of the pipe

The displacement of the pipe at the point of interaction is unknown prior to response simulations. Therefore, the value of $\delta p/V$ must be assumed (e.g. as $C_T.C_F.(m_t/k_w)^{1/2}/10$ and may be corrected after response simulations in some sort of iterative approach.

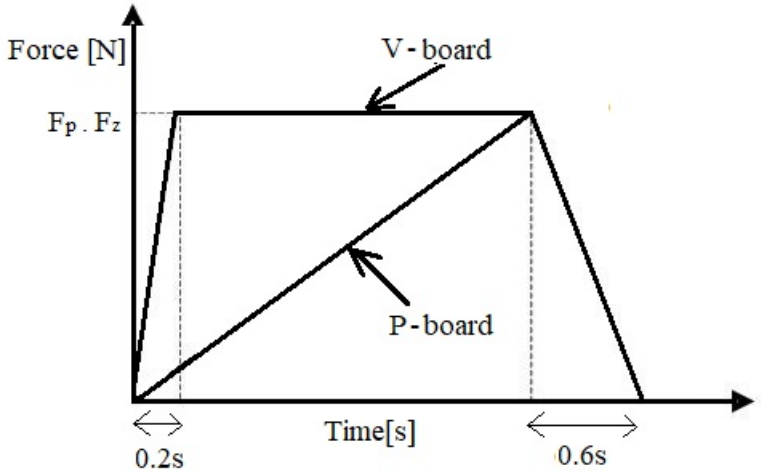

Figure 4.4 Force-time history for otter trawl board pull-over force on pipeline (DNV-RP-F111, 2014)

.

From the figure 4.4 fall time for trawl boards may be taken as 0.6 seconds, unless the total pull-over time given by 4.18. is less than this, in which case the fall time should be equal to the total time but still allowing for some force build-up say 0.1 second.

The coefficient for the trawl boards pull-over duration, C_T is given as

$$C_T = 2.0 \tag{4.19}$$

$$K_w = \frac{3.5 \times 10^7}{L_w} \text{N/m} \tag{4.20}$$

where L_w is the length of the warp line in meters. Typically, the warp line length is 2.5 to 3.5 times the water depth.

Chapter 5

SIMLA Model

5.1 Impact analysis

SIMLA is a nonlinear static and dynamic analysis program developed by MARINTEK. It is a special computer program used for engineering analysis of offshore pipeline during design, installation and operation. The impact model in this thesis is developed by IKM Ocean Design according to "Advanced impact calculation method". The model is developed with help of simla user manual (Svein Sævik et al., 2015). The simulation of the impact process

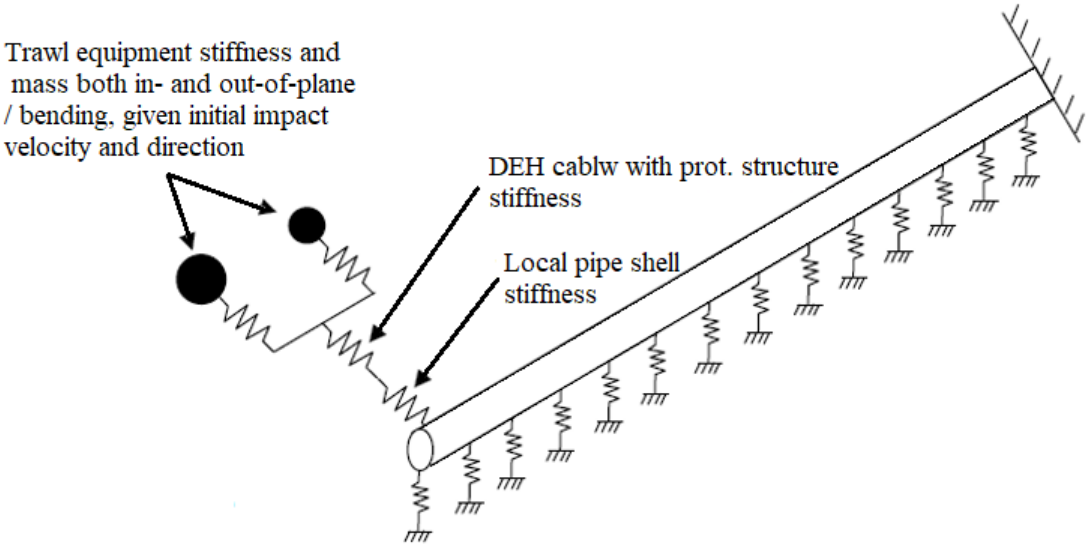

Figure 5.1 Configuration of mass spring with pipeline system (DNV-RP-F111, 2014)

is carried out in different steps. Initially the static analysis should be carried out and then the force dent relationship of the local pipe shell is established by using formula 4.12. Then the dynamic analysis is carried out and the maximum impact energy absorbed by local pipe shell is measured.

5.1.1 Trawl equipment

Trawl Board

The trawl board is considered as a point mass. The different masses are considered for the trawl board, one is dry steel mass and another is hydrodynamic added mass. The dry steel mass of the trawl board is applied through in-plane-stiffness and hydrodynamic added mass through out-of-plane stiffness. These stiffness values are used as per (DNV-RP-F111, 2014). The effect of impact is associated with the in-plane velocity of the steel mass of the board and hydrodynamic added mass acting through flexural stiffness of the board, which generally occur some hundredths of a second later.

Clump weight

For clump weight, the added mass is directly added to the mass of the clump weight and the mass are applied in the in-plane-stiffness. The effect of impact due to clump weight is categorized into two different types, one is the dynamic simulation to calculate input impact energy when the clump weight hits at one corner, which leads to the rotation of the clump weight. The other is the local stiffness of clump weight consider impact at corner and impact at mid-span of the clump weight. The added mass of the clump weight can be calculated according to the methodology in DNV-RP-C205 (2010) and typical mass of entrained water in clump weights are given in DNV-RP-F111 (2014).

5.1.2 Single pipe wall

The pipeline model was created using the parameters as shown in Appendix A, Table A-1. In general, the subsea pipelines laid on the uneven seabed. In this study, the pipeline is assumed

to be laid on the even seabed and no free span is considered. A sufficient length of pipeline should be included to avoid end effects influencing the results. According to DNV-RP-F111 (2014) the length of the pipelines is calculated by using the term 100D, where D is the diameter of the pipeline. Therefore, the length of the pipe is considered as 35.6 m. The base case simulation is performed by using the given input data as shown in Appendix A, Table A-1 and then by changing the different parameter for the pipeline and trawl board, different simulation cases was performed and the results are compared. These parameters included changing the pipe wall thickness, concrete thickness, content density and trawl velocity. The SIMLA model for single pipe wall with trawl equipment is shown in figure 5.2.

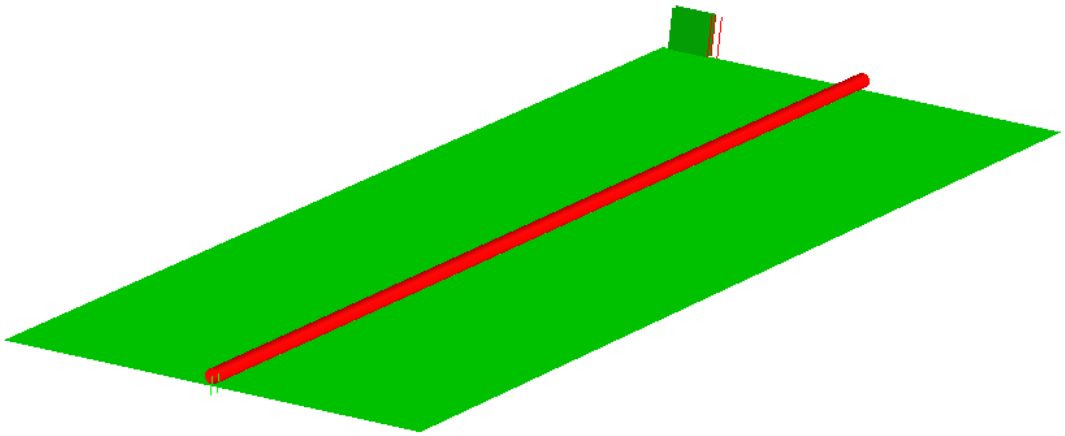

Figure 5.2 SIMLA impact model of single pipe

5.1.3 Pipe-in-pipe

The outer and inner pipe are separated by the centraliser. The centralisers are modelled using 3D spring element which connects inner pipe and carrier pipe. The stiffness is given in the vertical direction of the spring to keep the inner pipe concentric with the carrier pipe (Kristoffersen et al., 2012). The PIP also assumed to be laid on the even seabed and no free span is considered. A sufficient length of pipeline should be included to avoid end effects influencing the results. The length of the pipeline is calculated same as the single pipe and the length of the pipe is 39.4 m. The base case simulation is performed by using the given input data as shown in Appendix-A. The different cases are carried out by considering the position and node gap of the bearing spring and then the results are compared. The SIMLA

model for pipe-in-pipe with trawl equipment is shown in Figure 5.3 and Figure 5.4.

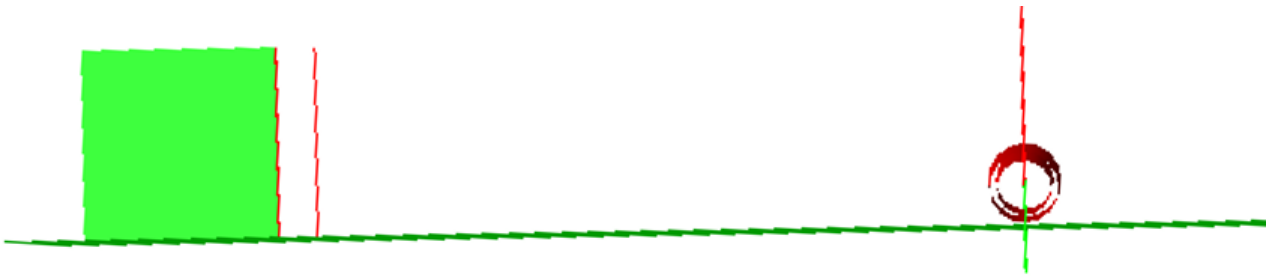

Figure 5.3 SIMLA impact model of a PIP (side view)

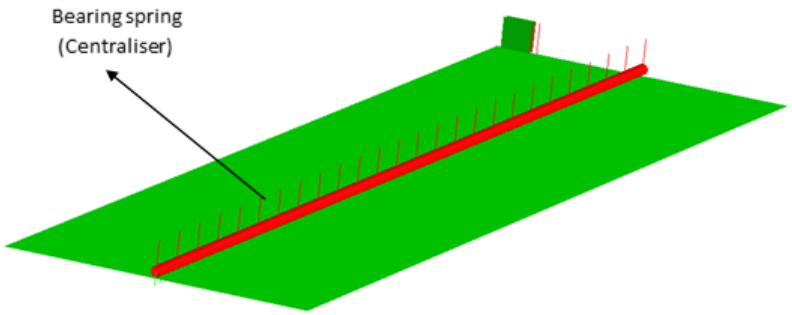

Figure 5.4 SIMLA impact model of a PIP

5.2 Pull-over analysis

Three different models have been established for trawl gear pull-over simulation cases.

- The experimental test model with new contact element to simulate clump weight interference with pipeline. This model was created for verification purposes of new contact element and is referred to as "The new contact clump weight model".
- New contact model to check the warp line tension of trawl board interference with single wall pipeline. This model was created for verification purpose and is referred to as "The new contact trawl board model".
- The trawl board interference with pipe-in-pipe model and is referred as "Free spanning pipe-in-pipe and trawl board model".

5.2.1 The new contact clump weight model

5.2.1.1 Clump weight and pipeline configuration

The trawl gear configuration of the new contact model is the same as in the previous model test performed at MARINTEK in 2004 with a Thyborøn roller clump type. All inputs and the SIMLA model are based on the master thesis written by Maalø (2011) and Johnsen (2012) from NTNU.The model configuration of the clump weight is shown in figure 5.5.

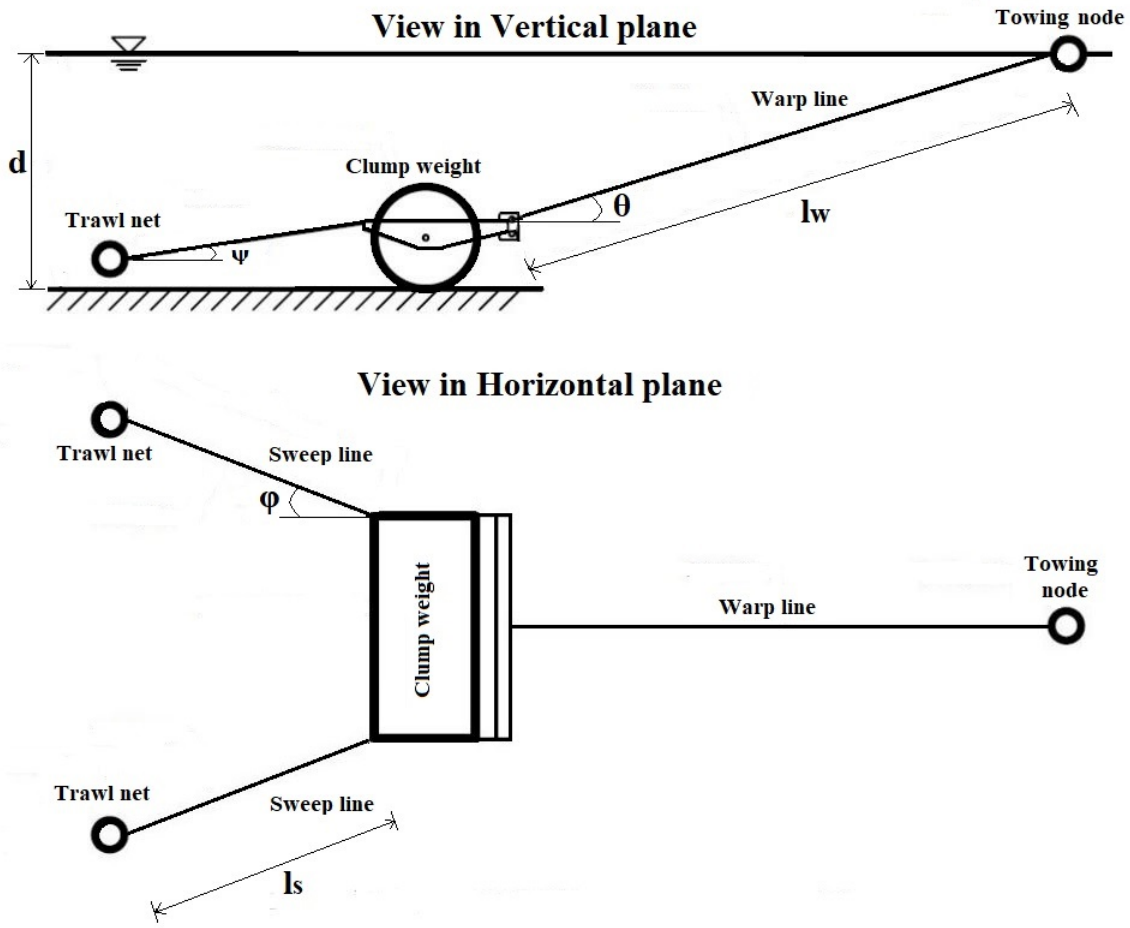

Figure 5.5 Configuration of a clump weight (Johnsen, 2012)

5.2.1.2 Clump Weight

The clump weight model is based on the Thyborøn roller type clump weight used in the previous model test. The SIMLA model is based on the model developed by Maalø (2011)

and Johnsen (2012). Additionally, the clump weight is modelled by using the new contact element (cont153) in SIMLA. The previously used contact element is based on beam to beam interaction and new contact element is based on body-pipe interaction. The new contact element is replaced in the place of previously used contact element to check the behaviour of new contact element. The new contact element is described detailly in trawl board section. The trawling velocity used for the clump weight is 1.95 m/s. Figures 5.6 and 5.7 shows the clump weight model with previous contact element and the new contact element.

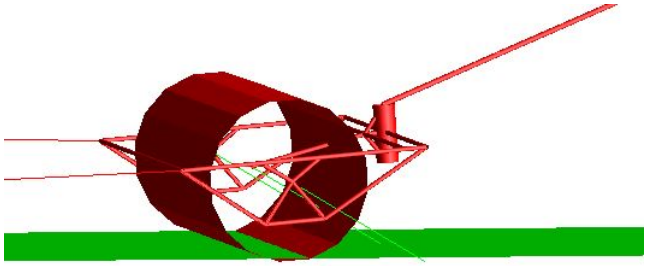

Figure 5.6 Clump weight with old contact element

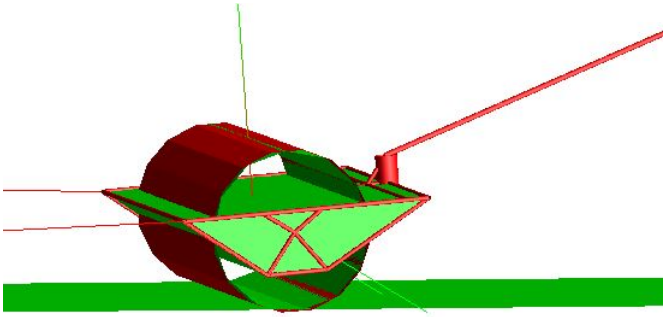

Figure 5.7 Clump weight with new contact element

Table 5.1 Clump weight properties

Quantity	**Symbol**	**Value**	**Unit**
Roller diameter	D_r	0.76	m
Roller length	l_r	1.55	m
Dry weight	m_t	6100	kg
Added mass	m_a	1.0	kg
Submerged mass	m_s	5316	kg

5.2.1.3 Pipeline Model

The new contact model and the pipeline data is similar to the model developed by Ingrid Berg Johnsen. The experimental tests were performed with only a small section of the pipeline. The length of the pipeline is 25m and the diameter is 350 mm. Two different span heights are considered for the simulation (0.50 m and 0.75 m). The pipeline is rigid with fixed end condition.

Table 5.2 350 mm pipeline properties

Quantity	Symbol	Value	Unit
Length of the pipeline model	L	25	m
Pipe diameter	OD	0.35	m
Structural mass of pipe	m_p	405.9	kg/m
Submerged weight of pipe	w_{sp}	307.3	kg/m
Added mass coefficient	C_a	1.0	-
Drag coefficient	C_d	1.0	-

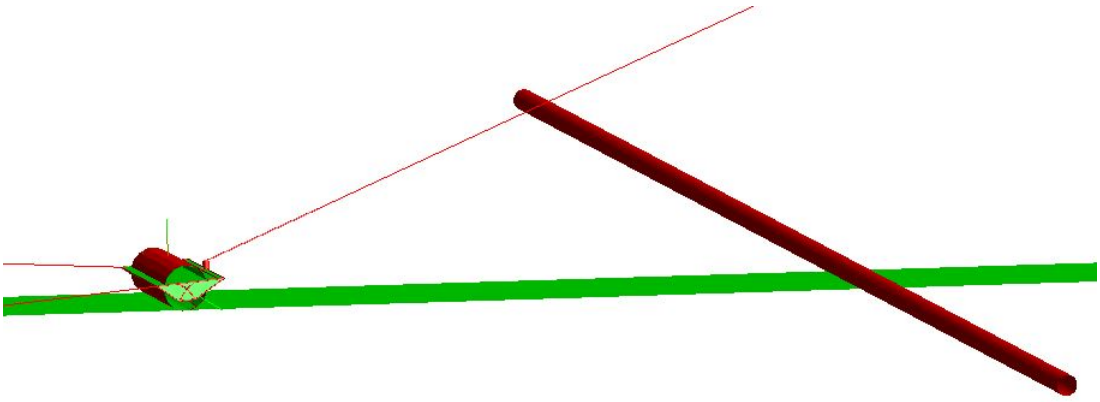

Figure 5.8 SIMLA model of clump weight and pipeline

The simulations are carried out to measure the horizontal pull-over force created by the new contact model and these results are compared with the results of old contact element and the model test results. This study is carried out to ivestigate the behaviour of the new contact element. The pipeline properties of the model are given in the table 5.2.

5.2.2 The new contact trawl board model

5.2.2.1 Trawl board and pipeline configuration

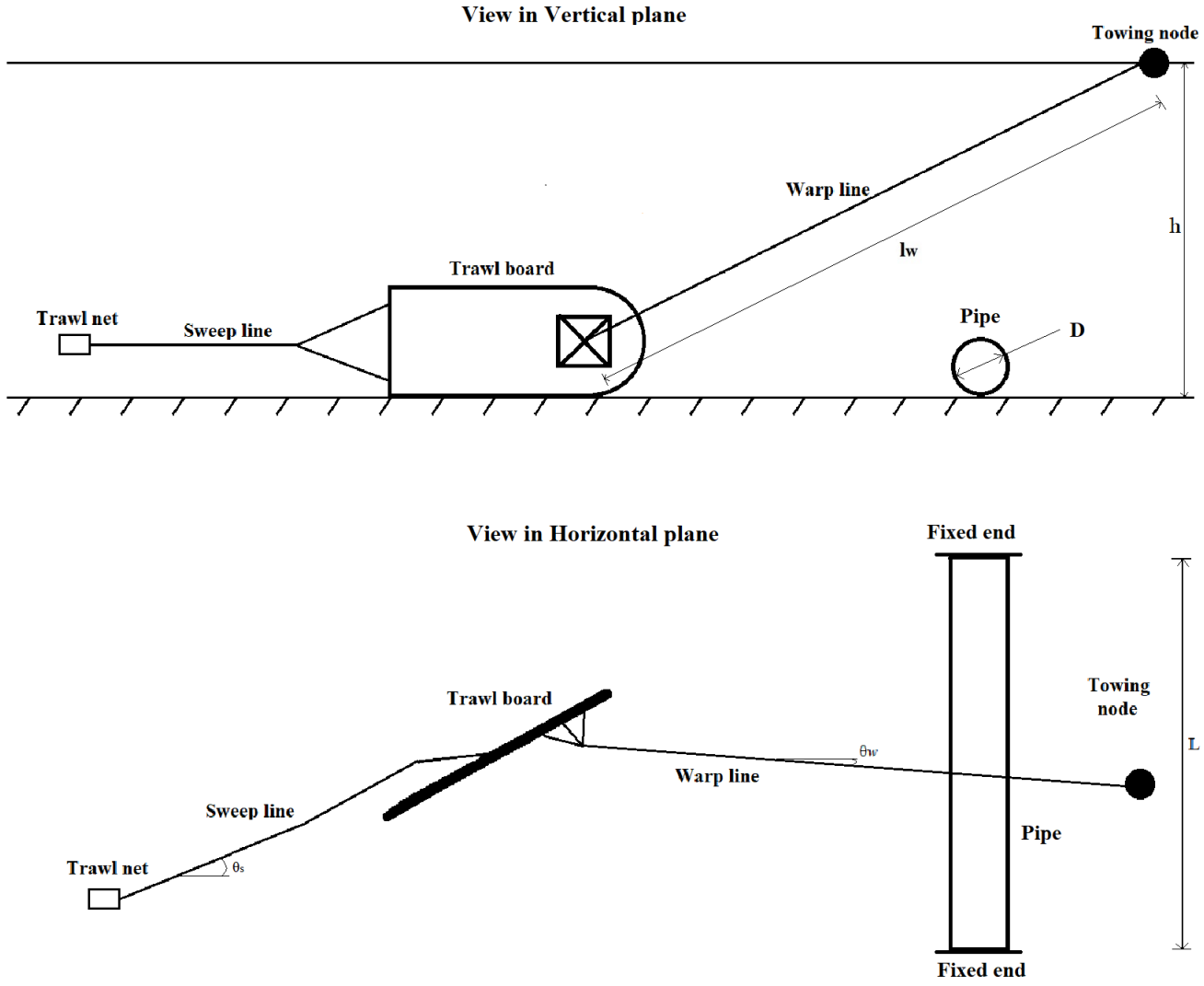

Figure 5.9 Configuration of trawl board model with single wall pipeline

The trawl board and pipeline configuration is shown in figure 5.9. THe trawl board has the trawling velocity 2 m/s. The model description will be discussed in detail in section 5.2.3. The new contact element used in the clum weight model is further developed into simplified trawl board model. In this validation study model, a single wall pipeline is used and the warp line tension is measured during pull-over analysis. The data used in validation study model is based on the experimental model test and the model developed by Wu et al. (2015).

5.2.2.2 Pipeline model

The single wall pipeline developed in the SIMLA model is rigid and fixed on both the ends. The diameter of the pipeline is 0.75 m and a length 1360 m. Figure 5.10 shows the pipeline model where OD represents the diameter of the pipeline and L represents the length. Pipeline data is represented in the Table 5.3.

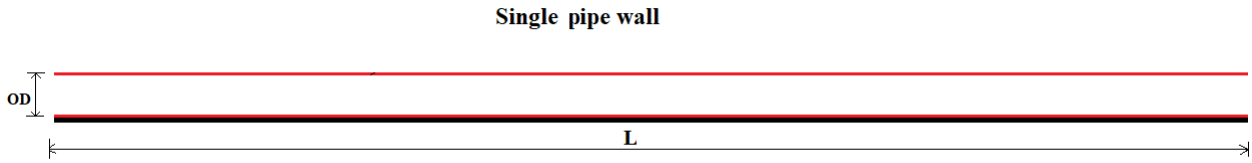

Figure 5.10 Configuration of single pipe wall

Table 5.3 750 mm pipeline properties

Quantity	Symbol	Value	Unit
Length of the pipeline model	L	1360	m
Pipe diameter	OD	750	mm
Pipe wall thickness	t	16	mm
Structural mass	m	289.62	kg/m
Submerged weight	W_s	253.72	kg/m
Added mass coefficient	C_a	1.0	-
Drag coefficient	C_d	1.0	-

The validation study is carried out for three different span heights say 0.5 m, 1.0 m and 5.0 m. The figure 5.11 shows the representation of span height (H_{sp}) of the rigid pipeline. Span height is the gap between the bottom of the pipe to the seabed, where L_s is the span length. Pipeline consists of 841 pipe elements. The element size is 3.0 m at the pipeline ends and it reduces gradually towards the midpoint of the pipeline where the element size is 0.3 m. The pipeline is modelled with empty condition which means that pipeline has no internal pressure or temperature. In this model, the warp line tension is measured and compared with the model test results when trawl board is pulled over the pipeline. Figure 5.12 shows the trawl board pipeline model in SIMLA.

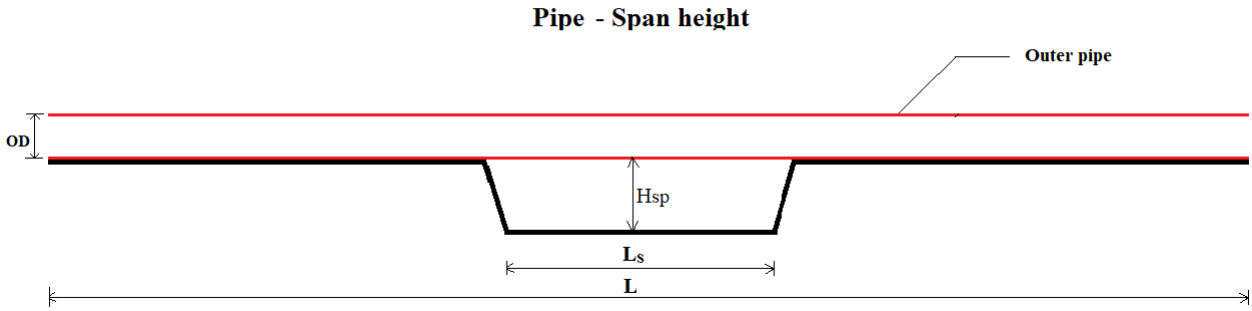

Figure 5.11 Pipeline representing span height

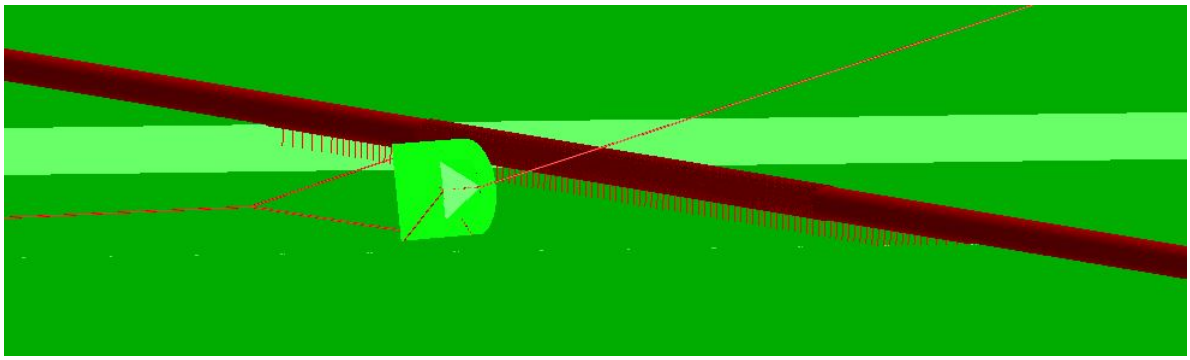

Figure 5.12 SIMLA model for trawl board and single wall pipeline

5.2.3 Free spanning pipe-in-pipe and trawl board model

The trawl gear configuration with pipe-in-pipe model is shown in Figure 5.13. The study was carried out to find the performance of the new contact element interaction with PIP. The configuration was developed in SIMLA for different span height of 0.0 m, 0.5 m, and 1.0 m. The trawl gear configuration consists of a single warp line, the port side trawl board, a single sweep line and the trawl net. To achieve a stable trawl board motion the trawl net and the sweep line were included in the simulation model. The trawl net is represented by a node, which is attached to the end of the sweep line. The water depth was set to 31.2 m. The model properties were illustrated in the Table 5.4.

5.2.3.1 Trawl board model

The trawl board is considered as a rigid body and modelled by using 3-dimensional mesh of geometry elements. This model of trawl board is based on edge-to-beam formulation method

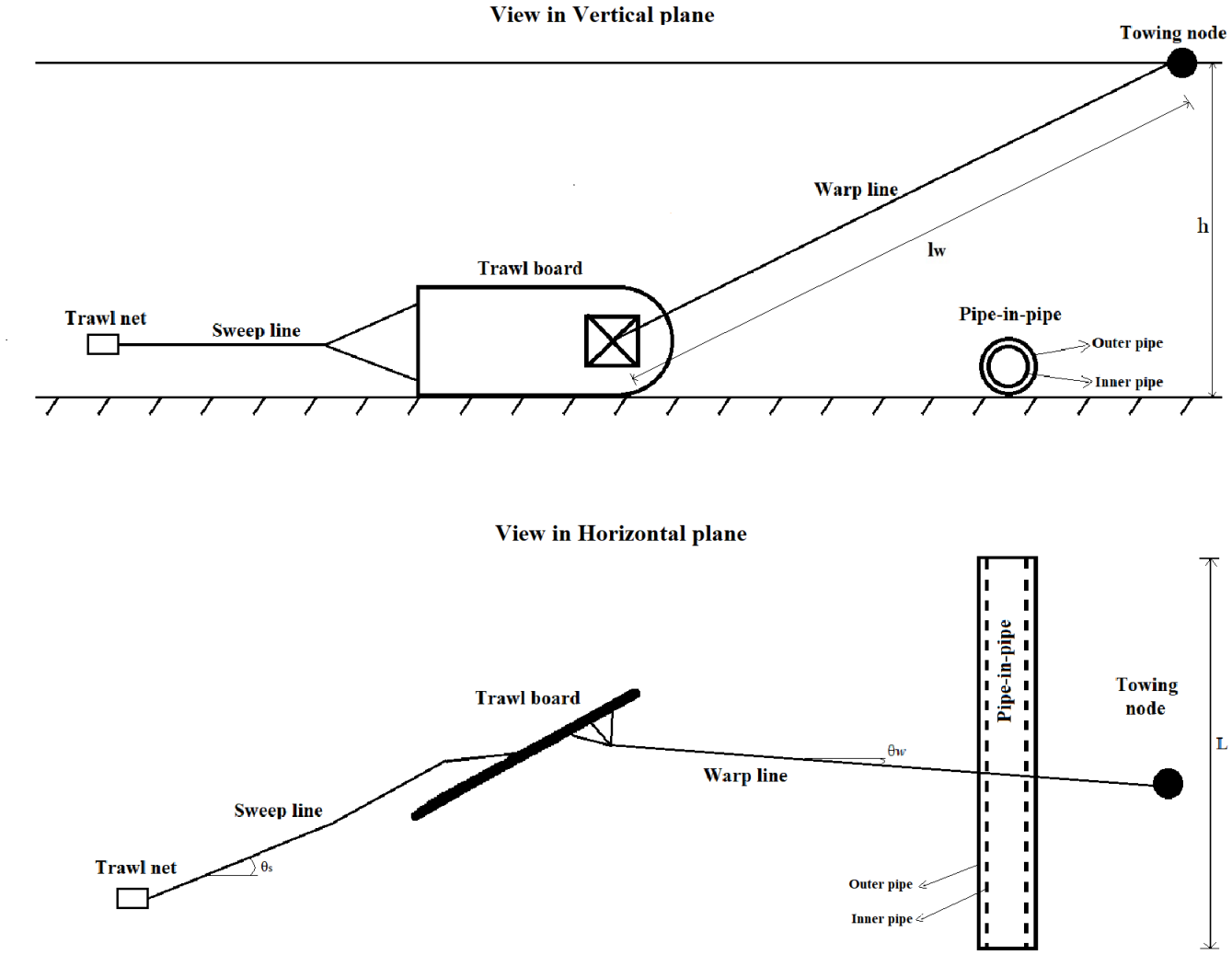

Figure 5.13 Configuration of trawl board PIP model

(cont153), previously it was node-to-surface contact formulation (cont164). This helps to improve the contact search. A single element of the trawl board geometry is shown in the Figure 5.14 and it consists of a triangular plate with thickness 2r surrounded by circular shaped edges and has a radius r with spherical shaped corners. To obtain a smooth surface, r is used along all the elements that develop the object. The full object is developed by defining nodes and coordinates of the nodes and connecting them in a sequential order. The trawl board considered in the model consists of steel mass 2600 kg, height of 2.2 m and a length of 4.0 m. The warp line and sweep line are connected in the trawl as shown in figure

Table 5.4 Model properties

Quantity	Symbol	Value	Unit
Water depth	d	31.2	m
Water density	ρ	1000	kg/m^3
Warp line stiffness		28	kN/m
Warp line angle	σ_w	18.3	deg
Sweep line angle	σ_s	30.0	deg
Trawl net resistance		40	kN
Trawling velocity	V	2.0	m/s

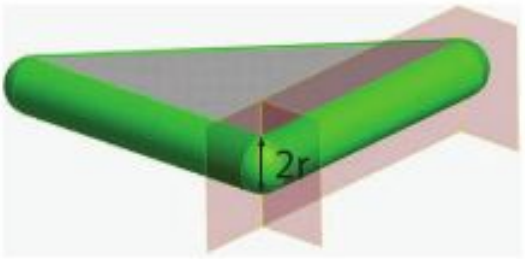

Figure 5.14 Body geometry element

5.15. The figure represents the model of the trawl board in SIMLA. Table 5.5 illustrates the properties of the trawl board.

Table 5.5 Trawl board properties

Quantity	Value	Unit
Height	2.2	m
Length	4	m
Mass	2600	kg
C. O. G. x-coordinate	-0.2	m
C. O. G. z-coordinate	-0.11	m
Roll mass moment of inertia	1885	kgm^2
Pitch mass moment of inertia	5245	kgm^2
Yaw mass moment of inertia	3358	kgm^2

Warp Line: The warp line connects the trawl board and towing vessel. The lower end of the warp line is connected to the trawl board and top end is connected to a towing node. The axial stiffness of the warp line is according to the experimental tests 28 kN/m. The warp line is modelled with 300 linear pipe elements.

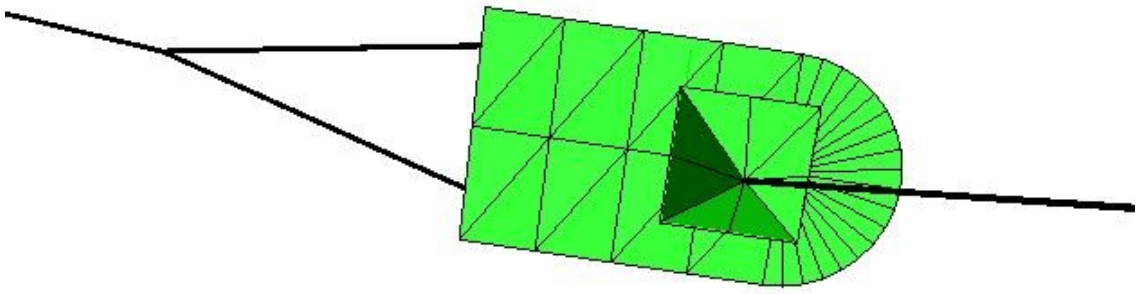

Figure 5.15 Trawl board model in SIMLA

Sweep lines: There are two short sweep lines that merged together and connected to a longer sweep line. The sweep lines are also modelled with linear pipe element.

5.2.3.2 Pipe-in-pipe model

The whole PIP was modeled together including both carrier pipe and inner pipe, centralizers and bulkheads. The bulkheads were used only at the pipe ends. The centralizers are modelled using a 3D spring element which connects the inner pipe and carrier pipe. The stiffness is given in the vertical direction of the spring to keep the inner pipe concentric with the carrier pipe all the time. The bulkheads are modelled at both ends of PIP by using a spring similar to the one used for centraliser and the stiffness is given in the axial direction. The configuration of PIP is shown in figure 5.16.

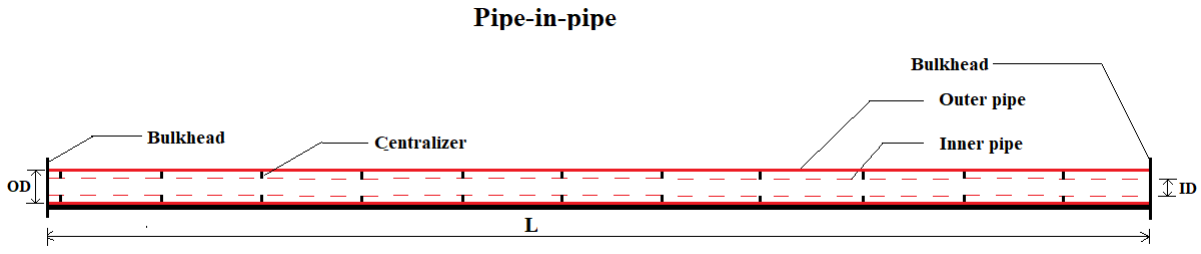

Figure 5.16 Configuration of PIP

The pipeline has a total length of 1120 m for both carrier pipe and outer pipe The carrier

pipe of the PIP has diameter 0.32 m and thickness 0.012 m with pressure of 1 bar and a temperature of 10^0c. The inner pipe has diameter 0.21 m and thickness 0.014 m with pressure of 300 bar and a temperature of 110^0c. The both the carrier pipe and inner pipe are just relatively flexible, but they are still rigid pipes. The PIP was modelled using 900 pipe elements. An element size of 4m was used at the outer edge of the model and it gradually reduces toward the middle with 0.25 m.

Table 5.6 PIP properties

Quantity	**Symbol**	**Value**	**Unit**
Pipe length	L	1120	m
Pipe span height	H_{sp}	0-1	m
Pipe span length	L_{sp}	25,50	m
	Outer pipe		
Outer pipe diameter	OD	0.32	m
Outer pipe thickness	t_o	0.012	m
Structural mass	m	79	kg/m
Submerged weight	w_s	68	kg/m
Pressure	P_o	1	bar
Temperature	T_o	10	^0c
	Inner pipe		
Inner pipe diameter	ID	0.21	m
Inner pipe thickness	t_i	0.014	m
Structural mass	m	86	kg/m
Submerged weight	w_s	86	kg/m
Pressure	P_i	300	bar
Temperature	T_i	110	^{0} C

The centralisers are placed at 2 m interval. At the midpoint of the modelled pipeline, a free span is included, see Figure 5.17. The length of the free span is measured in the direction of the pipeline Simulations were executed for four different span heights, 0.0 m, 0.5 m, and 1.0 m and respective span lengths are, no span, 25 m, 50 m . The span height H_{sp} is measured as a gap between bottom end of the pipeline to seabed.

The height is measured after applying static loads. Span height was varied by adjusting the seabed depth. The trawl gear configuration was kept at a constant depth in all simulations. The model properties of PIP are shown in Table 5.6.

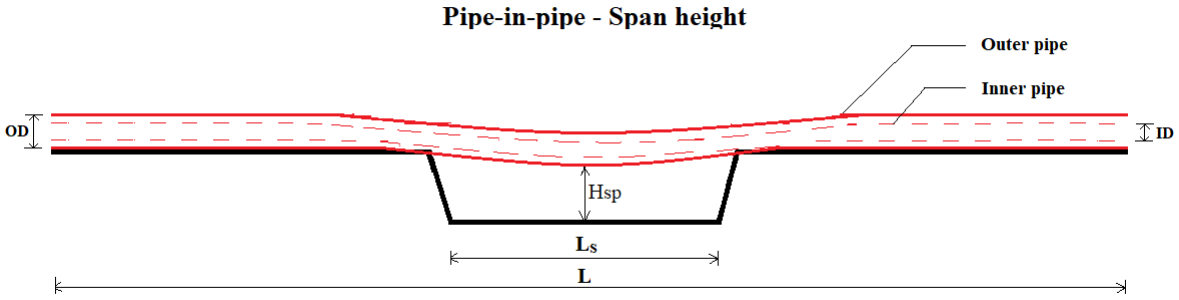

Figure 5.17 Flexible PIP representing span height

5.2.3.3 Seabed interaction

In this section, the trawl board and pipeline seabed interaction is described. The flat seabed is modelled along the entire length of the pipeline and the path of trawl board. In SIMLA, seabed interaction is modelled using special purpose seabed contact elements. The theory manual helps to choose the contact element and other parameters [8]. A contact surface representing the seabed is created between lines or routes along the seabed interaction is represented by applying springs at each node for the pipe segment in contact. Figure 5.18 shows the pipeline seabed interaction. For fee span pipeline model, the contact element for

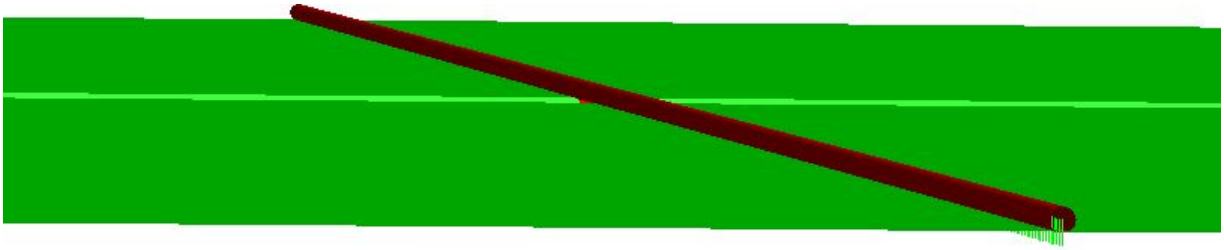

Figure 5.18 SIMLA model representing pipeline seabed interaction

seabed is included in all the pipeline nodes. The free span is modelled by lowering the seabed to the specific span length on each side, from the midpoint of the pipeline. Friction can be applied in axial and lateral direction, with interaction curves defining the unit friction force per meter displacement. The bottom of the trawl board has pipe element along its length. This pipe element has 5 nodes and are developed for the seabed contact. With this contact element configuration, it is possible for the trawl board to lay flat on the seabed. The contact forces between seabed and trawl board are is given in vertical direction. The soil stiffness

should be given such that the trawl board should not have large penetration. Figure 5.19 shows the SIMLA model for trawl board seabed interaction. In a real situation, the seabed will not be completely flat and the trawl board will thus bounce up and down during the trawling process.

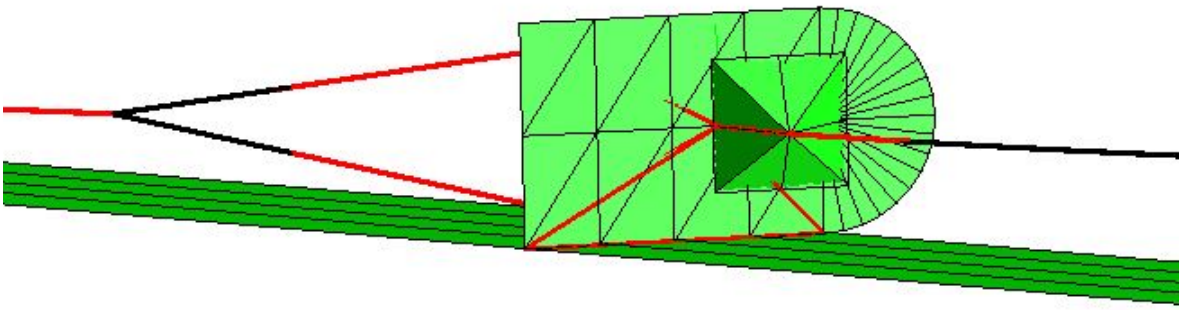

Figure 5.19 SIMLA mode representing trawl board seabed interaction

5.2.3.4 Warp line pipeline contact

The warp line interaction with pipeline was modelled using smaller circumferential master roller and it defines the outer shell of the pipeline as shown in Figure 5.21. The warp line was modelled with a single linear pipe element. The warp line with pipeline interaction is illustrated in the figure 5.20.

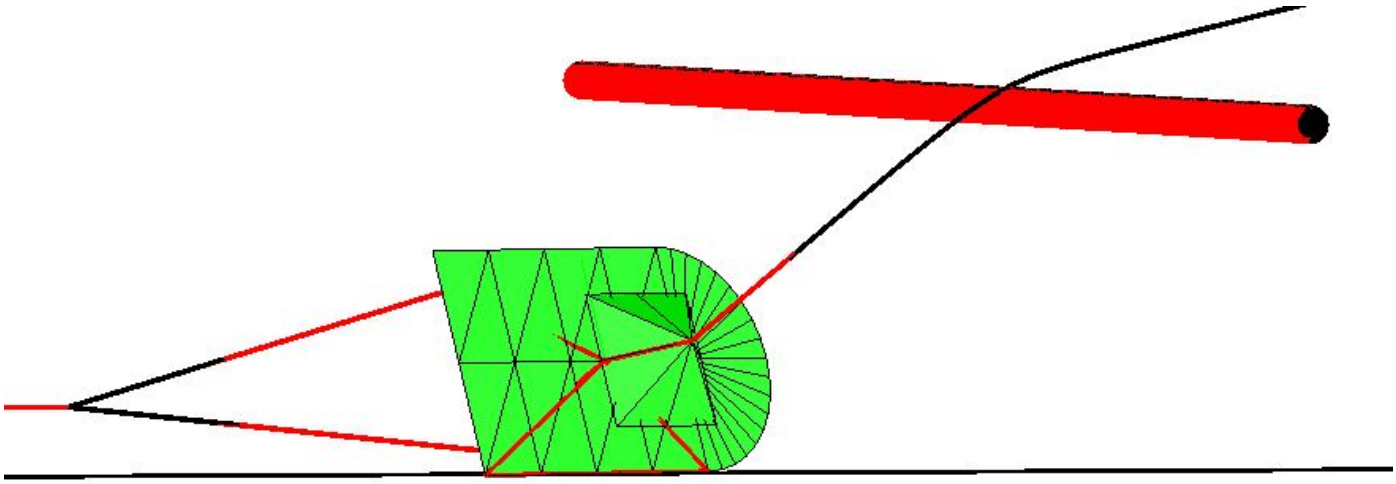

Figure 5.20 SIMLA model representing warp line interaction with pipeline

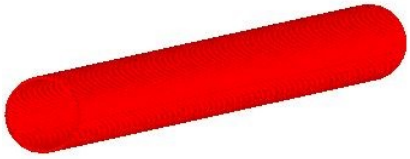

Figure 5.21 SIMLA model for roller contact elements

Chapter 6

Analysis Result

6.1 Comparison of simplified impact calculation and advance impact calculation

The calculation for simplified calculation method and the advanced impact calculation method is shown in Appendix-B. Table 6.1 shows the comparison of maximum impact force, the absorb energy and the permanent dent depth between simplified calculation and advanced impact calculation. The comparison case is considered according to example in (DNV-RP-F111, 2014) . The simplified case results are conservative, so advance impact

Table 6.1 Comparison of simplified calculation and advance impact calculation

Quantity	**unit**	**Simplified calculation**	**Advanced impact calculation**
Maximum impact force	kN	646.61	342.06
Absorbed energy	kJ	5.4	3.05
Permanent dent depth	mm	13.1	8.13

calculation is carried out to obtained accurate results. The below section contains the advanced impact calculation for different cases in single pipe wall and pipe-in-pipe

6.2 Advanced impact calculation for single pipe wall

This section presents the results of the cases for the single pipe wall pipe. The RP example is considered as the base case. For all the simulation cases the maximum impact force, the absorb energy and the permanent dent depth for each case are estimated and the results for each group is presented and discussed in detail. There are total five tasks carried out in the section, advanced impact calculation in single pipe wall. The first task cases are carried out based on different concrete coating thickness and the second task is based on different content density. These two tasks are based on how the mass influences the impact response. The third task is carried out with different specified minimum yield stress of the pipeline to check how the stiffness of the pipe shell influences the impact response. The fourth task the impact response is based on the combination both mass and stiffness of the pipe, for this task the thickness of the pipe wall is changed and then the simulations are carried out. The final task is based on different trawl types like comparing the results with same trawl type with different velocity and with different trawl board with same mass and same velocity All the simulations are carried out using the software SIMLA and the results are plotted for each of the above-mentioned task.

Table 6.2 Key parameters of cases with different coating thickness

Quantity	Unit	Case 1	Case 2	Case 3
Inner diameter of the pipe	mm	324	324	324
Pipe wall thickness	mm	16	16	16
Outer diameter of the pipe	mm	356	356	356
Concrete coating thickness	mm	40	20	60
Content density	kg/m^3	800	800	800
SMYS	N/mm^2	450	450	450
Trawl gear type	-	Polyvalent TB	Polyvalent TB	Polyvalent TB
Trawl board mass	kg	5000	5000	5000
Trawl velocity	m/s	2.6	2.6	2.6

6.2.1 Influence of coating thickness

Table 6.2 shows the key design parameters of different coating thickness and the remaining parameters are shown in appendix-a,table A-1. The comparison of impact force as a function of time obtained from finite element (FE) analysis is shown below in figure 6.1. Three different cases are carried out for the comparison of different concrete coating thickness. The case 1 is considered as a base case according to the DNV-RP-F111. This section is carried out to differentiate, how the concrete coating thickness of the pipe influence the impact response. Table 6.3 shows the results of maximum impact force, absorbed energy and the permanent dent depth for all the three cases. The maximum impact force is measured from figure 6.1, with help of the maximum impact force the absorbed energy and the permanent dent depth are calculated using the equation 4.13 and 4.10. Figure 6.2 shows the comparison of maximum impact force for different concrete coating thickness.

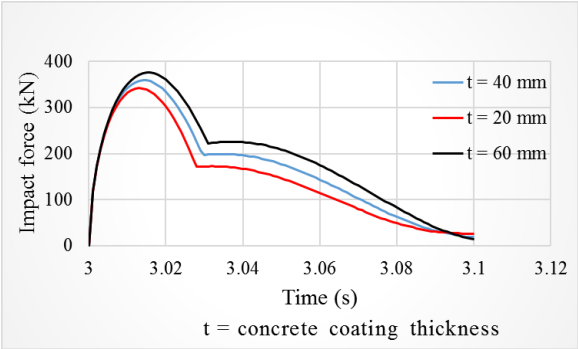

Figure 6.1 Comparison of impact force vs time for different coating thickness

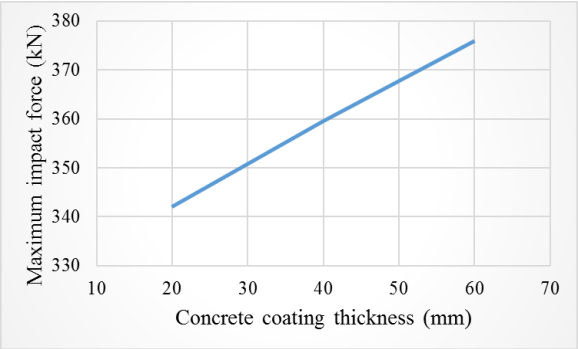

Figure 6.2 Maximum impact force vs concrete coating thickness

The change in thickness of concrete coating results in the change of dry mass and submerged mass of the pipeline. As the thickness of concrete coating increases the mass of the pipeline also increases. The increase in mass results in the increase of accelerating time period of the trawl board crossing the pipeline. So, the pipe absorbs more energy compared to pipe containing low concrete thickness or low mass.

From table 6.3, case 2 with concrete thickness 20 mm have low absorbed energy and low permeant dent depth when compared to case 1 and case 3. Whereas for case 3 with thickness 60 mm the absorbed energy and low permeant dent depth values are high.

Table 6.3 Results for different coating thickness

Quantity	Unit	Case 1	Case 2	Case 3
Coating thickness	mm	40	20	60
Maximum impact force	kN	359.556	342.06	375.85
Absorbed energy	kJ	3.51	3.05	3.99
Permanent dent depth	mm	9.17	8.13	10.20

6.2.2 Influence of content density

Table 6.4 Key parameters of cases with different content density

Quantity	Unit	Case 1	Case 2	Case 3
Inner diameter of the pipe	mm	324	324	324
Pipe wall thickness	mm	16	16	16
Outer diameter of the pipe	mm	356	356	356
Concrete coating thickness	mm	40	20	60
Content density	kg/m^3	800	500	1026
SMYS	N/mm^2	450	450	450
Trawl gear type	-	Polyvalent TB	Polyvalent TB	Polyvalent TB
Trawl board mass	kg	5000	5000	5000
Trawl velocity	m/s	2.6	2.6	2.6

Table 6.4 shows the key design parameters of different content density and the remaining parameters are shown in appendix-a, table A-1. The comparison of impact force as a function of time obtained from FE analysis is shown below in figure 6.3. The comparison in this section is based on three different content density. Here also, Case 1 is considered as a base case according to DNV-RP-F111 . This task is carried out to check the influence of impact response of the pipeline for different content density. The maximum impact force is obtained from the Figure 6.3 and with this maximum impact force the absorbed energy and the permanent dent depth for all the three cases are calculated using the equation 4.13 and 4.10 . The results are tabulated as shown in table 6.5

The change in content density results in the change of dry mass and submerged mass of the pipeline. As the thickness of content density increases, the mass of the pipeline also increases.

The increase in mass results in the increase of accelerating time period of the trawl board crossing the pipeline. So, the pipe absorbs more energy compared to pipe containing low concrete thickness. The mass of the pipe is the factor which influences the impact response.

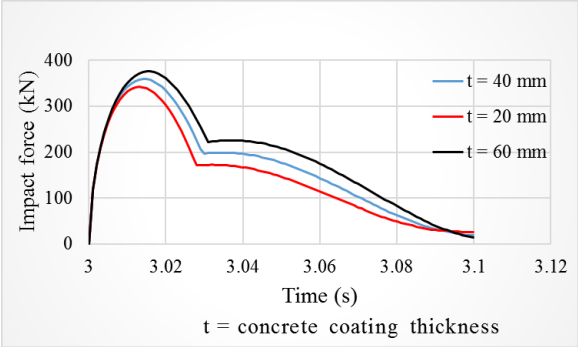

Figure 6.3 Comparison of impact force vs time for different content density

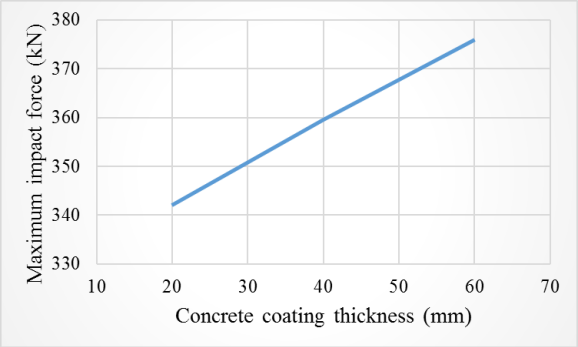

Figure 6.4 Maximum impact force vs content density

Table 6.5 Results for different content density

Quantity	Unit	Case 1	Case 2	Case 3
Content density	kg/m^3	800	500	1026
Maximum impact force	kN	359.55	355.06	362.85
Absorbed energy	kJ	3.51	3.42	3.59
Permanent dent depth	mm	9.17	8.95	9.33

6.5 shows that the maximum impact force, the absorbed energy and the permeant dent depth are low for case2 with content density 500 kg/m^3 and increases gradually for density 800 kg/m^3 and then for density 1026 kg/m^3.

6.2.3 Influence of specified minimum yield stress

Table 6.6 shows the key design parameters of different specified minimum yield thickness (SMYS) and the remaining parameters are shown in appendix-a, table A-1. The comparison of impact force as a function of time obtained from FE analysis is shown below in figure 6.5. The comparison in this section is based on three different SMYS. Here also Case 1 is considered as a base case according to DNV-RP-F111 (2014). The influence of impact

Table 6.6 Key parameters of cases with different SMYS

Quantity	Unit	Case 1	Case 2	Case 3
Inner diameter of the pipe	mm	324	324	324
Pipe wall thickness	mm	16	16	16
Outer diameter of the pipe	mm	356	356	356
Concrete coating thickness	mm	40	20	60
Content density	kg/m^3	800	500	1026
SMYS	N/mm^2	450	350	550
Trawl gear type	-	Polyvalent TB	Polyvalent TB	Polyvalent TB
Trawl board mass	kg	5000	5000	5000
Trawl velocity	m/s	2.6	2.6	2.6

response of the pipeline for different SMYS is measured in this task. This section is carried out to differentiate, how the SMYS of the pipe influence the impact response.

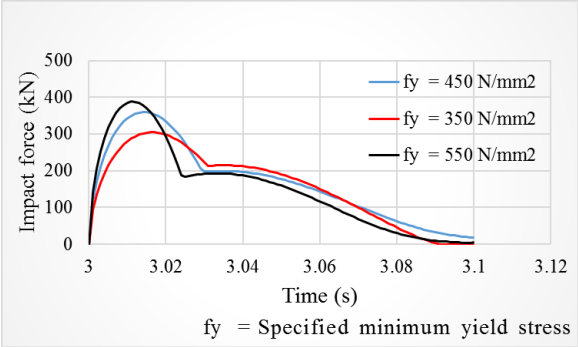

Figure 6.5 Comparison of impact force vs time for different SYMS

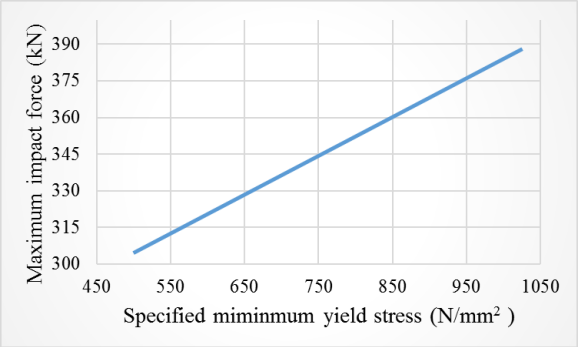

Figure 6.6 Maximum impact force vs SYMS

The stiffness of the pipeline changes according to SMYS. The spring is used in the design to show the pipe shell stiffness. The stiffness is calculated by using force-dent relation as shown in figure 6.7. The change in SYMS changes the stiffness of pipeline. If the stiffness of the pipe shell is increased, the resistance capacity for the deformation will be increased and the accelerating time period of the trawl board crossing the pipeline also increased. So, the pipe absorbs more energy compared to pipe containing low SMYS, also the absorbed energy and permeant dent depth will be low. The stiffness of the pipe shell is the important factor in this task which influence the impact response. The maximum impact force is obtained from

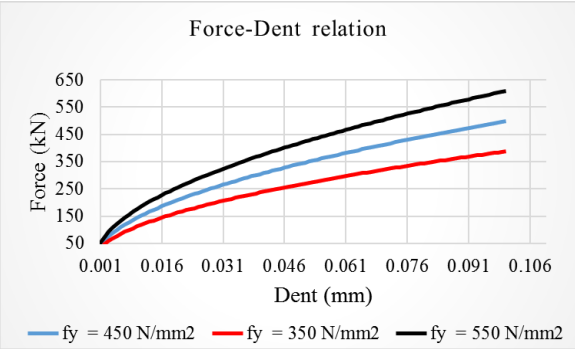

Figure 6.7 Force dent relation

the figure6.2 and with this maximum impact force the absorbed energy and the permanent dent depth for all the three cases are calculated using the equation 4.13 and 4.10 and the results are tabulated as shown in table 6.7 From the above table, the maximum impact force

Table 6.7 Results for different SYMS

Quantity	**Unit**	**Case 1**	**Case 2**	**Case 3**
SYMS	N/mm^2	450	350	550
Maximum impact force	kN	359.55	304.6	388.2
Absorbed energy	kJ	3.51	3.6	3.0
Permanent dent depth	mm	9.17	11.2	6.8

is higher for the case 3 with SMYS 550 N/mm^2 compared to case 2 with SMYS 350 N/mm^2 . The absorbed energy is low for case 3 when compared to case 1 and case 2.

6.2.4 Influence of pipe wall thickness

Table 6.8 shows the key design parameters of different pipe wall thickness and the remaining parameters are shown in appendix-a, table A-1. The comparison of impact force as a function of time obtained from FE analysis is shown in figure 6.8. The comparison is made between different pipe wall thickness, case 1 is considered as per DNV-RP-F111 (2014). And the parameters are changed only for the thickness of the pipe wall as in table **??** and the simulation are carried out. This task is carried out to check the influence of impact response of the pipeline for different content density.

Table 6.8 Key parameters of cases with different pipe wall thickness

Quantity	Unit	Case 1	Case 2	Case 3
Inner diameter of the pipe	mm	324	324	324
Pipe wall thickness	mm	16	14	18
Outer diameter of the pipe	mm	356	352	360
Concrete coating thickness	mm	40	40	40
Content density	kg/m^3	800	800	800
SMYS	N/mm^2	450	350	550
Trawl gear type	-	Polyvalent TB	Polyvalent TB	Polyvalent TB
Trawl board mass	kg	5000	5000	5000
Trawl velocity	m/s	2.6	2.6	2.6

The change in wall thickness of the pipeline results in the change of dry mass and submerged mass of the pipeline. The stiffness of the pipe is also influenced by the change in wall thickness of the pipe. In this simulation cases, the mass and the stiffness of the pipe shell is the important factor which influence the impact response.

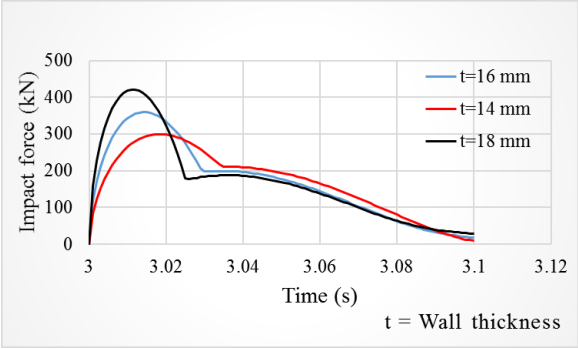

Figure 6.8 Comparison of impact force vs different pipe wall thickness

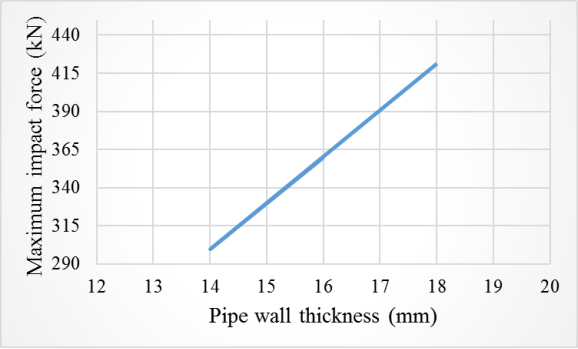

Figure 6.9 Maximum impact force vs pipe wall thickness

As the thickness of pipe wall increases the mass of the pipeline also increases. The increase in mass results in the increase of accelerating time period of the trawl board crossing the pipeline. So, the pipe absorbs more energy compared to pipe containing low wall thickness. The stiffness of the pipe shell is increased when the wall thickness of the pipe is increased. If the stiffness of the pipe increases it absorb more impact force and the dent formation will be low, due to high resisting force. The maximum impact energy absorbed from FE analysis

as shown in figure 6.8 is used to calculated the absorb energy and the permanent dent depth between three different cases by using the equation 4.13 and 4.10 defined in chapter 3 and the results are plotted as shown in table 6.9. The pipe wall with higher thickness 18 mm

Table 6.9 Results for different pipe wall thickness

Quantity	**Unit**	**Case 1**	**Case 2**	**Case 3**
pipe wall thickness	mm	16	14	18
Maximum impact force	kN	359.55	299.71	421.19
Absorbed energy	kJ	3.51	3.81	3.27
Permanent dent depth	mm	9.17	11.2	6.8

absorbs maximum impact force when compared to the remaining cases with thickness 16 mm and 14mm. The absorbed energy and the permeant dent depth for case 1 and case 2 is higher when compared with case 3 which is smaller with high wall thickness.

6.2.5 Influence of trawl gear

Table 6.10 Key parameters of cases with different trawl gear

Quantity	**Unit**	**Case 1**	**Case 2**	**Case 3**	**Case 4**
Inner diameter of the pipe	mm	324	324	324	324
Pipe wall thickness	mm	14	14	14	14
Outer diameter of the pipe	mm	360	360	360	360
Concrete coating thickness	mm	40	40	40	40
Content density	kg/m^3	800	800	800	800
SMYS	N/mm^2	450	450	450	450
Trawl gear type	-	Polyvalent TB	Clump weight	Polyvalent TB	Polyvalent TB
Trawl board mass	kg	6500	6500	5000	6500
Trawl velocity	m/s	1.7	1.7	1.7	2.6

Table 6.10 shows the key design parameters of cases with different trawl gear and the remaining parameters are shown in appendix-a,table A-1. In this task three different comparison are made for the impact response.

- The first comparison is between different trawl type with same mass and same velocity, that is with case 1 and case 2.
- The second comparison is between same trawl type with different mass and same velocity, that is with case 1 and case 3.
- The third comparison is between same trawl type with same mass and different velocity, that is with case 1 and case 3.

The comparison of impact force as a function of time obtained from FE analysis is shown below in figure 6.10, 6.11 and 6.12. The maximum impact energy absorbed from FE analysis is used to calculated the absorb energy and the permanent dent depth between three different cases by using the equation 4.13 and 4.10 defined in chapter 3. and the results are plotted as shown in table 6.11.

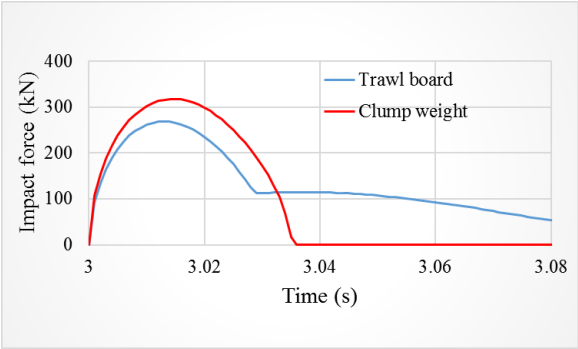

Figure 6.10 Comparison of impact force vs time, different type of trawl gear

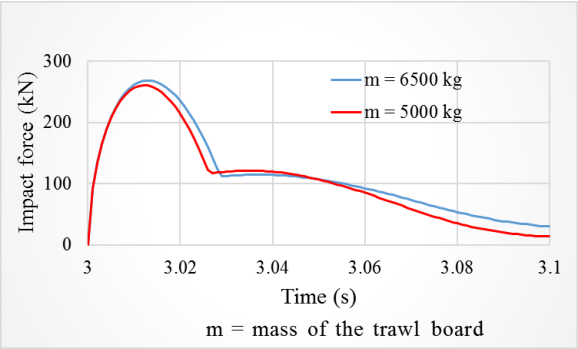

Figure 6.11 Maximum impact force vs time for, different mass of trawl board

Figure 6.10 shows the comparison different trawl gear type with same parameter. The simulation is carried out with two different types of trawl gear one is with polyvalent trawl board and the other is with clump weigh and the results are compared. The maximum impact energy observed from case 2 clump weight is higher than the case 1 trawl board, this is because the they have different configuration. The entire weight of the clump weight acts on the pipeline when it hits but for trawl board, one edge of the trawl board only hits the pipeline and the entire weight doesn't act on the pipeline. For trawl board the steel mass and added mass of the trawl board should be considered separately, but for clump weight the added mass is included with the steel mass of the clump weight.

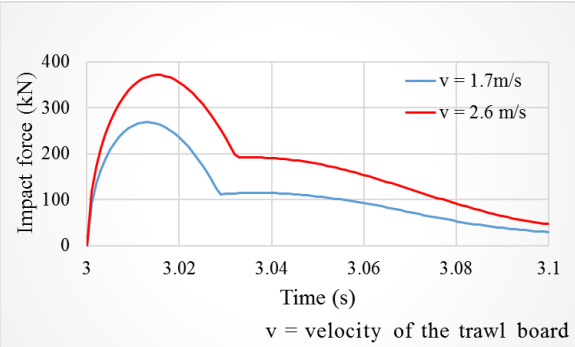

Figure 6.12 Comparison of impact force vs time for different trawling velocity

6.11 shows the comparison of trawl board with different mass. The maximum impact force is higher for case 1 with mass of 6500 kg when compared to case 3 with 5000 kg. This is because when the mass is larger it creates more energy on the pipeline when it hits on it. 6.12 shows the comparison of trawl board with different velocity. The maximum impact force is higher for case 4 with velocity 2.6 m/s when compared to case 1 with velocity 1.7 m/s. The velocity of the trawl board is increases the acceleration speed also increases. When the trawl gear hits the pipeline with higher velocity, the acceleration will be quicker and the time period it stays will be shorter. In shorter period, the pipeline absorbs the maximum impact force. Due to higher velocity, the dent depth and the absorbed energy also higher. 6.9.

Table 6.11 Results for different trawl gear parameters

Quantity	Unit	Case 1	Case 2	Case 3	Case 4
Maximum impact force	kN	268.7	317.7	260.8	371.1
Absorbed energy	kJ	1.5	2.5	1.4	3.8
Permanent dent depth	mm	4.4	6.8	4.0	9.9

6.3 Advance impact calculation in pipe-in-pipe

The Pipeline dimensions and material are considered as mentioned in table A-2 in appendix-a. The simulations for different cases are carried out using computer software SIMLA and the corresponding results are tabulated. The maximum impact force, the absorb energy and

the permanent dent depth are calculated using the equation 4.13 and 4.10 and the result are tabulated.

The simulation cases are carried out based on the interval gap of the centraliser. In SIMLA the centraliser is designed as a bearing spring and the pipeline is divided into several nodes. The bearing springs are placed in these nodal points on certain interval gap, by considering this aspect four different cases are simulated with one extreme case with centraliser at each node.

- Case 1 = The nodal interval between the bearing spring is 8
- Case 2 = The nodal interval between the bearing spring is 6
- Case 3 = The nodal interval between the bearing spring is 4
- Case 4 = extreme case with bearing spring at each node

There are two different tasks carried out for the above cases. The first task is based on the trawl board interference at the place of centraliser with different intervals between the centraliser and second task is based on the trawl board interference at the middle of two centralisers with different intervals between the centraliser.

6.3.1 Trawl board interference at the place of centraliser

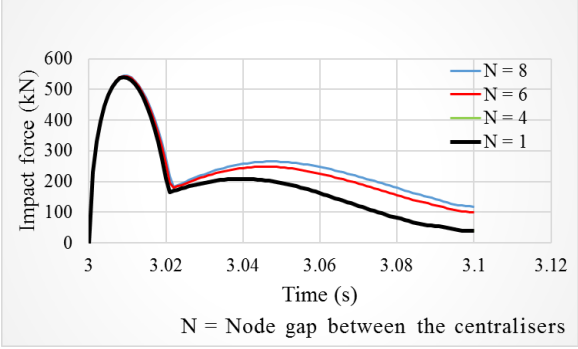

Figure 6.13 Comparison of impact force vs time obtained from FE analysis

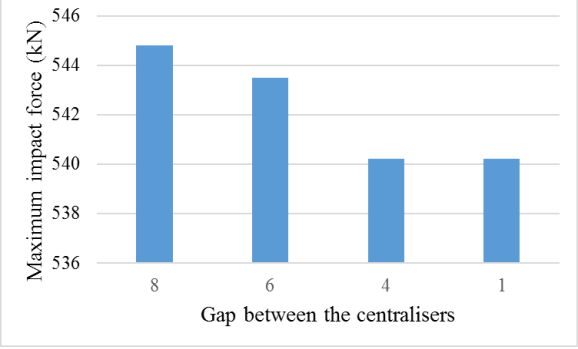

Figure 6.14 Maximum impact force for, TB interference at the place of centraliser

This task is based on the interference of trawl board at the position of bearing spring in pipe-in-pipe. Four different cases are carried out based on the interval gap between the centralisers. The simulations are carried out for all different cases and the results are plotted.

The comparison of impact force as a function of time obtained from FE analysis is shown in figure 6.13. The comparison is made between different interval gap of the centraliser placed in the pipeline. This task is carried out to check the influence of impact response of the pipeline when the trawl board hits pipeline at the place of centraliser for different interval gap of the centraliser. Figure 6.14 shows the difference in maximum impact force for all the cases. The maximum impact energy absorbed from FE analysis as shown in figure 6.14 is

Table 6.12 Results for the interference of trawl board at the place of centraliser

Quantity	**Unit**	**Case 1**	**Case 2**	**Case 3**	**Case 4**
bearing spring interval	-	8	6	4	1
Maximum impact force	kN	544.8	543.5	540.2	371.1
Absorbed energy	kJ	3.5	3.4	3.4	3.4
Permanent dent depth	mm	5.4	5.3	5.2	5.2

used to calculated the absorbed energy and the permanent dent depth between four different cases by using the equation 4.13 and 4.10. and the results are plotted as shown in table 6.12.

The maximum impact energy absorbed is in decreasing order from centraliser gap 8 to centraliser gap 1. The absorbed energy, the permanent dent depth for all the cases are similar. Therefore, the node gap of the centralizers will not make much difference in the impact but, there are small changes between the values. Table 6.12 shows the maximum impact force, the absorb energy and the permanent depth for all different case. The interval between centralisers and the impact location with respect to the centralizer have minor influence on the results. To make the PIP design simpler the centrlisers can be modelled at each node. In the same time the accuracy of the results are also maintained.

6.3.2 Trawl board interference at the middle of two centralisers

This task is based on the interference of trawl board at the middle of two centralisers. The simulations are carried out for four different cases and the results are plotted.

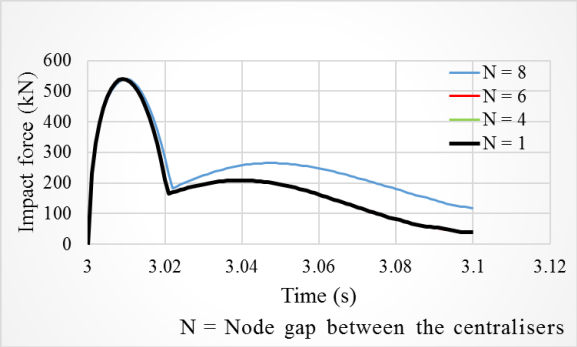

Figure 6.15 Comparison of impact force vs time obtained from FE analysis

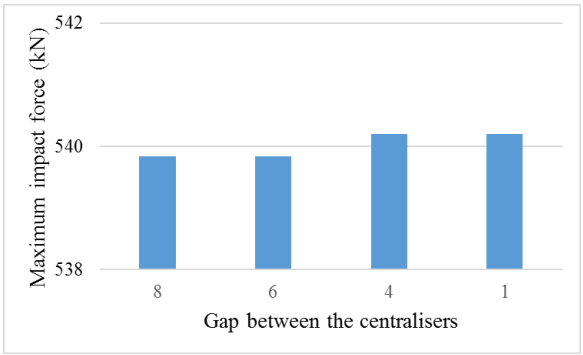

Figure 6.16 Maximum impact force for, TB interference at middle of centraliser interval

The main difference between the two tasks are, in task 1 the trawl board interference will be at the position of centraliser which is placed inside a PIP and in task 2 the trawl board interference will be at the middle of two centralisers.

The comparison of impact force as a function of time obtained from FE analysis is shown in figure 6.15. This task is carried out to check the influence of impact response of the pipeline when the trawl board hits pipeline at the middle of centraliser for different interval gap of the centraliser.

The maximum impact energy absorbed from FE analysis as shown in figure 6.16 is used to calculate the absorbed energy and the permanent dent depth between four different cases by using the equation 4.13 and 4.10. and the results are plotted as shown in table 6.13.

The maximum impact energy, the absorbed energy and the permanent dent depth in task 2 are all similar. From table 6.13, the results have minor change when the trawl board interacts between different interval gap of the centraliser.

Table 6.13 Results for the interference of trawl board at the middle of centraliser interval

Quantity	Unit	Case 1	Case 2	Case 3	Case 4
bearing spring interval	-	8	6	4	1
Maximum impact force	kN	539.8	539.8	540.2	540.2
Absorbed energy	kJ	3.4	3.4	3.4	3.4
Permanent dent depth	mm	5.2	5.2	5.3	5.2

6.4 Pull-over results

The results for different pull-over analysis are presented in this section. Firstly, the validation study "The new contact clump weight model" simulation is compared with the previous model test results and Johnsen (2012) results. In this study, the horizontal force experience by pipeline during the interaction of clump weight are measured and compared. The next validation study based on "The new contact trawl board model" is carried out for three different span heights. The study is based on comparison of warp line tension experienced during the interference of trawl board with single wall pipeline. Finally the results are compared with the model test results. Finally, the study based on trawl interference with "Free spanning of trawl board and pipe-in-pipe model" is carried out. The pull over results are compared with the RP load for different span heights of 0 m, 0.5 m, and 1 m. The filtering of results are done to make a clear comparison. This filtering reduces the high frequencies in the results, without affecting the maximum value of the results. The comparison of filtered and non-filtered results are shown in Appendix-D. These filterings are used in the place were required.

6.4.1 The new contact clump weight model

The study is carried out to obtain more understanding of the new contact (cont153) element, the clump weight model from mallø is taken and tested with new contact element. In this case the study is carrier out for a short pipeline of length 25 m with 350 mm diameter. The span of 0.50 m and 0.75 m are considered. These properties are same as the previous clump weight pull-over interaction carried out by Maaløe (2011) and Johnsen (2012) during their

master thesis. A similar model was reproduce using the contact element. The study is based on two different considerations one is based on the contact stiffness and the other is based on the contact friction.

6.4.1.1 Contact stiffness of new contact element

The study is carried out for three different levels of contact stiffness of the contact element. The span height considered here is 0.5 m and the three different stiffness values are, 100e6, 100e7 and 100e9 respectively. Friction coefficient 0.1 is used, which is same as the value used in mallø model.

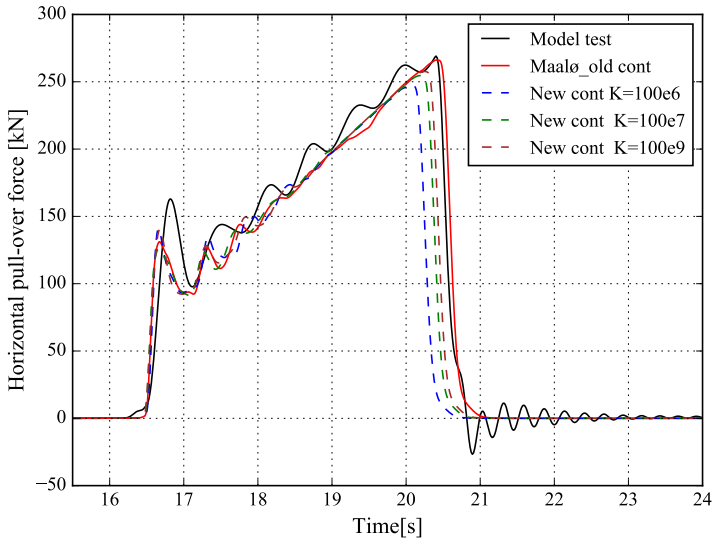

Figure 6.17 Horizontal pull-over force for different contact stiffness with friction 0.1

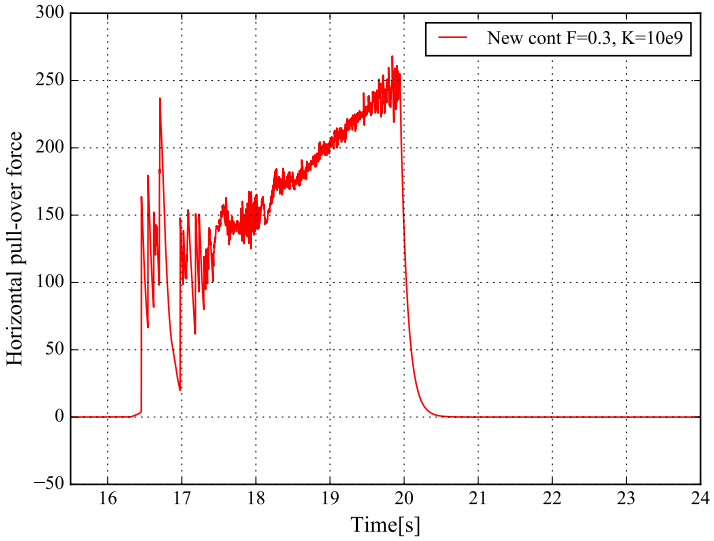

Figure 6.18 Horizontal pull-over force for high contact stiffness with friction 0.3

Figure 6.17 illustrates the horizontal pull over force for different contact stiffness. The results show that increase in stiffness of contact element increase the pull over force. Different simulation results could not match the model test and Maalø's result. The influence of different properties and behaviour between the new and old contact elements may be one of the reason for the mismatch of previous results. When the contact stiffness value is lower let's say 100e5, the clump weight has penetration in the pipe line as illustrated in 6.19 and for the increased contact stiffness of 100e6 the clump weight has good contact with the pipeline as illustrated in 6.20 . Further increase in contact stiffness does not affect the results in 0.1 friction coefficient, but for 0.3 friction coefficient there is non-physical resonance in pipeline which affects the horizontal pull over result. The figure 6.18 shows the unfiltered results for horizontal pull-over force caused by high stiffness value with 0.3 friction coefficient.

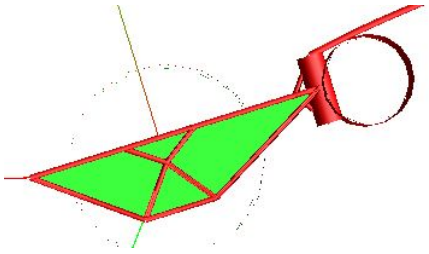

Figure 6.19 Clump weight with penetration due to low contact stiffness

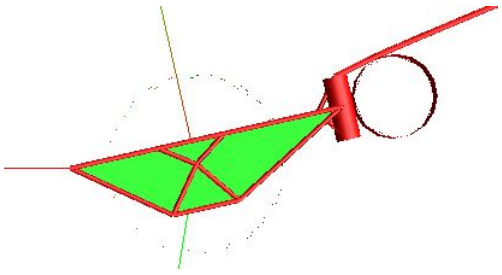

Figure 6.20 Clump weight with no penetration due to average stiffness

6.4.1.2 Friction coefficient of new contact element

The study is carried out for the two different span span heights, 0.5 m and 0.75 m. The contact stiffness with good contact behaviour obtained from the previous study is used here and the simulation is carried out for three different friction coefficient namely, 0.1 ,0.15, 0.3. The 0.1 friction coeffienct is used in Maalø (2011) and Johnsen (2012) study and as a results they concluded that the results are independent of the applied friction coefficient in the model. So, the study is continued with different friction coefficient values to see the influence of friction coefficient for the new contact element. Figure 6.21 and 6.22 shows the comparison of horizontal pull over force for different friction coefficient for 0.5 m and 0.75 m span height.In the figure the model test represents the model test results, Maalo-old cont represents the results of Maalø (2011) and New cont F=0.10 represent the simulation results of new contact element with different friction. For 0.5 m span height, the result doesn't match the previous research results for 0.1 friction coefficient, so the friction coefficient is increased to 0.15, which has a better match with model test and mallø result. For 0.75 m span height the 0.1 friction coefficient has a closest match with malø results. Friction coefficient 0.3 results in the increase of the horizontal pull over force for both 0.5 m and 0.75 m span height. Thus the contact friction coefficient has an important influence on the horizontal pull-over results.

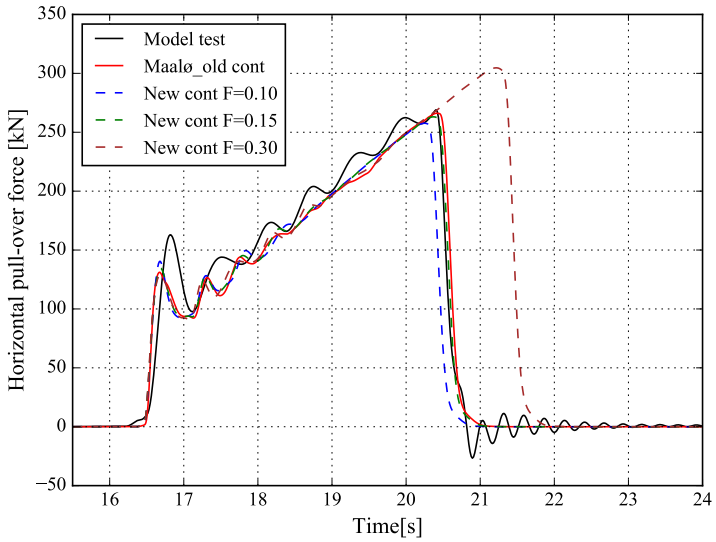

Figure 6.21 Horizontal pull over force for different contact stiffness with friction 0.1

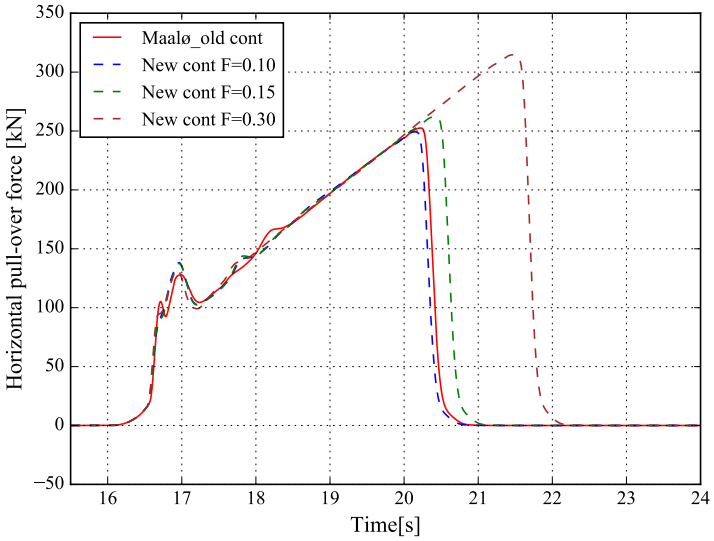

Figure 6.22 Horizontal pull over force for high contact stiffness with friction 0.3

6.4.2 The new contact trawl board model

The new contact element used in clump weight model is fthe trawl board model. The contact stiffness value with good contact behaviour obtained from the clum weight model case is used here . The reasonable steel to steel friction coeffiecient 0.3 is used for the contact element. The simulation for pull over analysis is carried to compare the warp line tension results with previous model test results. The warp line tension is measure for three different span height 0.5 m, 1 m and 5 m. The detail of model test is described detailly by (Wu et al., 2013) and the model data from (Wu et al., 2013) is used here. The study is carried out to check the response of new contact element in the trawl board model. The study consists of two different tasks, one is comparison of warp line stiffness of SIMLA model with model test results and other one is comparison of warp line tension for three different warp line angle say 10^0, 20^0 and 30^0.

6.4.2.1 Warp line tension – SIMLA vs model test

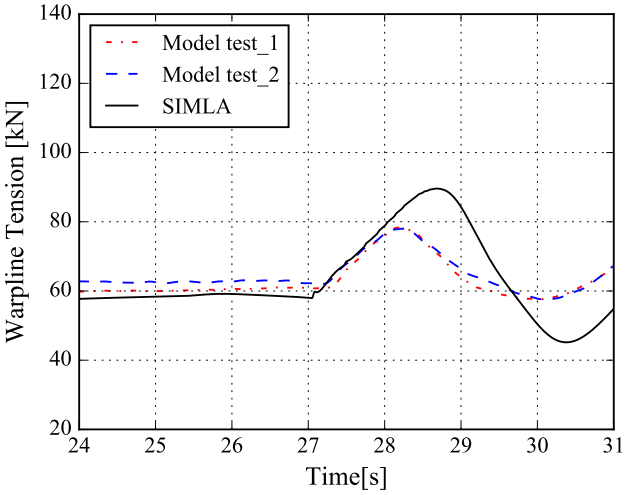

Figure 6.23 Warp line tension $H_{sp} = 0.5m$

The trawl board with velocity $2m/s$ is pulled over the pipeline. The trawling path is perpendicular to the pipeline section ($\alpha = 90^0$). The simulation is carried for three different span heights with same warpline angle 30^0. The maximum warp line tension and the pull over duration are tabulated in table 6.14. The warp line tension for smaller span heights has reasonable agreement with the model test results as illustrated in figure 6.23 and 6.24 . The same level of maximum warp line tension in absorbed in both the cases. However, the warp line tension for 5 m span has a greater deviation in results as shown in figure 6.25 . This is because the hydrodynamic load induced in vertical direction is not captured in FE analysis software, since SIMLA is a developing version software. So, the simulation is accounted for smaller span heights, to get valuable results.

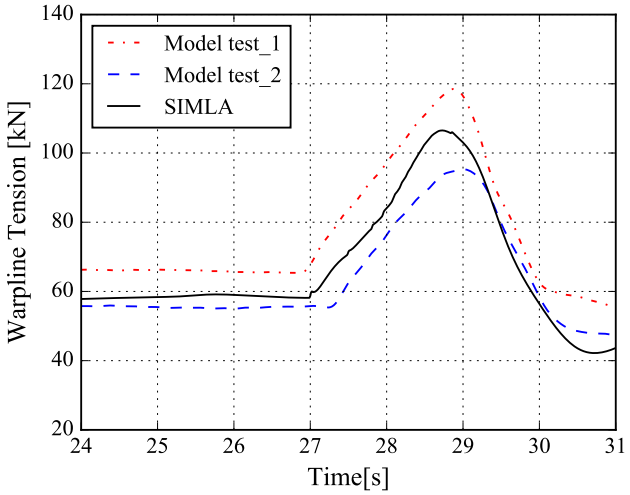

Figure 6.24 Warp line tension $H_{sp} = 1m$

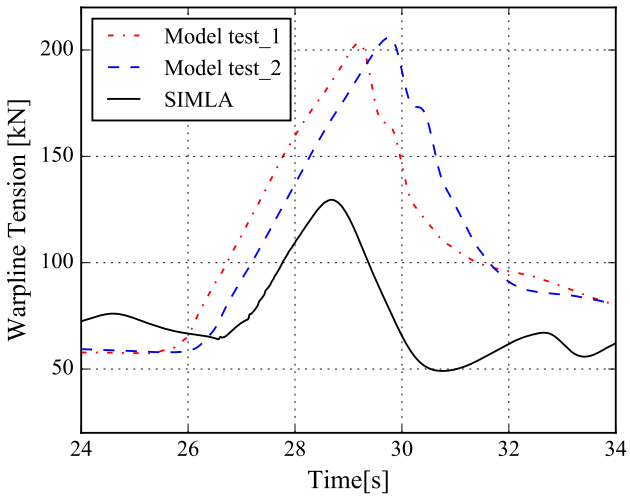

Figure 6.25 Warp line tension $H_{sp} = 5m$

Table 6.14 Summary of warp line tension results for model test and SIMLA model

	Maximum Tension [kN]		**Pull over duration[s]**	
Case	Simulation	Model test	Simulation	Model test
H_{sp}= 0.5 m	92.7	83	1.8	1.1
H_{sp}= 1 m	104.5	109.4	2.1	1.5
H_{sp}= 5 m	127.4	213.5	2.8	3.8

6.4.2.2 Warp line tension for different warp line angle– SIMLA vs model test

The next study is based on the simulation carried out for different warp line angle of 100, 200, and 300. The simulation is accounted for different span heights as well 0.5 m, 1 m and 5 m. The results are illustrated in figure 6.26, 6.27 and 6.28.

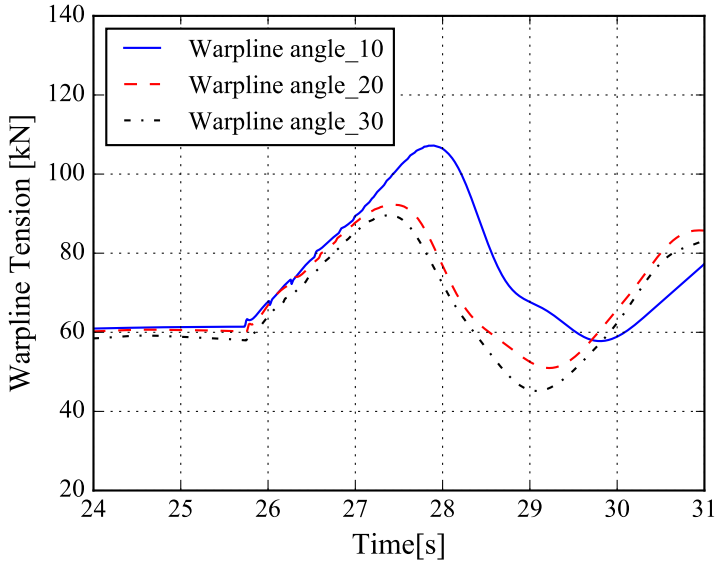

Figure 6.26 Warp line tension $H_{sp} = \ 0.5m$, $\sigma_w = 10^0, 20^0, 30^0$

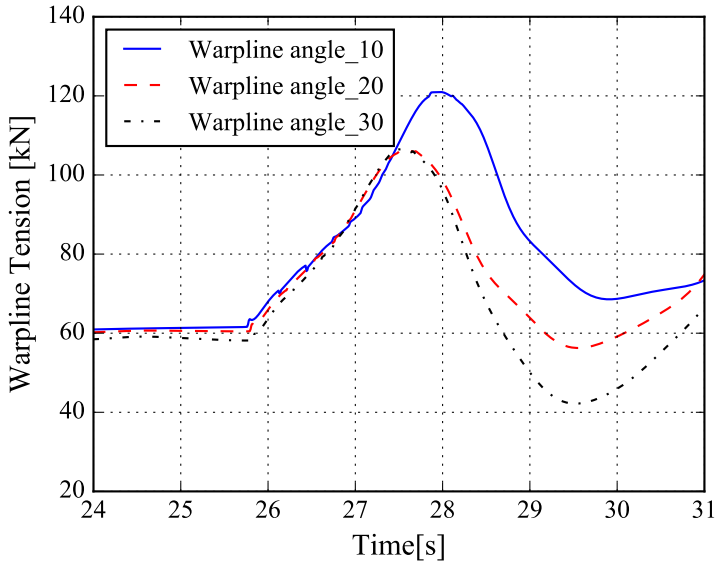

Figure 6.27 Warp line tension $H_{sp} = \ 1m$, $\sigma_w = 10^0, 20^0, 30^0$

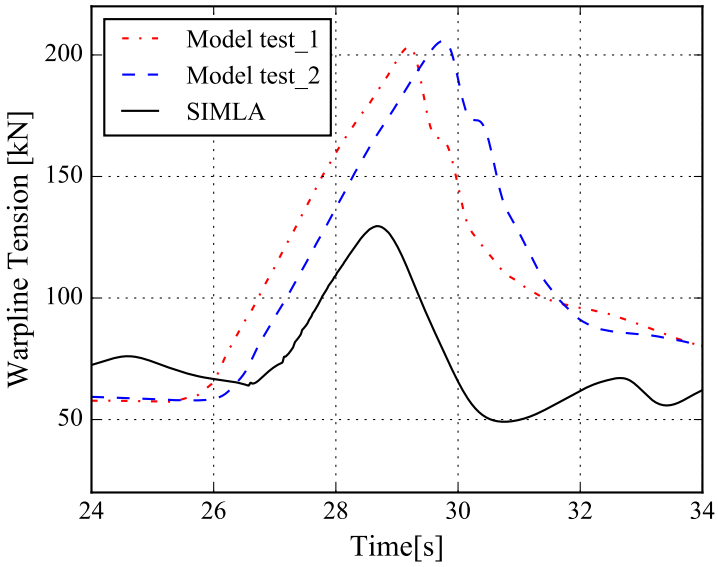

Figure 6.28 Warp line tension $H_{sp} = \ 5m$, $\sigma_w = 10^0, 20^0, 30^0$

The result indicated that decrese in warpline angle increses the tensin in the warpline. For the smaller span height 0.5 m, 1 m , the warp line tension is higher for the warp line angle 10^0, when compared to angle 20^0 ,30^0 . The warpline tension for the follows the same trend. For 5 m span height, the warp line tension is larger for the smaller angle. This influence in result is due to the trawl board hit angle because the angle will differ for different warp line angle. Figure 6.29 and 6.30 shoes the interaction position of trawl board model for 10^0 and 30^0 warp line angle.

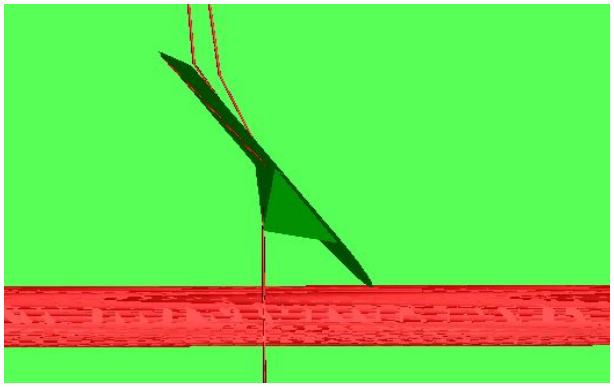

Figure 6.29 Trawl board interaction with pipeline for 10^0 warp line angle

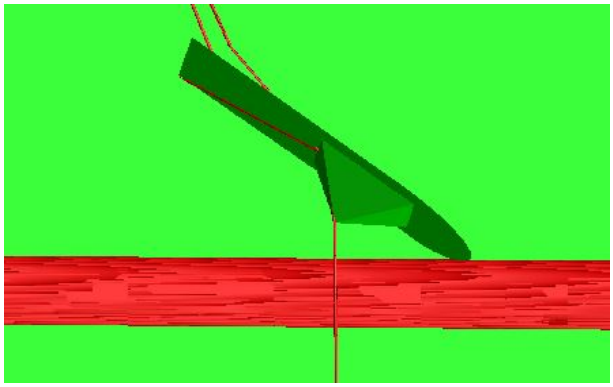

Figure 6.30 Trawl board interaction with pipeline for 30^0 warp line angle

6.4.3 Free spanning pipe-in-pipe and trawl board model

The pull over analysis is carried out for the interaction of trawl board with the PIP and also the simualtion for RP load is also carried out. The RP load is based on the DNV-RP-F111 (2014) as described in chapter 4. The RP load in applied on both horizontal and vertical direction on the pipe element. The different RP loads and pull over duration is illustrated in the table 6.15. The trawl board developed during the the new contact trawl board model case is used here , additionally the PIP configuration is modelled in the place of single wall pipele. The simulation is carried out for three different span height 0 m, 0.5 m, and 1 m, with respective span length of 25 m, and 50 m. The trawling velocity is 2m/s. The pull over results of trawl load is compared with the RP load. The horizontal force, horizontal displacement, vertical force, strains and the bending moments results are compared for both inner pipe and out pipe. The contact stiffnes with good contact behaviour achieved in the new contact clump weight model is used here. The different loading on pipeline are applied stage by stage in SIMLA. First the gravitational load and buoyancy are applied, followed by the residul tension loads are applied. Later the pressure loads and temperature loads are applied with 20 seconds each. Finally the trawl boards starts started moving to causes the interference.

Table 6.15 RP load and pull over duration for various span heights

	Unit	**Span height** H_{sp}		
Quantity		0 m	0.5 m	1 m
Horizontal force	kN	29.23	59.79	81.87
Vertical force	kN	117.05	20.25	20.48
Pull-over duration	S	1.10	2.25	3.08

6.4.3.1 Horizontal force on inner pipe and outer pipe

The horizontal pull over force induced by the trawl board are compared with RP load. Both the outer pipe and inner pipe are taken into account for the comparison. Figure 6.31 and 6.32 shows the comparison for the pipeline laid flat on the seabed.

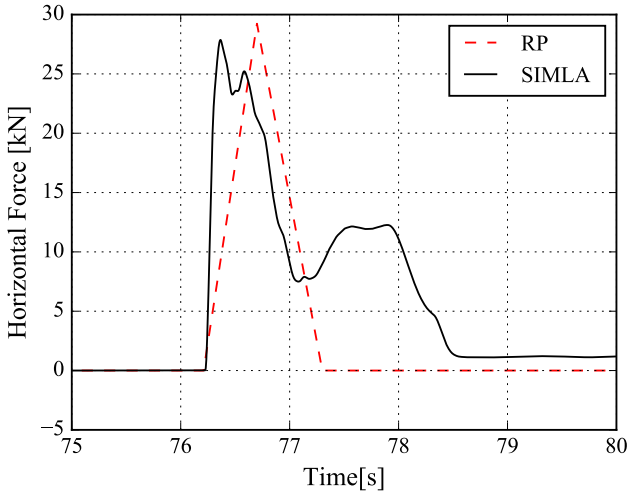

Figure 6.31 Horizontal force-OP, $H_{sp} = 0$ m

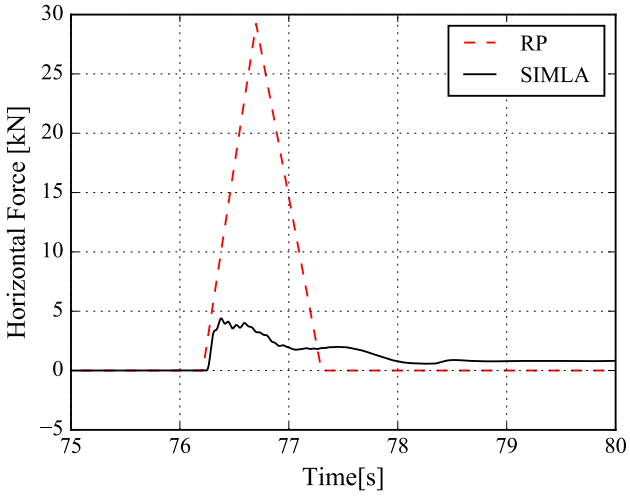

Figure 6.32 Horizontal force-IP, $H_{sp} = 0$ m

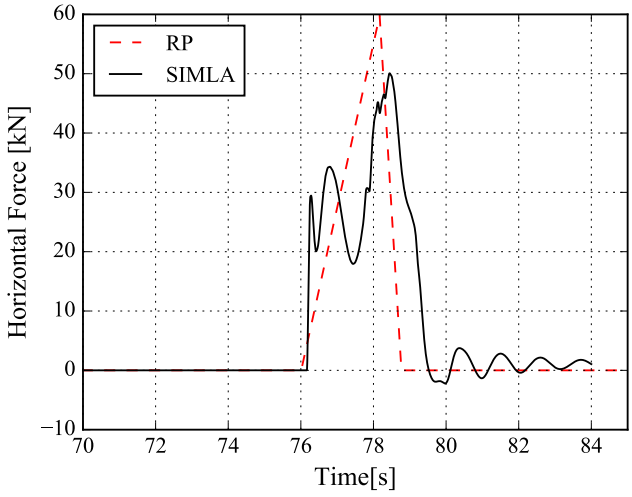

Figure 6.33 Horizontal force-OP, $H_{sp} = 0.5$ m

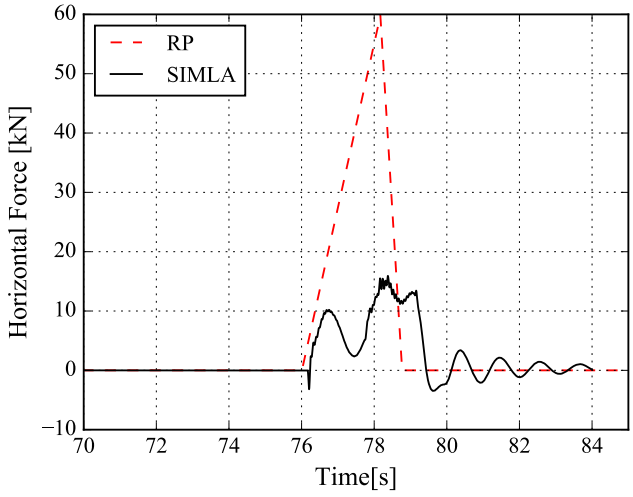

Figure 6.34 Horizontal force-IP, $H_{sp} = 0.5$ m

The comparision shows that for outer pipe the trend follows the RP load results, but for the inner pipe the trawl load is lower when compared to the RP load. This is because, the trawl board hits initially the outer pipe which experience the maximum horizontal force when compared to inner pipe. The same trend for the 0.5 m and 1 m span heights. When the horizontal force is compared between different span heights the result shows that increse in span height increses the horizontal pull-over force. The horizontal pull over force for trawl board interaction has two peaks in the result, the first peak occurs when the trawl board

hits the pipeline initially and when it hits the pipeline the upward force will be created in trawl board due to pull over, so it jumps after the first hit and after few second it will come again in contact with the pipeline, during this time the second peak of horizontal force is created and it will reduce once the trawl slides completely over the pipeline. The pull-over screen short are illustrated in appendix-d. The horizontal pull-over force for 1 m and 2 m span height for outer and inner pipe is shown in figure 6.39,6.34, 6.35, 6.36 . In figure the legend RP represents the RP load model and SIMLA represent the trawl board croosing the PIP model.

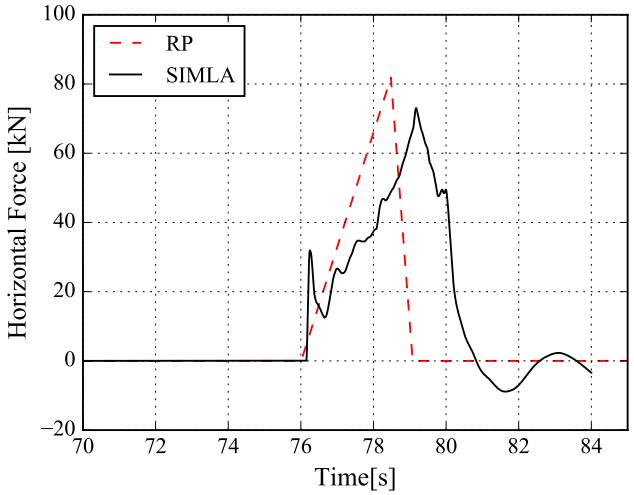

Figure 6.35 Horizontal force-OP, $H_{sp} = 1$ m

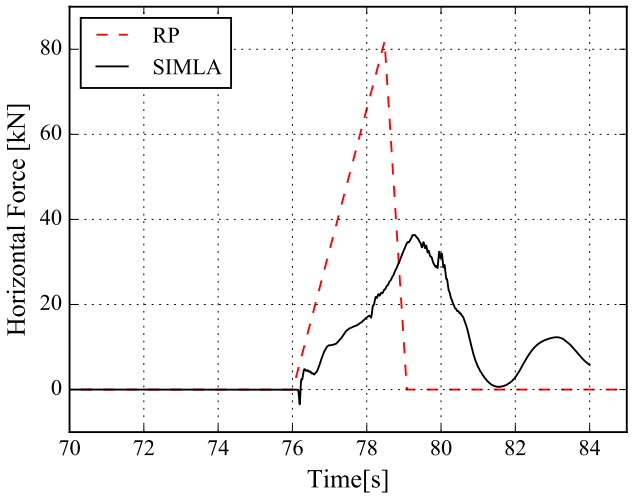

Figure 6.36 Horizontal force-IP, $H_{sp} = 1$ m

6.4.3.2 Lateral displacement of inner pipe and outer pipe

The lateral displacement of the pipeline occurs when the trawl board hits the pipe laterally and pulled over it. The displacement of inner pipe and outer pipe will be same, this is because the outer pipe and inner pipe are place concentric with each other by help of the centralisers. When the displacement occurs due to trawl load the inner pipe will follow the path of outer pipe. Thus, both the displacement is similar. The displacement due to trawl load is compared with RP load for different span height.The RP load calculations are based on several real time experiments. For 2 m span height, the displacement is larger than the RP load For 0 m ,0.5 m and 1 m span height the displacement is lower than that of displacement due to RP load. But the displacement increase if the span height increase this is due to

the hitting position of the trawl board. The lower edge of the trawl board hits the pipeline when it is resting on the seabed and the hitting position will differ based on different span heights. The displacement results for various span height are shown from figure 6.37 to 6.42. The larger displacement occurs after the trawl board hits the pipeline. The displacement is reduced after the trawl board completely slides over the pipeline. The pipeline will not returned to its initial position because there might be small displacement caused by trawl board even after it crossed the pipeline.

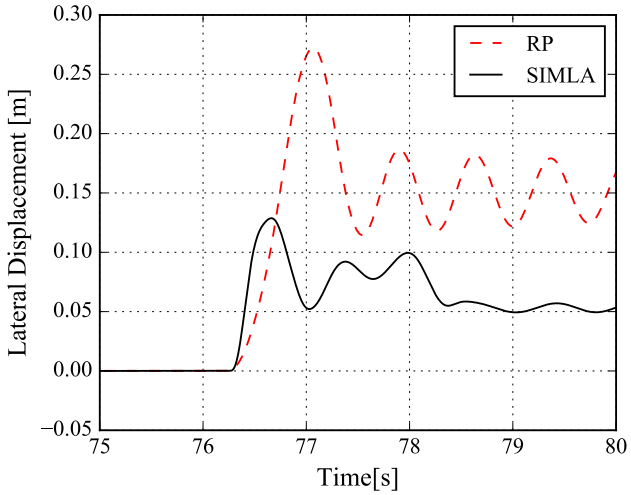

Figure 6.37 Lateral displacement-OP, $H_{sp} = 0$ m

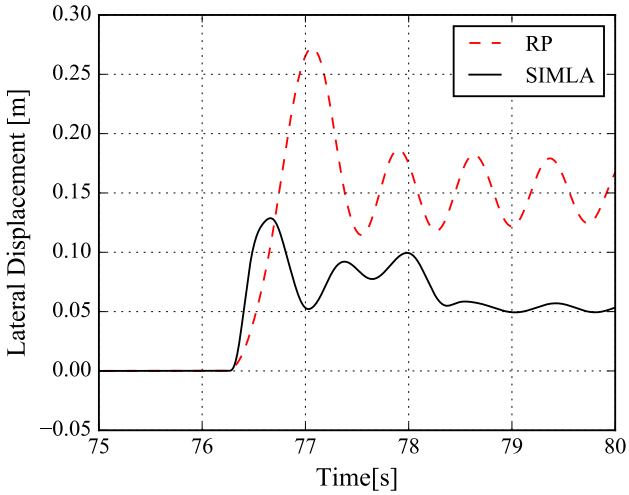

Figure 6.38 Lateral displacement-IP, $H_{sp} = 0$ m

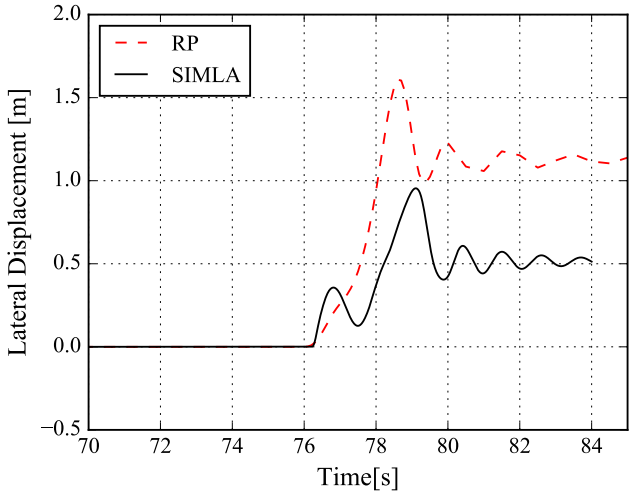

Figure 6.39 Lateral displacement-OP, $H_{sp} = 0.5$ m

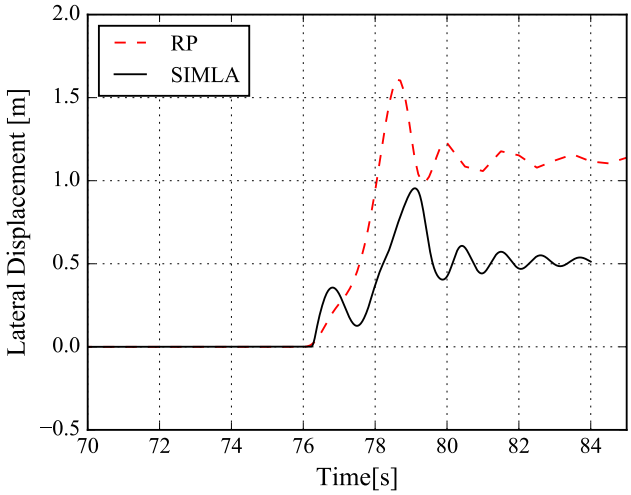

Figure 6.40 Lateral displacement-IP, $H_{sp} = 0.5$ m

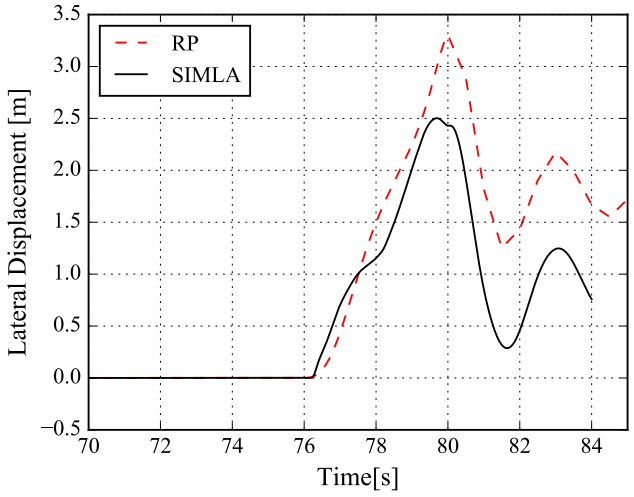

Figure 6.41 Lateral displacement-OP, $H_{sp} = 1$ m

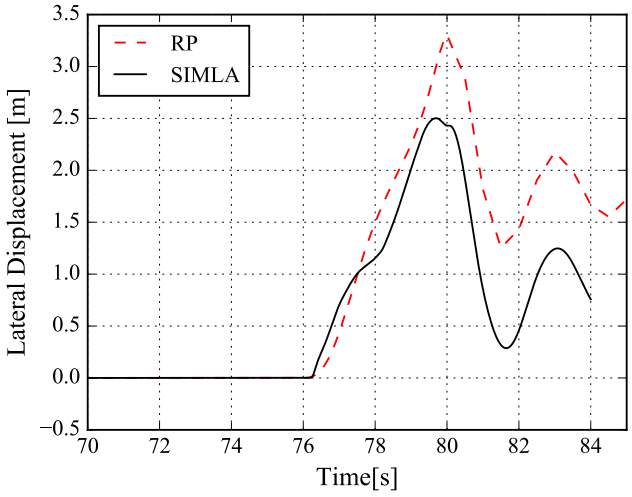

Figure 6.42 Lateral displacement-IP, $H_{sp} = 1$ m

6.4.3.3 Vertical force of inner pipe and outer pipe

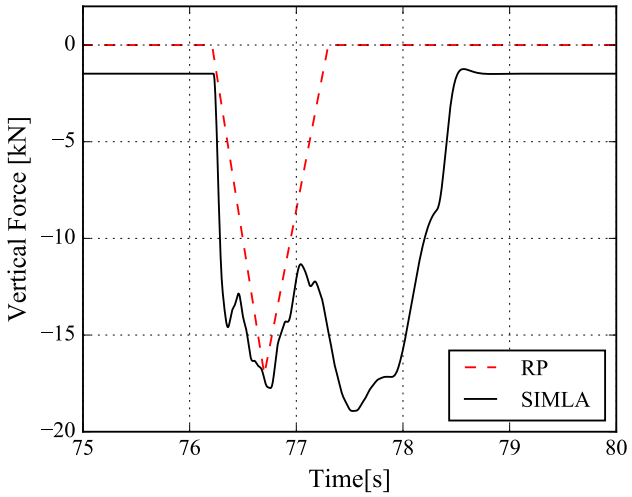

Figure 6.43 Vertical force-OP, $H_{sp} = 0$ m

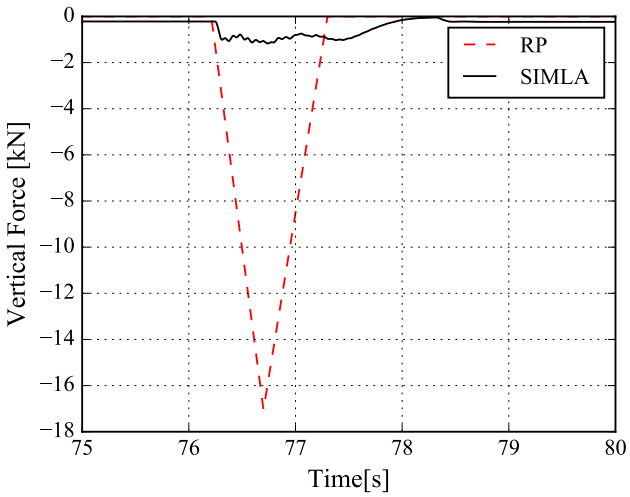

Figure 6.44 Vertical force-IP, $H_{sp} = 0$ m

The vertical force is acting in downward direction for both RP case and trawl board case. As per, DNV-RP-F111 (2014) the vertical force should be applied on downward direction. The vertical force is also measured for different span heights for both inner pipe and outer pipe and the comparison is made with RP load . The comparison results for all the three span height agree with RP model results for outer pipe. For the inner pipe the reson for lower

vertical force is because the maximum vertical force is absorbed initially by outer pipe when exposed to trawl board. The vertical force for inner pipe and outer pipe is shown from figure 6.43 to 6.48.

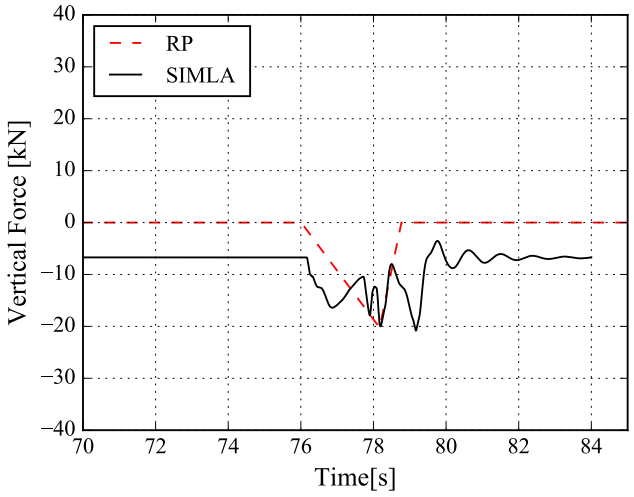

Figure 6.45 Vertical force-OP, $H_{sp} = 0.5$ m

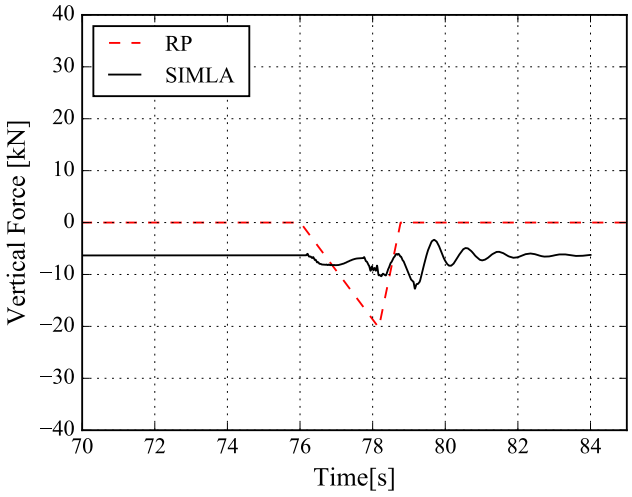

Figure 6.46 Vertical force-IP, $H_{sp} = 0.5$ m

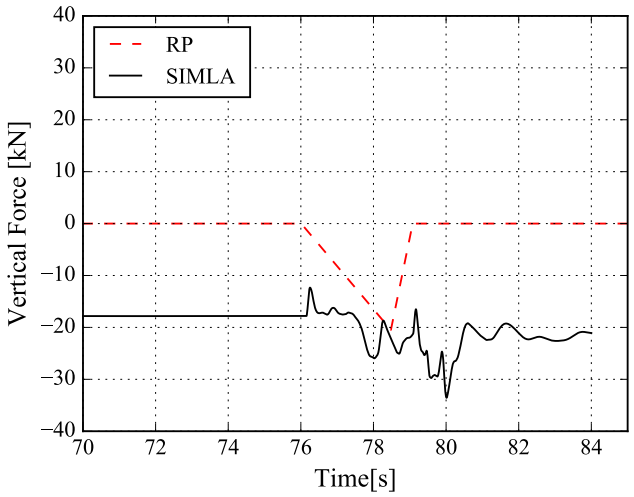

Figure 6.47 Vertical force-OP, $H_{sp} = 1$ m

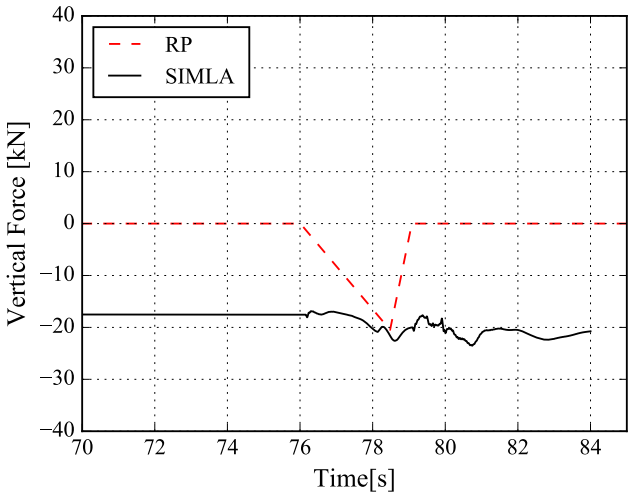

Figure 6.48 Vertical force-IP, $H_{sp} = 1$ m

6.4.3.4 Strains on the outer pipe and inner pipe

The strain results for RP load and trawl load are compared for outer pipe and inner pipe for different span heights. Both tensile strain and compressive strain are compared. For both outer and inner pipe, the strains are lower than the RP load results for all span heights. In

general, when certain load acts on a pipe or beam, there might be strain induced in that object. Different type of strains are compared with RP load and the results are illustrated from figure 6.49 to 6.54. When compared to different span height, both the tensile and compressive strain increases when the span height increses.

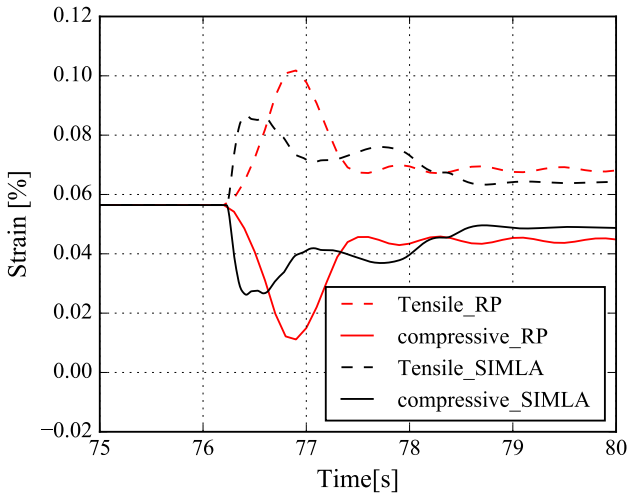

Figure 6.49 Strain-OP, $H_{sp} = 0$ m

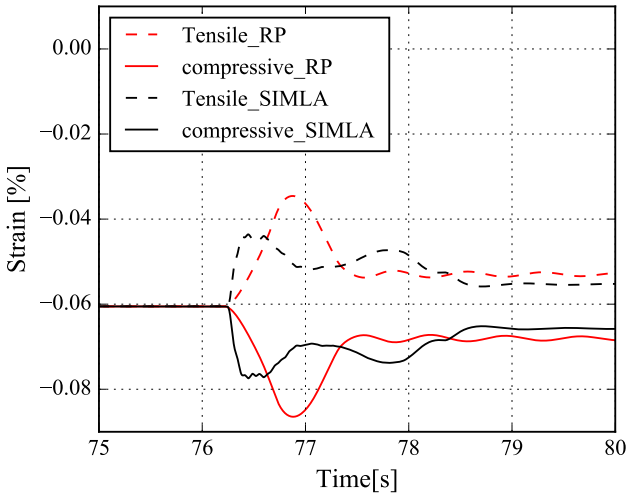

Figure 6.50 Strain-IP, $H_{sp} = 0$ m

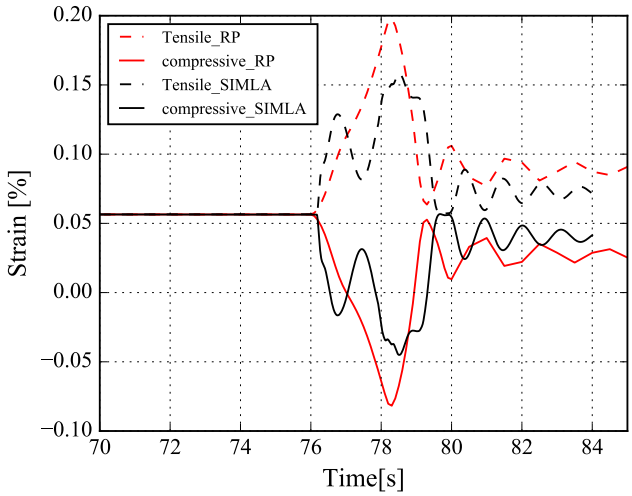

Figure 6.51 Strain-OP, $H_{sp} = 0.5$ m

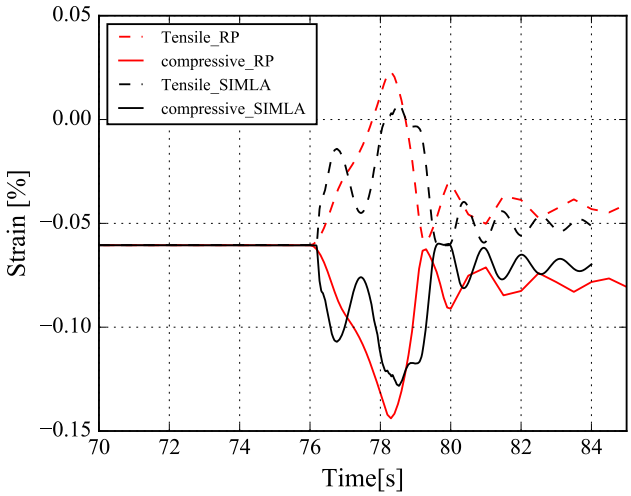

Figure 6.52 Strain-IP, $H_{sp} = 0.5$ m

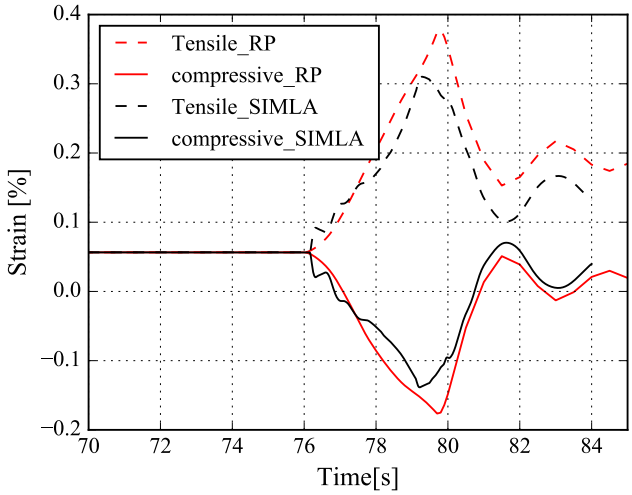

Figure 6.53 Strain-OP, $H_{sp} = 1$ m

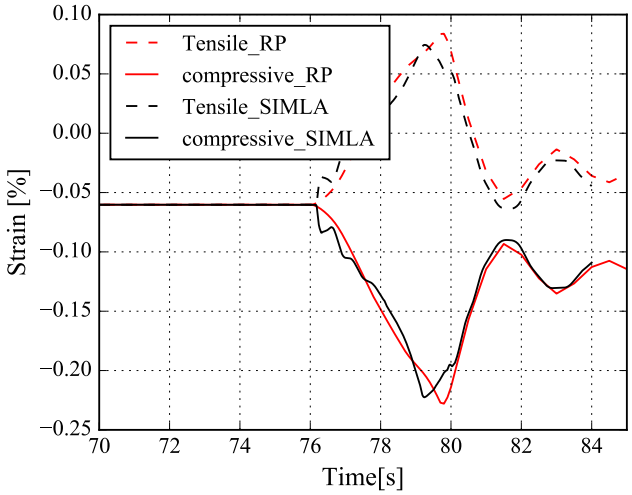

Figure 6.54 Strain-IP, $H_{sp} = 1$ m

6.4.3.5 Resultant bending moment for outer pipe and inner pipe

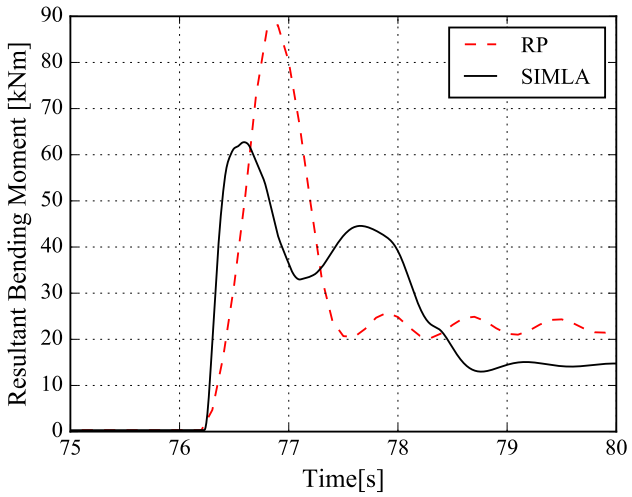

Figure 6.55 Resultant bending-OP, $H_{sp} = 0$ m

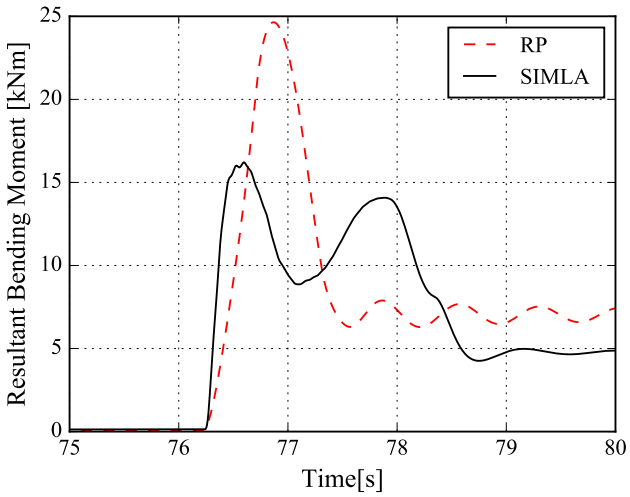

Figure 6.56 Resultant bending-IP, $H_{sp} = 0$ m

The resulting bending moment is calculated by using lateral bending moment and vertical bending moment. The results of both the bending moment is described in Appendix E . The resultant bending moment for inner pipe follows the same trend as outer pipe. But the the inner pipe has less bending moment when compared to the outer pipe where it is very high. Figure from 6.55 to 6.60 illustrates the resultant bending moment in th pipe. For 0.0

m and 0.5 m span, the result has two peaks this is because during pull-over the trawl board hits twice the pipeline as it jumps over the pipeline. In other word the traw board has two different contact point during ots pull-over.

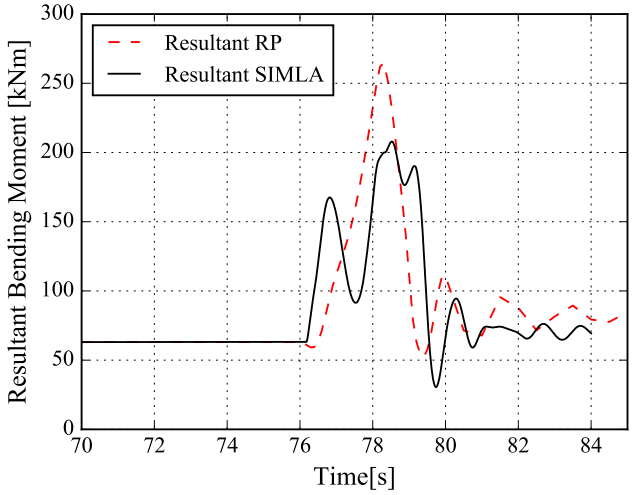

Figure 6.57 Resultant bending-OP, H_{sp} = 0.5 m

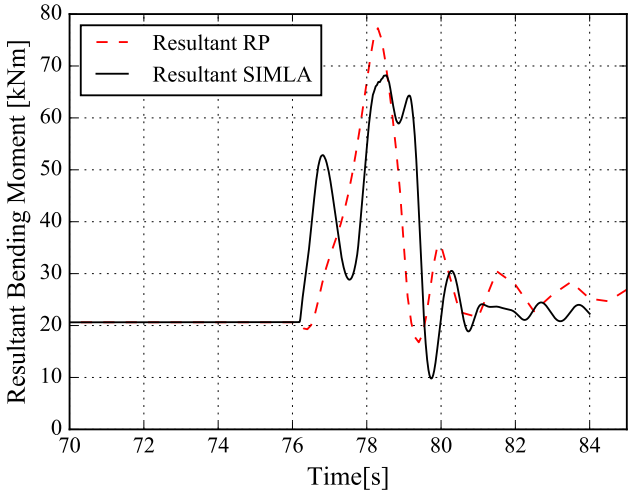

Figure 6.58 Resultant bending-IP, H_{sp} = 0.5 m

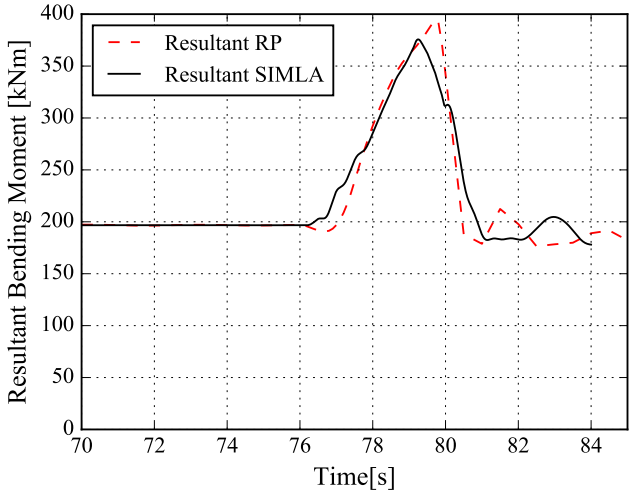

Figure 6.59 Resultant bending-OP, $H_{sp} = 1$ m

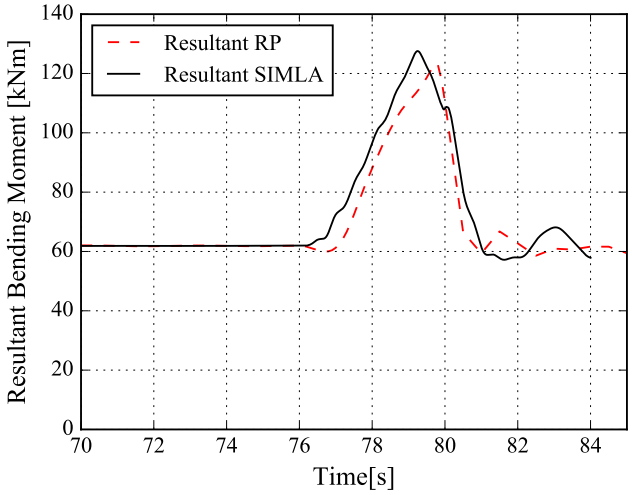

Figure 6.60 Resultant bending-IP, $H_{sp} = 1$ m

Chapter 7

Conclusions

7.1 Impact analysis

The impact responses of single pipe wall and pipe-in-pipe were obtained based on advanced impact calculation method as mentioned in DNV-RP-F111 (2014) and the simulations are done by using FEM software SIMLA.

7.1.1 Impact on single pipe wall

First, the finite element impact model for single pipe wall was used to study the influence from different important parameters, including coating thickness, content density, SYMS, pipe wall thickness, and the trawl gear types. The impact response for coating thickness 60 mm and content density 1026 kg/m^3 is high. The mass of the pipe will change for different coating thickness and density. Increase in mass or density of the pipe results in the increase of the total mass of the pipe. Therefore, more energy is required to mobilize the pipe and results in larger energy absorption. The cases with different specified minimum yield stress indicates that the change in stiffness of the pipe shell. When stiffness of the pipeline decreases, the impact force reaches the maximum in a shorter period of time. Therefore, the total impact energy absorbed by the pipe walls become lower. When the pipe wall thickness changes, the mass and stiffness of the pipe will change. The pipe with high wall thickness 16 mm has

high impact response. The trawl board with high mass or high velocity creates high impact response on the pipeline.

7.1.2 Impact on pipe-in-pipe

The finite element model was developed for pipe-in-pipe to study the impact response. The different case are based on the interval between the centralisers and the impact location either at the start or middle of two centralisers. Both the cases with respect to impact location and the interval between the centraliser have minor influence on results. Therefore, for pipe-in-pipe, the centralizers can be modelled at each node for simplicity, without losing accuracy on the predicted results.

7.2 Pull-over analysis

7.2.1 New contact clump weight model

The purpose of this exercise is to obtain more understanding of cont153 element. The Maalø (2011) model was tested by replaceing the old contact (cont164) with the new contact element. Different study is carrried out based on the contact stiffness and the friction coefficient. For the lower contact siffness the clump weight has penetration on the pipeline, whereas for the higher contact stiffness the contact creates non-physical resonance in the pipeline. So, for the average contact stiffness the clump weight will have good contact with the pipeline. As a result of this study, a contact stiffness with good contact behaviour was acheived and then used for further studies.

By considering the good contact stiffness, the next simulation cases is carried out for different friction coefficient. The simulation is carried out for two different span heights of 0.50 m and 0.75 m, with trawling velocity of 1.95 m/s. Three different friction coefficient are considered for the simulations are 0.10 , 1.5 and 0,30. The 0.1 is the friction coefficient used in previous contact model. 0.15 is found to be the best match with the previous model results (Johnsen,

2012) and 0.30 the reasonable friction coefficient for steel to steel contact. For both 0.50 m and 0.75 m span, the 0.3 friction coefficient has higher force than the others. The 0.1 friction coefficient did not match the previous contact element results and a good match was achieved by increasing to 0.15 friction cofiicient. In contrast to the previous study which states that the friction coeffient does not have any influence on the results, this study shows that the friction coefficient has important influence in the results.

7.2.2 New contact trawl board model

This study is carried out to investigate the influence of warp line angle in the results. The new contact element cont153 is further used in the trawl board model with a simplified geometry, with the contact stiffness defined in the clump weight case. The simulation are carried out for three different span heights of 0.5 m, 1.0 m and 5.0 m with trawl velocity of 2 m/s. The pipeline is rigid and has a 750 mm diameter. The warpline tension results are analyzed from the model and compared with previous model test results (Wu et al., 2015). For each span heights the results are compared and it shows that, for smaller span heights (0.5 m and 1.0 m) the results has good agreement with the previous model test result. But for the high span height (5 m) notable deviations were found in the results. This indicates that the established trawl board pull-over model in this thesis is more reliable for low span height than high span height.

The next study is based on the comparison of different warpline angle (10^0 ,20^0, 30^0). The result shows that, for all the span heights decrease in warpline angle increases the warpline tension.

7.2.3 Free spanning pipe-in-pipe and trawl board model

The final study is based on the interaction of detailed trawl board model with PIP. The simulations are carried out for three different span heights 0.0 m, 0.5 m and 1.0 m (low span height). The pull-over response from the detailed model is compared with those from RP Load. The various pull-over response such as, horizontal force, horizontal displacement,

vertical force, strains, bending moments are taken into account and compared with RP load. The comparison shows that the pull-over responses increases as the span height increses, and in general all the results from the detailed model is lower than that of RP load case. This findings indicates the possiblity to further optimise PIP design in the view point of trawl board pull-over loads at the low span heights.

7.3 Future work

In this thesis, first the impact analysis is carried out for PIP by using advanced impact calculation method. Followed by, trawl gear pull-over analysis is carried out. In which the geometry,hydrodynamics and contact mechanism of the trawl gear are modelled and are compared with simplified analysis methods based on semi-empirical formulas proposed for trawl gear pull-over analysis in the RP (DNV-RP-F111, 2014). The analysis is carried out for the interaction of this detailed pull-over model with a pipe-in-pipe system by using SIMLA software. The pipeline are installed using different laying methods. In that, reeling is one of the methods used for laying pipelnes.The pipe-in-pipe system is usually installed after different stages in the reeling process and they are classified as reel-on, reel-off, through aligner, through straightener and release pipe. The reeling process produces residual loading in the pipe-in-pipe system. Such effect will have an influence on the subsequent trawl load analysis, especially for the pull-over phase. Therefore, it is very important to study the response of trawl gear interaction with the pipe-in-pipe system, considering the effect of the reeling history on the trawl load responses.

To combine the reeling process and the detailed trawl gear pull-over analysis on the pipe-in-pipe system, all the model should be developed under the same framework in SIMLA. The key aspects of the possible future work are therefore summarised as follows:

- Sensitivity study should be carried out for the proposed model
- Develop a reeling model for a pipe-in-pipe system in SIMLA.
- Combine the reeling model and the pull-over model in the same model.

- Investigate the pull-over phenomena of a pipe-in-pipe system considering the reeling effect.
- Compare the results between models with and without the reeling effect.

Bibliography

Bai, Y. and Bai, Q. (2005). *Subsea pipelines and risers*. Elsevier.

Berhe, D. (2014). *Controlled lateral buckling design of pipelines*. PhD thesis, University of Stavanger, Norway.

DNV-RP-C205 (2010). Dnv-rp-c205: Environmental conditions and environmental loads. *Norway: DetNorskeVeritas*.

DNV-RP-F111 (2014). Interference between trawl gear and pipelines. Technical report.

Ellinas, C., King, B., and Davies, R. (1995). Evaluation of fishing gear induced pipeline damage. In *The Fifth International Offshore and Polar Engineering Conference*. International Society of Offshore and Polar Engineers.

FRDC (December 2014). Frdc fisheries reserch and development corporation,.

Fyrileiv, O. and Collberg, L. (2005). Influence of pressure in pipeline design: effective axial force. In *ASME 2005 24th International Conference on Offshore Mechanics and Arctic Engineering*, pages 629–636. American Society of Mechanical Engineers.

Horenberg, J. and Sriskandarajah, T. (1987). An analytical and experimental analysis of trawl gear-pipeline interaction. In *Offshore Technology Conference*. Offshore Technology Conference.

Hval, M., Brækstad, L., and Olsø, E. (2009). Structural integrity of submarine pipelines subjected to large strains caused by trawl pull-over. In *The Nineteenth International Offshore and Polar Engineering Conference*. International Society of Offshore and Polar Engineers.

Igland, R. T. and Søreide, T. (2008). Advanced pipeline trawl gear impact design. In *ASME 2008 27th International Conference on Offshore Mechanics and Arctic Engineering*, pages 271–277. American Society of Mechanical Engineers.

Johnsen, I. B. (2012). *Clump-weight trawl gear interaction with submarine pipelines*. PhD thesis, Norges teknisk-naturvitenskapelige universitet, Fakultet for ingeniørvitenskap og teknologi, Institutt for marin teknikk.

Kristoffersen, A. S., Asklund, P. O., and Nystrøm, P. R. (2012). Pipe-in-pipe global buckling and trawl design on uneven seabed. In *The Twenty-second International Offshore and Polar Engineering Conference*. International Society of Offshore and Polar Engineers.

Longva, V. (2010). *Simulation of trawl loads on subsea pipelines*. PhD thesis, Norges teknisk-naturvitenskapelige universitet, Fakultet for ingeniørvitenskap og teknologi, Institutt for marin teknikk.

Longva, V. and Sævik, S. (2012). A penalty-based body-pipeline contact element for simulation of pull-over events. In *ASME 2012 31st International Conference on Ocean, Offshore and Arctic Engineering*, pages 241–250. American Society of Mechanical Engineers.

Maaløe, K. (2011). *Clump-weight Trawl Gear Interaction with Submarine Pipelines*. PhD thesis, Norges teknisk-naturvitenskapelige universitet, Fakultet for ingeniørvitenskap og teknologi, Institutt for marin teknikk.

Mellem, T., Spiten, J., Verley, R., and Moshagen, H. (1996). Trawl board impacts on pipelines. Technical report, American Society of Mechanical Engineers, New York, NY (United States).

Moshagen, H. and Kjeldsen, S. (1980). Fishing gear loads and effects on submarine pipelines. In *Offshore Technology Conference*. Offshore Technology Conference.

Norwegian petroleum directorate, D. O. F. (2010). Description of relevant fishing gear and fishery activities in the norwegian economic zone. Technical report.

Palmer, A. C. and King, R. A. (2004). *Subsea pipeline engineering*. PennWell Books.

Palmer, A. C. and Ling, M. T. (1981). Movements of submarine pipelines close to platforms. In *Offshore Technology Conference*. Offshore Technology Conference.

Skibssmedie/Thyborøn. Polyvalent board, http://thyboron-trawldoor.dk/products/bottom-trawldoors/type-16-oval-standard-light/.

Sriskandarajah, T., Ragupathy, P., Anurudran, G., and Wilkins, R. (1999). Fishing gear interaction on hp/ht pipe-in-pipe systems. In *The Ninth International Offshore and Polar Engineering Conference*. International Society of Offshore and Polar Engineers.

Svein Sævik, O. D. Ø., Gjøsteen, G. S. B., and K.Ø., J. (2015). Simla - user manual. Technical report.

Technip. Pipe-in-pipe, http://www.technip.com/fr/sites/default/files/technip/fields.

Verley, R. (1994). Pipeline on a flat seabed subjected to trawling or other limited duration point loads. In *The Fourth International Offshore and Polar Engineering Conference*. International Society of Offshore and Polar Engineers.

Verley, R., Moshagen, B., Moholdt, N., and Nygaard, I. (1991). Trawl forces on free-spanning pipelines. In *The First International Offshore and Polar Engineering Conference*. International Society of Offshore and Polar Engineers.

Wu, X., Longva, V., Sævik, S., and Moan, T. (2013). Simulation of hooking event in fish trawling operation. In *ASME 2013 32nd International Conference on Ocean, Offshore and Arctic Engineering*, pages V04AT04A036–V04AT04A036. American Society of Mechanical Engineers.

Wu, X., Longva, V., Sævik, S., and Moan, T. (2015). A simplified approach to estimate the probability of otter board hooking at pipelines. *Journal of Offshore Mechanics and Arctic Engineering*, 137(6):061702.

Zheng, J., Palmer, A., Brunning, P., and Gan, C. (2014a). Indentation and external pressure on subsea single wall pipe and pipe-in-pipe. *Ocean Engineering*, 83:125–132.

Zheng, J., Palmer, A., Brunning, P., Lim, G., and Shu, S. (2014b). Method to assess

the overtrawlability of pipe-in-pipe. In *Offshore Technology Conference-Asia*. Offshore Technology Conference.

Zheng, J., Palmer, A., Lipski, W., and Brunning, P. (2012). Impact damage on pipe-in-pipe systems. In *The Twenty-second International Offshore and Polar Engineering Conference*. International Society of Offshore and Polar Engineers.

Appendix A

Design data for impact analysis

Table A.1 Design data for single pipe (DNV-RP-F111, 2014)

Quantity	Symbol	Value	Unit
Pipeline Property			
Outer diameter	D	—	mm
Wall thickness	t_{nom}	—	mm
Corrosion allowance	t_{corr}	0.3	-
Steel quality	-	SML450IU	-
Specified minimum yield stress	SYMS	450	N/mm^2
Specified minimum tensile strength	-	535	N/mm^2
Coating			
Type	-	Concrete	-
Thickness	t_{con}	40	mm
Specific weight	-	1900	kg/m^3
Content			
Type	-	OIL	-
Design temperature	-	40	^0c
Design pressure	-	100	bar
Environmental data			
Water depth	d	300	m
Soil conditions			
Sand, friction angle	ϕ	35	deg
Axial friction coefficient	-	0.5	-
Lateral friction coefficient	-	0.6	-
Safety Philosophy			
Fluid category	-	B	-
Location class	-	1	-
Safety class	-	Medium	-

Table A.2 Design data for pipe-in-pipe (DNV-RP-F111, 2014)

Quantity	Symbol	Value	Unit
Outer pipeline dimensions			
Outer diameter	D	394	mm
Wall thickness	t_{nom}	20.5	mm
Corrosion allowance	t_{corr}	0	-
Derating at design temperature	-	0	MPa
Inner pipeline dimensions			
Outer diameter	D	251	mm
Wall thickness	t_{nom}	11.5	mm
Corrosion allowance	t_{corr}	0	-
Derating at design temperature	-	0	MPa
Steel material outer pipe			
Steel quality	-	SML450IU	-
Specified minimum yield stress	SYMS	360	N/mm^2
Steel material inner pipe			
Steel quality	-	SML450IU	-
Specified minimum yield stress	SYMS	550	N/mm^2
Coating			
Thickness	t_{coat}	3	mm
Specific weight	-	950	kg/m^3
Content			
Type	-	OIL	-
Specific weight	-	534	-
Design temperature	-	90	^0c
Design pressure	-	150	bar
Environmental data			
Water depth	d	300	m
Ambient temperature	-	5	^0c
Soil conditions			
Sand, friction angle	ϕ	35	deg
Axial friction coefficient	-	0.4	-
Lateral friction coefficient	-	0.6	-
Safety Philosophy			
Fluid category	-	B	-
Location class	-	1	-
Safety class	-	Medium	-

Appendix B

Calculation of different impact scenarios

The calculation of maximum impact force, the absorb energy and the permanent dent depth for the simplified method and the advanced impact calculation method are as follows According to 4.4 calculation of m_p is

$$m_p = \frac{1}{4}.f_y.t^2 \tag{B.1}$$

$$m_p = \frac{1}{4} \times 450 \times 13^2 \tag{B.2}$$

$$m_p = 19.01kN \tag{B.3}$$

According to 4.7 calculation of α is

$$\alpha = 37\left[ln\frac{D}{t} - \frac{1}{2}\right] \tag{B.4}$$

$$\alpha = 37\left[ln\frac{356}{13} - \frac{1}{2}\right] \tag{B.5}$$

$$\alpha = 37\left[ln\frac{356}{13} - \frac{1}{2}\right] \tag{B.6}$$

$$\alpha = 103.97 \tag{B.7}$$

According to 4.6 calculation of α

$$\beta = 0.125\left[ln\frac{D}{t} + \frac{1}{2}\right] \tag{B.8}$$

$$\beta = 0.125\left[ln\frac{356}{13} + \frac{1}{2}\right] \tag{B.9}$$

$$\beta = 0.53 \tag{B.10}$$

B.1 Simplified Calculation

The absorbed energy due to impacting steel mass is calculated using the equation 4.1.

$$E_s = R_{fs}.\frac{1}{2}.m_t.(C_h.V^2) \tag{B.11}$$

$$E_s = 0.55.\frac{1}{2} \times 4000 \times (0.85 \times 2.6^2) \tag{B.12}$$

$$E_s = 5.4kJ \tag{B.13}$$

The impacting force caused by the hydrodynamic added mass is calculated by using equation 4.5.

$$F_b = c_b.V.(m_a.k_b)^{0.5} \tag{B.14}$$

$$F_b = 0.85 \times 2.6 \times (4000.10 \times 10^7)^{0.5} \tag{B.15}$$

$$F_b = 646.6kN \tag{B.16}$$

The absorbed energy of hydrodynamic mass is calculated using the equation 4.3.

$$E_a = R_{fa}.\frac{\alpha.m_p.D}{\beta+1}.\left[\frac{F_b}{\alpha.m_p}\right]^{(\beta+1/\beta)} \tag{B.17}$$

$$E_a = 0.25.\frac{103.9 \times 19010 \times 0.356}{0.54+1} \times \left[\frac{646.6}{103.9 \times 19.012}\right]^{(1.54+1/0.54)} \leq \frac{\text{ffl}1}{2} m_t (C_h.V)^2 \tag{B.18}$$

$$E_a = 4.7kJ \leq 20.9kJ \tag{B.19}$$

The impact force experienced by the pipe shell is given by equation 4.11.

$$F_{sh} = m_p.\alpha.\left[\frac{z_{LOC}}{m_p.D}.\frac{B+1}{\alpha}\right]^{\beta/(\beta+1)} \tag{B.20}$$

$$F_{sh} = 19.01 \times 103.97 \times \left[\frac{5.4}{19.01 \times 0.356} \times \frac{0.54+1}{103.9}\right]^{0.54/(0.54+1)} \tag{B.21}$$

$$F_{sh} = 417.05kN \tag{B.22}$$

The permanent dent depth is calculated by using the equation 4.10.

$$H_{pc} = D\left[\frac{F_{sh}}{m_p.\alpha}\right]^{1/\beta} - \left[\frac{F_{sh}}{m_p.6 \times 10^3}.\sqrt{\frac{D^3}{t}}\right] \tag{B.23}$$

$$H_{pc} = 0.356 \times \left[\frac{371.39}{19.01 \times 103.9}\right]^{1/0.5} - \left[\frac{371.39}{19.01 \times 6 \times 10^3}.\sqrt{\frac{0.356^3}{0.14}}\right] \tag{B.24}$$

$$H_{pc} = 13.1mm \tag{B.25}$$

The simplified analysis will lead to conservative results for smaller and lighter pipes. In this

case the advanced assessment is recommended.

B.1.1 Advanced Impact Calculation

The energy absorbed by the steel pipe can be calculated directly from the maximum force obtained from the impact analysis by, equation 4.13'

$$E_{ab} = \int F_{sh}(H_t)dH_t = \frac{\alpha.m_p.D}{(\beta+1)}.\left[\frac{F_{sh}}{\alpha.m_p}\right]^{(\beta+1)/\beta} \tag{B.26}$$

$$E_{ab} = \frac{103.9 \times 19.01 \times 0,356}{(0.54+1)} \times \left[\frac{359.55}{103.97 \times 19.012}\right]^{(0.54+1)/0.54} \tag{B.27}$$

$$E_{ab} = 3.3kJ \tag{B.28}$$

The permanent dent depth is calculated by using the equation

$$H_{pc} = D\left[\frac{F_{sh}}{m_p.\alpha}\right]^{1/\beta} - \left[\frac{F_{sh}}{m_p \times 6 \times 10^3}.\sqrt{\frac{D^3}{t}}\right] \tag{B.29}$$

$$H_{pc} = 0.356 \times \left[\frac{359.55}{19.01 \times 103.9}\right]^{1/0.5} - \left[\frac{359.55}{19.01.6 \times 10^3}.\sqrt{\frac{0.356^3}{0.14}}\right] \tag{B.30}$$

$$H_{pc} = 13.1mm \tag{B.31}$$

Appendix C

Calculation of RP load

C.1 Trawl board

Table C.1 Model properties

Quantity	**value**
Water depth, (d)	400 m
Trawl board height, ($h = 2B$)	2.46
Span height, (H_{sp})	0.5 m
Warp line diameter	0.028 m
Drag coefficient	2.0
Added mass coefficient	2.0
Axial friction coefficient	0.4
Lateral friction coefficient	0.6
Load effect factor	1.1
Condition load effect factor, (γ_c)	1.07

The pull-over load is divided into Horizontal force and vertical force. The loads for trawl board is calculated as follows

$$\bar{H} = \frac{H_{sp} + (OD/2) + 0.2}{B} \tag{C.1}$$

$$\bar{H} = \frac{0 + (0.32/2) + 0.2}{1.23} \tag{C.2}$$

$$\bar{H} = 0.7 \tag{C.3}$$

The empirical coefficient for polyvalent and rectangular boards is calculated by using equation 4.15

$$C_F = 8.0(1 - e^{-0.8\bar{H}}) \tag{C.4}$$

$$C_F = 8.0(1 - e^{-0.8\bar{0.7}}) \tag{C.5}$$

$$C_F = 3.43 \tag{C.6}$$

The maximum horizontal pull-over force is calculated according to the following equation 4.14 and it is denoted by Fp.

$$F_P = c_F.V(m_t.k_w)^{1/2} \tag{C.7}$$

$$F_P = 3.43 \times 2(2600 \times 1.23)^{1/2} \tag{C.8}$$

$$F_P = 59kN \tag{C.9}$$

The maximum vertical force for Polyvalent and rectangular boards acting in the downward direction can be estimated by using equation 4.17

$$F_z = F_p(0.2 + 0.8.e^{-2.5\bar{H}}) \tag{C.10}$$

$$F_z = 59(0.2 + 0.8.e^{-2.5\bar{0.7}}) \tag{C.11}$$

$$F_z = 20kN \tag{C.12}$$

calculation of stiffness according to equation 4.20

$$K_w = \frac{3.5 \times 10^7}{L_w} \text{N/m} \tag{C.13}$$

$$K_w = \frac{3.5 \times 10^7}{3 \times 400} \text{N/m} \tag{C.14}$$

$$K_w = 29KN/m \tag{C.15}$$

The total pull-over time, T_P is calculated by using equation 4.18

$$T_P = C_T.C_F.\left(\frac{m_t}{k_w}\right)^{1/2} + \frac{\delta p}{V} \tag{C.16}$$

$$T_P = (1 + 0.1) \times 2 \times 3.43\left(\frac{2600}{29}\right)^{1/2} \tag{C.17}$$

$$T_P = 2.25s \tag{C.18}$$

The displacement of the pipe at the point of interaction is unknown prior to response simulations. Therefore, the value of $\delta p/V$ must be assumed (e.g. as $C_T.C_F.(m_t/k_w)^{1/2}/10$ and may be corrected after response simulations in some sort of iterative approach.

Appendix D

Low pass filter results

The low pass filtering of results were performed for various cases .The same low pass filtering results are presented for previous model test results for clump-weight pipeline interaction. This filtering is executed by appling a butter low pass function in PYTHON, with cutt-off frequency 1.54 Hz. This filtering reduces the high frquencies, but it did not lower the original value of the results. The comparison of filtered and non-filtered results are shown below.

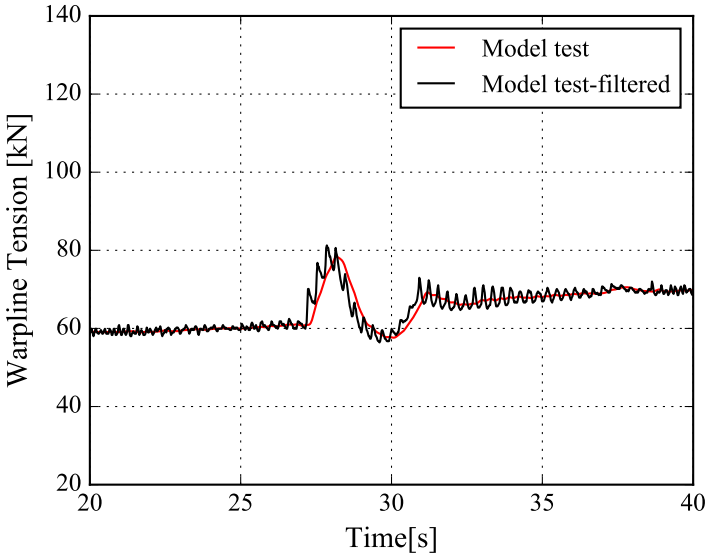

Figure D.1 comparison of Low pass filtered result with non filtered results $H_{sp} = 0.5m$

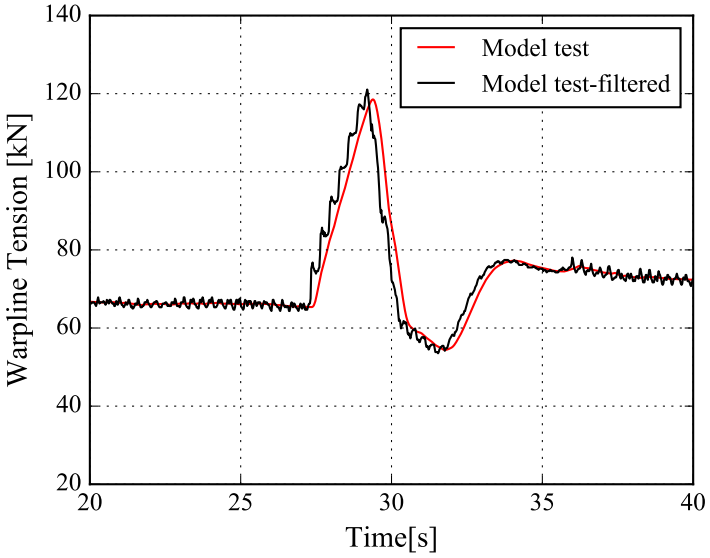

Figure D.2 comparison of Low pass filtered result with non filtered results $H_{sp} = 1m$

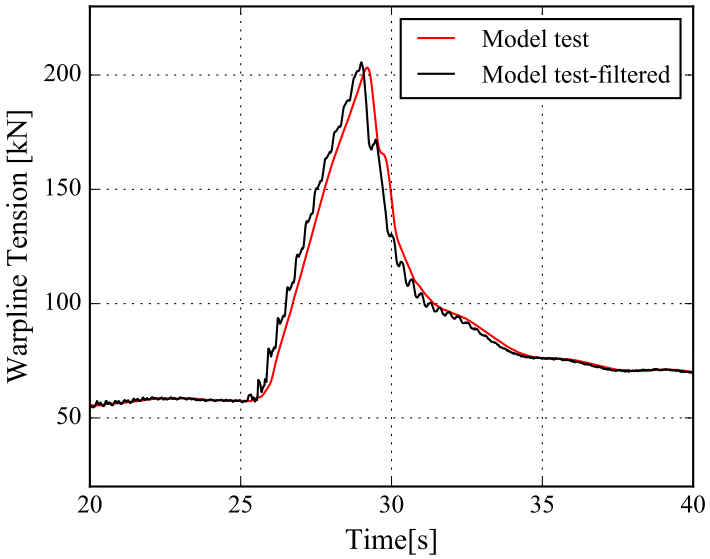

Figure D.3 comparison of Low pass filtered result with non filtered results $H_{sp} = 5m$

Appendix E

Free spanning pipe-in-pipe and trawl board model - bending moment results

The comparison of trawl load with RP load is illustrated. The simulation is carried out for three different span heights and the results are plotted. Figure E.1 to E.6 shows the comparison of lateral bending moment and from figure E.7 to E.12

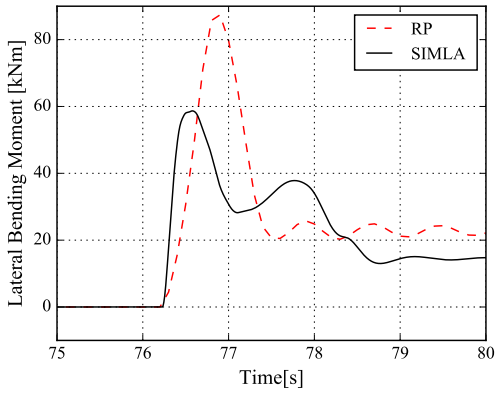

Figure E.1 Lateral bending moment-OP, H_{sp} = 0 m

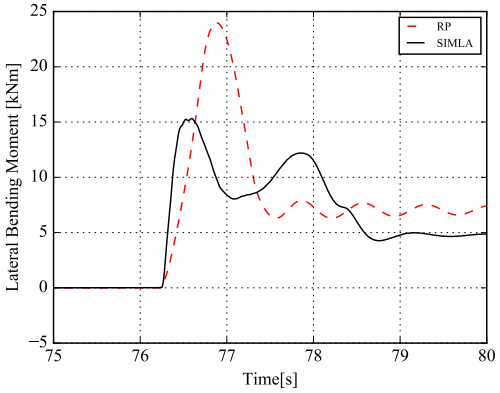

Figure E.2 Lateral bending moment-IP, H_{sp} = 0 m

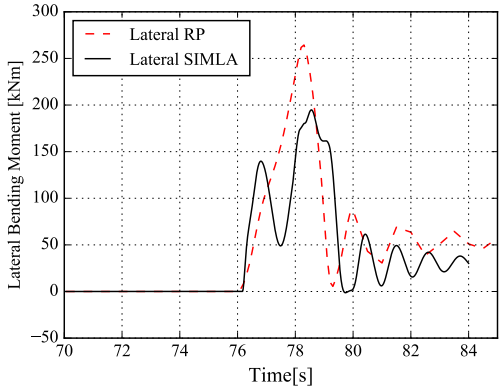

Figure E.3 Lateral bending moment-OP, H_{sp} = 0.5 m

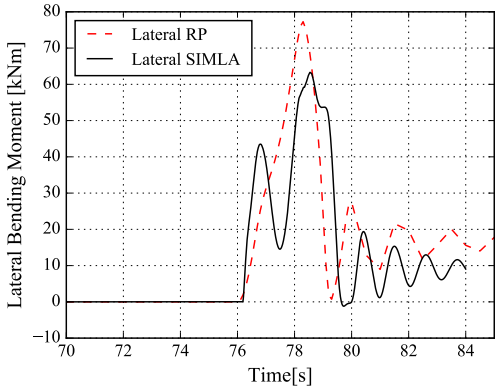

Figure E.4 Vertical bending moment-IP, H_{sp} = 0.5 m

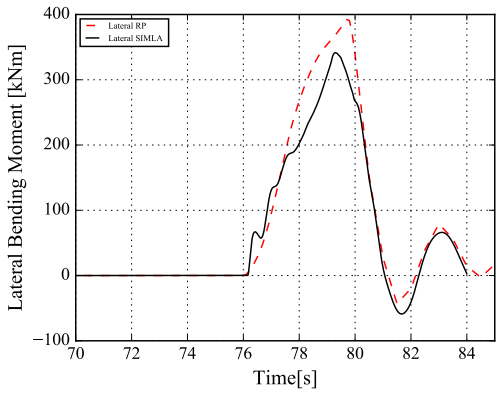

Figure E.5 Lateral bending moment-OP, H_{sp} = 1 m

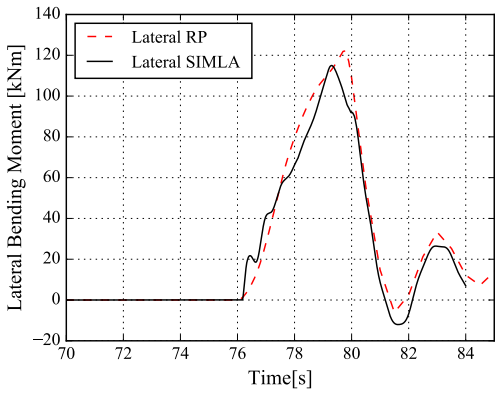

Figure E.6 Lateral bending moment-IP, H_{sp} = 1 m

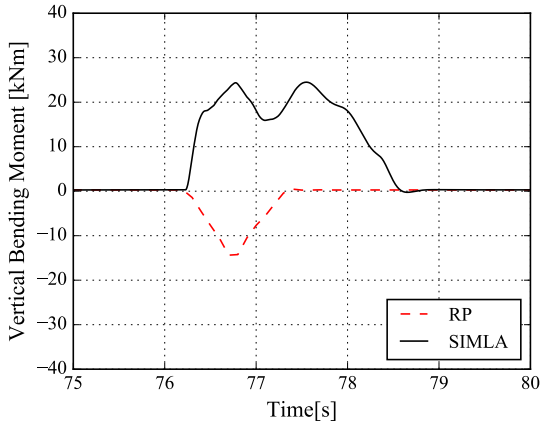

Figure E.7 Vertical bending moment-OP, $H_{sp} = 0$ m

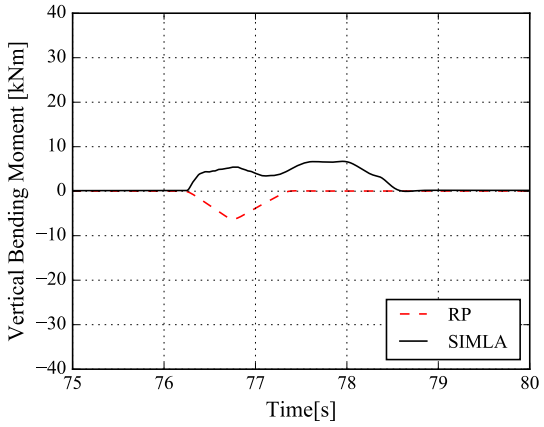

Figure E.8 Vertical bending moment-IP, $H_{sp} = 0$ m

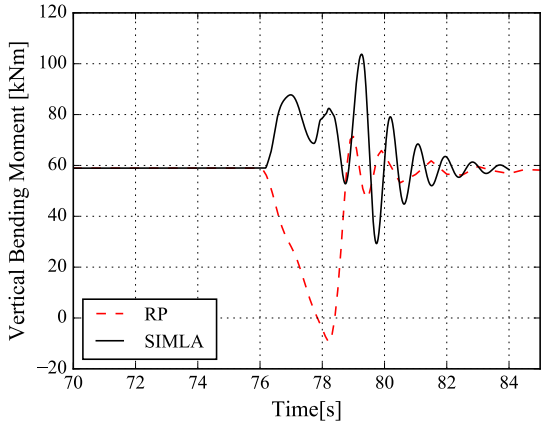

Figure E.9 Vertical bending moment-OP, $H_{sp} = 0.5$ m

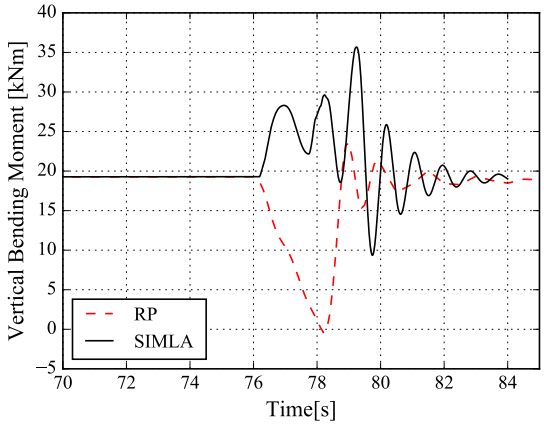

Figure E.10 Vertical bending moment-IP, $H_{sp} = 0.5$ m

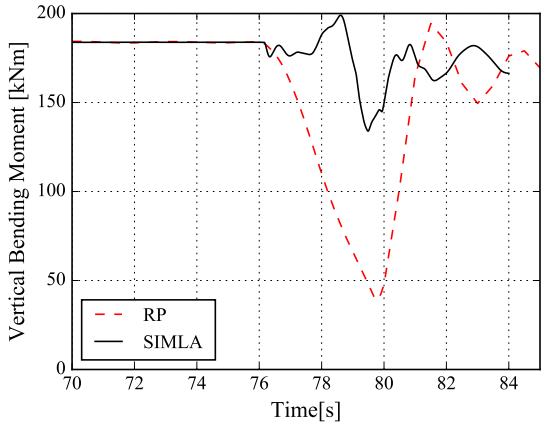

Figure E.11 Vertical bending moment-OP, $H_{sp} = 1$ m

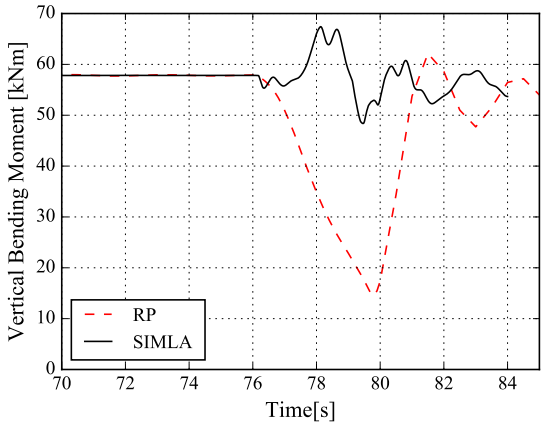

Figure E.12 Vertical bending moment-IP, $H_{sp} = 1$ m